

**Josip Juraj Strossmayer University of Osijek**  
**University of Dubrovnik**  
**Ruđer Bošković Institute**  
**University Postgraduate Interdisciplinary Doctoral Study of Molecular  
biosciences**

**Željka Trumbić**

**DEVELOPMENT AND APPLICATION OF A DNA  
MICROARRAY FOR GENE EXPRESSION PROFILING IN  
CAPTIVE ATLANTIC BLUEFIN TUNA (*THUNNUS  
THYNNUS* L., 1758)**

**PhD THESIS**

**Osijek, 2015.**

---

## BASIC DOCUMENTATION CARD

---

**Josip Juraj Strossmayer University of Osijek**  
**University of Dubrovnik**  
**Ruđer Bošković Institute**  
**University Postgraduate Interdisciplinary**  
**Doctoral Study of Molecular biosciences**

**PhD thesis**

**Scientific Area:** Biotechnical Sciences

**Scientific Field:** Biotechnology

### **DEVELOPMENT AND APPLICATION OF A DNA MICROARRAY FOR GENE EXPRESSION PROFILING IN CAPTIVE ATLANTIC BLUEFIN TUNA (*THUNNUS THYNNUS* L., 1758)**

Željka Trumbić

**Thesis performed at:** Institute of Aquaculture, University of Stirling, Stirling, Scotland, United Kingdom; Laboratory of Aquaculture, Institute of Oceanography and Fisheries, Split, Croatia

**Supervisor/s:** Prof. Ivona Mladineo, DVM, PhD, senior research fellow  
John Bernard Taggart, PhD, senior lecturer

#### **Short abstract:**

Atlantic bluefin tuna *Thunnus thynnus* is migratory fish with distinct physiology and high economic value. In this study mixed-tissue normalized cDNA library was constructed, pyrosequenced, assembled and annotated. It was used as a template for construction of *T. thynnus*-specific DNA microarray with 15 000 probes used to infer tissue-specific gene expression profiles. The relationship between bluefin as a host and digenean trematode *Didymosulcus katsuwonicola* was further investigated employing DNA microarray and transmission electron microscopy.

**Number of pages:** 115

**Number of figures:** 25

**Number of tables:** 9

**Number of references:** 253

**Original in:** English

**Key words:** *Thunnus thynnus*, *Didymosulcus katsuwonicola*, transcriptome sequencing, DNA microarray, Trematoda, ultrastructure

**Date of the thesis defense:** September 15<sup>th</sup> 2015

#### **Reviewers:**

1. Prof. Đurđica Ugarković, PhD, senior research fellow, president of the committee
2. Prof. Ivona Mladineo, PhD, senior research fellow, supervisor and reviewer
3. Oliver Vugrek, PhD, research associate, reviewer
4. Maja Herak Bosnar, PhD, research associate, substitute

**Thesis deposited in:** National and University Library in Zagreb, Ul. Hrvatske bratske zajednice 4, Zagreb; City and University Library of Osijek, Europska avenija 24, Osijek; Josip Juraj Strossmayer University of Osijek, Trg sv. Trojstva 3, Osijek

## TEMELJNA DOKUMENTACIJSKA KARTICA

---

Sveučilište Josipa Jurja Strossmayera u Osijeku  
Sveučilište u Dubrovniku  
Institut Ruđer Bošković  
Poslijediplomski interdisciplinarni sveučilišni  
studij Molekularne bioznanosti

Doktorska disertacija

**Znanstveno područje:** Biotehničke znanosti  
**Znanstveno polje:** Biotehnologija

### IZRADA I PRIMJENA DNA MIKROČIPA ZA ODREĐIVANJE EKSPRESIJE GENA KOD KAVEZNE ATLANTSKE PLAVOPERAJNE TUNE (*THUNNUS THYNNUS* L., 1758)

Željka Trumbić

**Disertacija je izrađena u:** Institutu za akvakulturu Sveučilišta u Stirlingu, Stirling,  
Škotska, Velika Britanija; Laboratoriju za akvakulturu Instituta za oceanografiju i ribarstvo  
Split, Hrvatska

**Mentor/i:** Prof. dr.sc. Ivona Mladineo, znanstvena savjetnica  
Dr. sc. John Bernard Taggart

#### **Kratki sažetak doktorske disertacije:**

Atlantska plavoperajna tuna *Thunnus thynnus* je migratorna vrsta ribe sa specifičnom fiziologijom i značajnom ekonomskom vrijednošću. U ovoj studiji je sintetizirana normalizirana cDNA knjižnica iz različitih tkiva odraslih jedinki, pirosekvencirana, sastavljena i anotirana. Ista je iskorištena kao kalup za konstrukciju DNA mikročipa specifičnog za ovu vrstu od 15 000 probi koji je upotrijebljen za profiliranje genske ekspresije između metabolički različitih tkiva. Nadalje, istražen je odnos između tune kao domaćina i dvorodnog metilja *Didymosulcus katsuwonicola* korištenjem DNA mikročipa i transmisivne elektronske mikroskopije.

**Broj stranica:** 115

**Broj slika:** 25

**Broj tablica:** 9

**Broj literaturnih navoda:** 253

**Jezik izvornika:** Engleski

**Ključne riječi:** *Thunnus thynnus*, *Didymosulcus katsuwonicola*, sekvenciranje transkriptoma, DNA mikročip, Trematoda, ultrastruktura

**Datum obrane:** 15. rujna 2015.

#### **Stručno povjerenstvo za obranu:**

1. Prof. dr. sc. Đurđica Ugarković, znanstvena savjetnica, predsjednica povjerenstva
2. Prof. dr. sc. Ivona Mladineo, znanstvena savjetnica, mentor i član
3. Dr. sc. Oliver Vugrek, viši znanstveni suradnik, član
4. Dr. sc. Maja Herak Bosnar, viša znanstvena suradnica, zamjena člana

**Disertacija je pohranjena u:** Nacionalnoj i sveučilišnoj knjižnici Zagreb, Ul. Hrvatske bratske zajednice 4, Zagreb; Gradskoj i sveučilišnoj knjižnici Osijek, Europska avenija 24, Osijek; Sveučilištu Josipa Jurja Strossmayera u Osijeku, Trg sv. Trojstva 3, Osijek

---

This doctoral thesis was performed at The Laboratory of Aquaculture, Institute of Oceanography and Fisheries Split, Croatia, supervised by Prof. dr. sc. Ivona Mladineo, and The Institute of Aquaculture, University of Stirling, Stirling, Scotland, United Kingdom, under the supervision of Dr. sc. John Bernard Taggart. The supporting grants include the Business Innovation Croatian Agency (BICRO) Proof of Concept (POC) grant: MikroTuna - a new diagnostic tool for monitoring disease in tuna farms (PoC\_01\_07-U-1), Unity Through Knowledge Fund (UKF): Development of a Health Genomic Profile for the captive Atlantic bluefin tuna (*Thunnus thynnus*) (23/08) and a personal Fellowship for Doctoral Students from the Croatian Science Foundation to Željka Trumbić.

---

## **Acknowledgments**

*I would like to express my sincere gratitude to all who supported, participated and contributed to this project. Most importantly, my supervisors, Dr Ivona Mladineo without whose ideas and initiative the project would not have happened and for always being a source of scientific inspiration; and Dr John Taggart for extending me a warm and unreserved welcome to his laboratory and for providing advice and support every step of the way. I would like to thank Dr Michaël Bekaert, Dr James Bron, Dr Stephen Carmichael for their time and expert guidance and all the staff, colleagues and friends at the Stirling Institute of Aquaculture, for making it a great learning and life experience. Especially you, Beatrix!*

*I would like to thank to Dr Svjetlana Krstulović Šifner for patience and understanding. Many thanks to all dear friends and colleagues at the Department of Marine Studies and Institute of Oceanography and Fisheries (Mirela, Zvezdana, Josipa, Jure, Tanja, Ivana LP), for their encouragements and for making everyday life interesting, dynamic and enjoyable.*

*Finally, deepest gratitude to my family, for unconditional love and support!*

# Table of contents

<b>1 Introduction .....</b>	<b>1</b>
1.1 Biological and ecological characteristics of <i>Thunnus thynnus</i> .....	1
1.2 Tuna aquaculture and management .....	3
1.3 Health status of Atlantic bluefin tuna .....	7
1.4 Digenenas as parasites of tuna .....	8
1.5 Application of transcriptomics in aquaculture .....	10
1.6 Research objectives .....	12
<b>2 Materials and Methods.....</b>	<b>13</b>
2.1 Animal tissue collection .....	13
2.2 RNA extraction .....	13
2.3 Normalized cDNA library preparation.....	14
2.4 Pyrosequencing .....	18
2.5 Data filtering and assemblies .....	19
2.6 Sequence annotation and functional assignments .....	20
2.7 Genome mapping .....	20
2.8 <i>In silico</i> mining of EST-associated SSRs (EST-SSRs) .....	21
2.9 <i>Thunnus thynnus</i> microarray design .....	21
2.10 Microarray experiments .....	22
2.10.1 Preparation of total RNA samples for hybridization .....	23
2.11 Microarray data analyses .....	25
2.11.1 Profiling of tissue-specific gene expression signatures .....	25
2.11.2 Inference of transcriptomic changes between infected and uninfected gills.....	26
2.12 Quantitative reverse transcription PCR (RT-qPCR).....	27
2.13 Transmission electron microscopy .....	31
2.14 Data access .....	31
<b>3 Results .....</b>	<b>32</b>
3.1 Pyrosequencing and transcriptome assembly .....	32
3.2 Functional inference by searching against public databases .....	34
3.3 Genome mapping .....	36
3.4 <i>In silico</i> EST-SSRs mining .....	37
3.5 Results of microarray inference of tissue-specific gene expression profiles and qPCR validation .....	40
3.6 Microarray profiling of transcriptomic changes in gill epithelium induced by <i>D.</i>	

<i>katsuwonicola</i> infection and qPCR validation .....	46
3.7 Heterologous hybridization of <i>D. katsuwonicola</i> to <i>T. thynnus</i> arrays .....	54
3.8 Ultrastructure of <i>Didymosulcus katsuwonicola</i> cysts.....	55
<b>4 Discussion .....</b>	<b>59</b>
4.1 Functional interpretation of tissue-specific expression profiles .....	59
4.2 Functional interpretation of transcriptomic and ultrastructural changes associated with <i>D. katsuwonicola</i> infection in <i>T. thynnus</i> gills.....	65
<b>5 Conclusions .....</b>	<b>76</b>
<b>6 References.....</b>	<b>77</b>
<b>7 Summary .....</b>	<b>96</b>
<b>8 Sažetak.....</b>	<b>97</b>
<b>9 Supporting Information .....</b>	<b>100</b>
<b>10 Curriculum Vitae .....</b>	<b>114</b>

# 1 Introduction

Fish represent the oldest and most diverse vertebrate group, inhabiting every available aquatic environment (Froese & Pauly 2014). They display remarkable heterogeneity of life trait characteristics and occupy a historically important place in human culture as a source of nutritionally valuable food. Marked by genome duplication events, the diversification and adaptive radiation of fish represent an attractive evolutionary model to study ecological, behavioural and physiological aspects of biodiversity (Volff 2005). The object of investigation in this thesis is a teleostean species with important and unique physiological adaptations, ecological traits and high socio-economic impact, the Atlantic bluefin tuna *Thunnus thynnus* (Linnaeus, 1758).

## 1.1 Biological and ecological characteristics of *Thunnus thynnus*

Migratory tunas (family *Scombridae*, order *Perciformes*: suborder *Scombroidei*), are pelagic oceanodromous top predators, which display a set of extreme adaptations to life in a prey depauperate pelagic environment. They are obligate ram ventilators with streamlined bodies for rapid locomotion, have increased aerobic scope and metabolic rates that allow them to satisfy the energy needs of multiple high performance functions without compromise, including high digestive rates, increased somatic and gonadal growth and incredibly fast recovery from oxygen debt after exhaustive exercise compared to other teleosts (Brill 1996; Block & Stevens 2001). A key characteristic of tunas is their regional endothermy, the ability to retain metabolic heat and maintain elevated temperature in the brain, eye, myotomal muscle and viscera comparing to the external environment (Block & Stevens 2001). Primarily, heat is generated within slow-twitch oxidative myotomal muscles (red muscles, RM) during sustained swimming. Comparing to other teleosts, except for the swordfish (*Xiphias gladius*), RM is situated more anterior and nearer to the vertebral column and is completely surrounded by white muscle in tuna. Thermal exchange occurs within vascular specializations called *rete mirabile*, which comprise numerous juxtaposed arterial and venous vessels acting as a counter-current heat exchange system (Block & Stevens 2001). Heat from the venules exiting the RM is equilibrated with oppositely flowing cool arterioles. This heterothermic physiology shares characteristics of both poikilothermic and homoeothermic organisms and is

considered to have developed in order to permit thermal niche expansion, especially in correlation with maintenance of central nervous system function (Block *et al.* 1993) or to sustain a rise in aerobic capacity and muscular performance (Block & Finnerty 1994).

The largest of the tuna species, Atlantic bluefin tuna, *Thunnus thynnus*, inhabits the North Atlantic Ocean and the Mediterranean Sea (Figure 1.1). They are long-lived fish with average lifespan of 15 years (Ottolenghi 2008). At 10 years of age they measure approximately 200 cm and 150 Kg and can reach 400 cm and 700 Kg as they get older and growth in weight increases (Fromentin & Powers 2005). Males have been known to grow faster than females. Atlantic bluefin tuna undertake extensive migrations to cold temperate waters in search for prey. They reside mostly in subsurface waters, but can dive to depths of 500 – 1000 m sustaining temperatures from 3 °C to 30 °C while preserving stable internal body temperature (Block *et al.* 2001, 2005; Walli *et al.* 2009). When mature, they annually or biennially return to warm waters to spawn within a narrow spatial and temporal window. Based on the observed homing behaviour to two major spawning grounds: the Gulf of Mexico and the Mediterranean Sea (Rooker *et al.* 2008), the International Commission for the Conservation of Atlantic Tunas (ICCAT) recognizes smaller Western and larger Eastern populations respectively as separate management units divided by the 45°W meridian (Figure 1.1). Age at maturity in the Eastern stock has been estimated at 4 years (length at maturity is about 110 –120 cm (30 – 35 Kg)) and at around 8 years for the Western stock (about 200 cm (150 Kg)) (Fromentin & Powers 2005), with the latter data being the subject of debate (Knapp *et al.* 2014). Spawning peaks during May in the Gulf of Mexico and June for the Mediterranean Sea, correlating with water temperatures exceeding 24 °C. Although the differentiation between these populations has been corroborated by molecular markers (Carlsson *et al.* 2007; Boustany *et al.* 2008), results of electronic tagging reveal a complex ecology, with extensive trans-Atlantic migrations and mixing of the individuals at the foraging and spawning grounds (Block *et al.* 2005; Walli *et al.* 2009), complicating *T. thynnus* stock management. Furthermore, the population structure within the Mediterranean is not completely resolved. Although it needs further research, it appears that there is significant differentiation between tuna populations of the Eastern and Western Mediterranean basins (Boustany *et al.* 2008; Riccioni *et al.* 2010; Viñas *et al.* 2011).

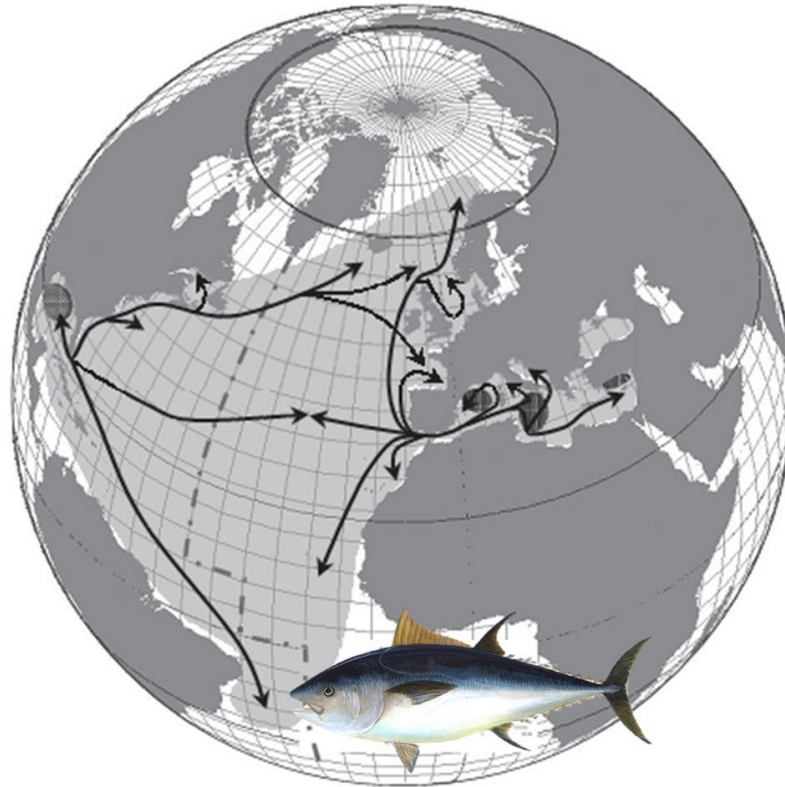


**Figure 1.1** Distribution of Atlantic bluefin tuna *Thunnus thynnus* in the North Atlantic and the Mediterranean Sea. Spawning grounds (black areas), migration routes (arrows) and stock differentiation border, 45°W meridian (dashed line), are depicted. Adapted from Fromentin & Powers (2005).

## 1.2 Tuna aquaculture and management

*T. thynnus* form large schools during their migrations to the Mediterranean Sea in order to spawn during summer months. Schools can be heterogeneous regarding their age and body size, although they usually school according to size. Juveniles can be found mixed with smaller tuna species such as skipjack (*Katsuwonis pelamis*) or bonito (*Sarda sarda*) (Ottolenghi 2008). It is during this time that lean breeders, who have consumed their fat reserves in the process of migration, are caught by purse seiners, transferred to towing cages and slowly towed for weeks, or even months, to near-shore facilities for tuna out-growth and rearing. After the transfer to rearing cages, they are allowed a 10 to 15 days acclimation period before the commencement of feeding (Mylonas *et al.* 2010). In order to increase marketable value by increasing body size and the muscle fat content, tunas are fed daily with fresh and/or defrosted mixture of baitfish such as sardine (*Sardinella aurita*), pilchard (*Sardina pilchardus*), mackerel (*Scomber japonicus*), bogue (*Boops boops*), anchovy

(*Engraulis encrasicolus*), herring (*Clupea harrengus*) and squid (*Illex* sp.) (Katavic *et al.* 2003; Mišlov Jelavić *et al.* 2012). At harvest in the Adriatic, the fish are killed as quickly as possible by a combination of techniques involving a blow or shot to the head, followed by bleeding of the animals from lateral arteries, coring the brain case and pushing the metal wire through the hind brain and spinal cord in order to stop any involuntary muscle movement. Accumulation of lactic acid in the muscles and increase in body temperature during intensive swimming and fighting can cause severe deterioration of the flesh quality for sushi and sashimi market, and care is taken to minimize these effects.

Tuna aquaculture is therefore dependent on the yearly renewal from the wild and referred to as fattening, if rearing is done for 3 – 7 months using mature fish (> 30 Kg), characteristic for most Mediterranean countries, or farming, if it involves juvenile fish (8 – 30 Kg) that need to be reared for at least two years to reach exploitable size (30 Kg), specific only for Croatia (Mylonas *et al.* 2010). However, this activity is not sustainable in the long run as tuna wild populations are considered critically endangered (Fromentin & Powers 2005; MacKenzie *et al.* 2009; Taylor *et al.* 2011). Tuna fattening/farming operations were first introduced to Croatia and Spain in 1996, based on successful experiences from Southern bluefin tuna (*Thunnus maccoyii*) rearing in Australia (Miyake *et al.* 2003). They have been expanding throughout the region ever since and today five leading countries with highest capacity to produce farmed tuna are Spain, Malta, Turkey, Italy and Croatia (Ottolenghi 2008). Over 70 % of Atlantic bluefin tuna global catch is landed in the Mediterranean Sea, of which 99 % is destined for fattening/farming operations (Mylonas *et al.* 2010). This has however greatly increased fishing mortality and load on already collapsing tuna stocks (Figure 1.2). In order to control fishing activities, the International Commission for the Conservation of Atlantic Tunas (ICCAT) has introduced restrictive catch limits since 1982 for the Western Atlantic and 1998 for the Eastern Atlantic and Mediterranean stocks (Ottolenghi 2008). As part of a multiannual recovery plan and under the increasing pressure of NGOs (non-governmental organizations), ICCAT reduced the TAC (total allowable catch) for 2010 to only 13,500 t, a threefold reduction from 2007, and restricted the purse seine fishing period from May 15<sup>th</sup> – June 15<sup>th</sup>. The implementation of these management measures resulted in detectable increase in spawning stock biomass, allowing for moderate catch quotas increase after a long time in 2015 (ICCAT 2014). Nevertheless, the reports stress the high

uncertainty associated with these assessments and vigilance is recommended as populations remain under threat. Consequently, it is considered that only domestication of *T. thynnus* and development of high welfare aquaculture practices independent of wild resources can preserve the species for future generations.

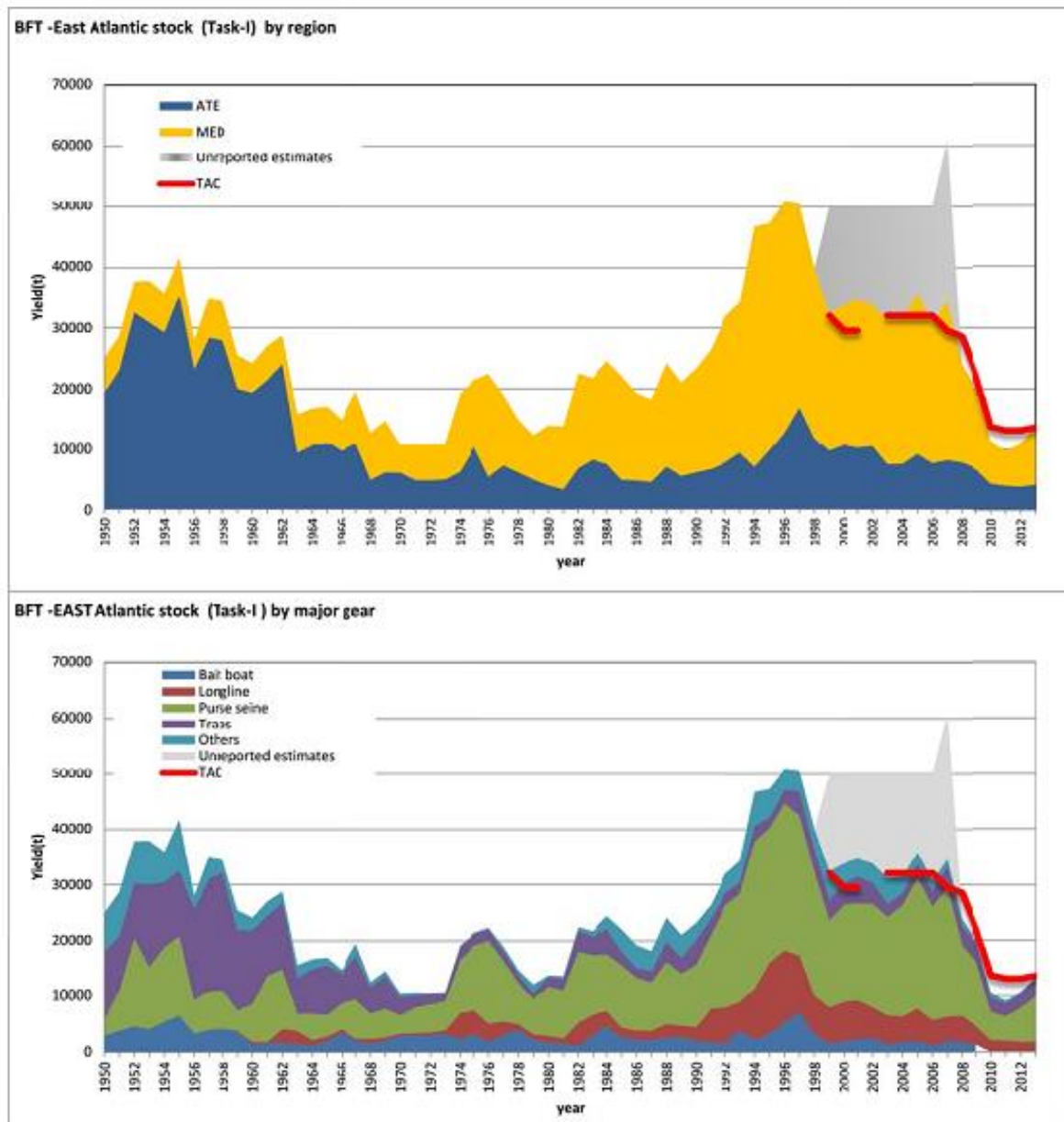


**Figure 1.2** Reported catch of *T. thynnus* for the East Atlantic and Mediterranean from 1950 – 2013 split by main geographic areas (top panel) and by gears (bottom panel). TAC levels (red line) and unreported catch estimates are also reported. Reused from ICCAT (2014).

The first bluefin tuna species successfully grown in captivity from larvae to adults is Pacific bluefin tuna *Thunnus orientalis* in Japan (Sawada *et al.* 2005). Fish are maintained in large cages and allowed to spawn naturally. The technology is the result of a 30 year old research effort and highlights many challenges that need to be solved, such as unpredictable spawning, poor larval post-hatch survival, cannibalism, collisions with the tank or net wall and diseases. Today, a limited quantity of entirely farmed Pacific bluefin tuna can be found at the Japanese market. Extensive research efforts have been made regarding the control of *T. thynnus* reproduction in captivity using gonadotropin-releasing hormone agonist (GnRHa) implants to induce final oocyte maturation and ovulation (Corriero *et al.* 2007; Rosenfeld *et al.* 2012), although spontaneous spawning has also been recorded (Grubišić *et al.* 2013). The technology is in its infancy and holds great promise for the completion of *T. thynnus* rearing cycle in captivity independent of wild resources.

Tuna industry is associated with substantial socio-economic impact, generating significant income, new job opportunities, driving the modernization of entire fishing fleets and the development of a new set of professional specializations, like expert divers, inspectors, teams of skilled personnel to assure fish wellbeing and appropriate handling throughout the rearing cycle (Ottolenghi 2008). It has substantially transformed the Japanese sushi and sashimi market by introducing a middle quality meat category that was previously non-existent, consisting of small fish fattened by farming and available in abundance, influencing the trade and prices overall (Miyake *et al.* 2003). In Croatia, it constitutes one of the main fisheries export products. However, tuna farming operations are in conflict with other sectors, such as traditional longline and trap fisheries, as well as tourism as dense farming introduces substantial amount of organic matter into the environment from uneaten bait fish, excreted feces or processing at harvest, in form of grease stains and unpleasant odour. There is also an issue of possible negative environmental impacts. Studies have shown that benthic communities are transformed (Vita & Marin 2007; Vezzulli *et al.* 2008), especially *Posidonia oceanica* meadows (Kružić *et al.* 2014), below-cage sediment composition is altered (Vezzulli *et al.* 2008; Matijević *et al.* 2012), although not as much as with other aquaculture species (Vita *et al.* 2004), while water column physico-chemical properties remain unchanged. These effects can however vary greatly depending on local hydro-dynamic and biotic variables, but are generally considered to be non-detrimental in the long term. Positioning tuna cages in off-shore

deep oligotrophic areas with strong currents is highlighted as an important contributor towards reduction of negative effects and also essential for satisfying physiological needs of these fast-swimming and energetic fish. The studies report that seasonal character of tuna farming/fattening is also an important factor in mitigation of adverse consequences for the environment, in which case additional caution is advised in the Adriatic where tuna farming is all-year-round activity.

### 1.3 Health status of Atlantic bluefin tuna

Intense rearing environment has been known to facilitate pathogen dissemination and spread of diseases, the reason why industries of many aquacultured species suffer extensive losses. Generally, tuna are hosts to many types of pathogens, including viruses, bacteria, protozoa and many metazoan organisms (Munday *et al.* 2003), however reports of associated mass mortalities are rare, especially for the Mediterranean. There are few reports of losses of Atlantic bluefin tuna due to environmental factors, such as water turbidity (Mylonas *et al.* 2010), a case of pan-steatitis induced mortality associated with feed (Roberts & Agius 2008) and a mass mortality due to *Photobacterium damsela* subsp. *piscicida* outbreak (Mladineo *et al.* 2006). Parasite-induced morbidity and mortality seem to be more common issues in other bluefin tuna species, although still considered of a low risk. In Southern bluefin tuna *T. maccoyii* advents of mortalities have been associated with debilitating encephalitis caused by scuticociliate *Uronema nigricans*, known as the "swimming syndrome" (Munday *et al.* 1997), or seasonally correlated with epizootic hyperinfections of sea lice *Caligus chistos* and blood fluke *Cardicola forsteri* (Hayward *et al.* 2010).

Metazoan parasite communities of *T. thynnus* are diverse and composed of different taxonomic groups, such as trematodes, cestodes, nematodes, crustaceans, myxozoans and microsporidians (Mladineo *et al.* 2008). Most abundant and prevalent group constitute digenean trematodes, with *Didymosulcus katsuwnicola* and *Koellikerioides intestinalis* core parasite species (Mladineo & Tudor 2004; Mladineo *et al.* 2011). It has been observed that total parasite richness and mean abundance decline during farming in the Adriatic Sea, with complete loss of species with direct life cycle such as copepods and monogeneans, and significant decrease of heteroxenous digeneans with a shift in community structure (Mladineo *et al.* 2011).

Multiple factors in combination could be responsible for this phenomenon, from environmental variables, tuna rearing conditions, inadequate trophic propagation of parasite infective stages or host intrinsic immune factors, a subject requiring further investigation. Culurgioni *et al.* (2014) reported differentiation of *T. thynnus* parasite assemblages according to host size, with the largest ones bearing most diverse parasitofauna, opposite of what is observed in captivity. This is a reflection of their migratory life style. The authors also noted spatial differentiation of composition of parasite communities within the Mediterranean. The Western Mediterranean group was characterized as a mixture of poorly infected resident tunas and heavily infected tunas migrating from the Atlantic Ocean.

Current fattening/farming practices rely on regular renewal from the wild with mature or juvenile immunocompetent fish already naturally selected for resistance. Towing fish to rearing facilities is a stressful activity with 2 – 4 % mortality rate (Ottolenghi 2008), additionally exerting pressure on weak individuals. With intensification of production in an anthropogenically controlled environment, it is possible that new tuna health issues might emerge and will have to be resolved.

#### **1.4 Digeneas as parasites of tuna**

As already mentioned, digeneans (Trematoda) constitute most diverse and core group parasitizing Atlantic bluefin tuna. Hermaphroditic trematode species exhibit a remarkable plasticity of their evolution and physiology that enables colonization of all available niches in the vertebrate host: from the digestive system to epidermis (Galaktionov & Dobrovolskij 2003). Although their primary environment represents the digestive tract, a smaller number of species migrated to new habitats. One of them is represented by a peculiar group of tissue cyst-forming trematodes of family Didymozoidae parasitizing pelagic oceanic and coastal fish, particularly scombrids (Munday *et al.* 2003). It is believed that their switch from digestive system to peripheral parasitism sites has been induced by histophagy (Ginetsinskaya 1988), although their feeding strategy is still not fully solved. Didymozoids have world-wide distribution in tropical to subtropical areas, but still they are considered one of the most taxonomically complex digenean families, whose intricate migration patterns are complex and largely unknown (Pozdnyakov & Gibson 2008). Their life cycle might involve three or four hosts and follows typical digenean pattern encompassing small

pelagic fish and cephalopods as intermediate, and pelagic fish as final hosts (Lester & Newman 1986; Pozdnyakov 1996). The exact migration route of didymozoid cercariae from final host's digestive tract to its preferred sites of parasitization is unknown, limited by sampling of large pelagic fish or impossibility to develop *in vitro* assays. In the Atlantic bluefin tuna, didymozoids inhabit practically all conceivable niches (Mladineo 2006; Mladineo et al. 2011), encyst mostly in pairs in a connective-tissue capsule of varying size and thickness, formed mutually by the parasite and host reaction (Mladineo 2006; Di Maio & Mladineo 2008). *Didymosulcus katsuwonicola* (syn. *Didymocystis wedli*) (Figure 1.3) is the most abundant didymozoid species infecting farmed bluefin tuna (Mladineo et al. 2011), which in particular rearing conditions may elicit inflammatory and necrotic changes in the gill tissue (Mladineo 2006; Mladineo & Bočina 2009). However, in most cases infections terminate without any gross pathology, characterized by a significant decrease of cysts per host after couple of months of tuna rearing (Mladineo et al. 2011). Therefore, gill didymozoids could represent an interesting model for parasite-host interaction study, moreover because in contrast to internal organs, regional heterothermy in tuna impedes elevated temperature in gill tissue where *D. katsuwonicola* originates (Block & Stevens 2001).

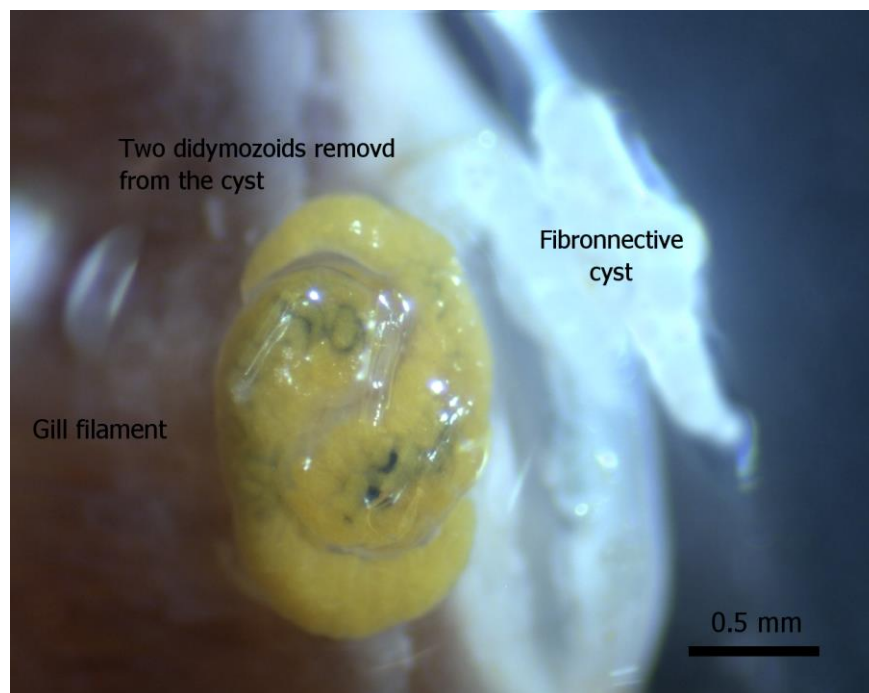


**Figure 1.3** *Didymosulcus katsuwonicola* pair excised from the connective tissue capsule (cyst) attached to *T. thynnus* gill filaments, using scalpel under the dissecting microscope.

## 1.5 Application of transcriptomics in aquaculture

Genetic and molecular approach to investigating important ecological questions and life history traits, such as migration rates, population size, kinship, adaptation, disease resistance, etc. has become powerful, flexible, efficient and widespread in the past decade (Selkoe & Toonen 2006). Molecular markers allow us to establish the hidden link between observed phenotypic effects, at a population or individual level, and their genetic background. Since the advent of second generation high-throughput sequencing technologies (Margulies *et al.* 2005), the focus is shifting from single gene oriented to genome-wide studies employing thousands of markers in search of systemic solutions. Development of the necessary tools and resources can now be achieved in a relatively short period of time, even for species with a low level of background information (Ekblom & Galindo 2011), such as non-model organisms and economically important species. Sequence data, such as genome or, more commonly, expressed sequence tags (ESTs) constitute initial resource for such studies. ESTs are single-read sequences produced from partial sequencing of a bulk mRNA pool within a given set of tissues, developmental stages, environmental conditions and genotypes (Bouck & Vision 2007). They represent a sample of coding sequences associated with a certain phenotype and can serve for various purposes, differential gene expression analyses, alternative splicing detection, gene discovery, development of single nucleotide polymorphism (SNPs) markers or simple sequence repeats (SSRs), to name a few. Classical approach to building EST libraries involved the production of bulk cDNA by reverse transcription of template mRNA present in sampled cells which was then cloned into a vector library and each clone was individually end-sequenced (Bouck & Vision 2007). Normalization procedures can be applied during cDNA library construction in order to eliminate abundant transcripts and increase sequencing coverage of rare genes (Zhulidov *et al.* 2004). Today, cDNA material can be directly sequenced with one of the high-throughput technologies, referred to as transcriptome characterization. However, higher sequencing error rate is associated with these technologies and a hybrid approach is often advised (Ekblom & Galindo 2011).

Available genomic resources for *T. thynnus* were until recently relatively scarce, most derived from a single EST sequencing project comprising adult liver, ovary and testis mRNA transcripts contributed by Chini *et al.* (2008). This collection served as the basis for the construction of the first *T. thynnus*-specific oligonucleotide microarray, employed for the description of the Gulf of Mexico *T. thynnus* gonad

transcriptome (Gardner *et al.* 2012). It was also utilized for the profiling of cardiac transcriptome response to temperature acclimation in congeneric *T. orientalis* (Jayasundara *et al.* 2013), highlighting the applicability of such a tool for gene expression analyses in phylogenetically related species. The release of congeneric genome of *T. orientalis* (Nakamura *et al.* 2013) opens new opportunities for tuna comparative genome studies and ongoing transcriptome characterization projects.

Developed in 1995 (Schena *et al.* 1995), DNA microarray technology today represents the benchmark for quantitative analyses of gene expression variation at transcriptome level, with applications in biomedical and life sciences research. A microarray slide consists of thousands of gene-specific probes imprinted or directly synthesized on a glass surface. Hybridization between transcripts and their complementary probes is measured by the intensity of fluorescent signal proportional to initial transcript quantity in the sample. Regarding the type of probes used, oligonucleotides have become preferred alternative to cDNAs as they are more specific, reproducible, easily designed (Hughes *et al.* 2001) and allow for standardization between different experiments (Kuo *et al.* 2006). By providing large scale transcriptomic insight into important life trait characteristics, such as growth, maturation, environmental tolerance and disease resistance, DNA microarray technology contributes valuable knowledge assisting in the development of welfare-centred and sustainable management strategies for aquaculture and fisheries sectors (Nielsen & Pavey 2010). Microarray development for teleost species was motivated primarily by toxicogenomics and environmental stress research, followed by developmental and commercial aquaculture application studies (Miller & Maclean 2008). Within the latter, examples of explored themes include immune response to pathogens (Liu *et al.* 2008; Tadiso *et al.* 2011), dietary lipid metabolism (Taggart *et al.* 2008), larval development (Douglas *et al.* 2008), skeletal deformities (Ferraresso *et al.* 2010), molecular phenotypic selection for improved broodstock characteristics (Melamed *et al.* 2002), search for superior embryo quality (Mommens *et al.* 2014) or effects of domestication (Bicskei *et al.* 2014). Although direct massively parallel sequencing of RNA population (RNA-seq) is replacing microarrays as a method of choice for transcriptome investigation (Wang *et al.* 2009), microarrays show good correlation with RNA-seq data, still being a more familiar, cost-effective and versatile tool (Zhao *et al.* 2014).

## 1.6 Research objectives

The objectives of this thesis were:

- to build on and expand existing transcriptomic resources for studying *T. thynnus* using high-throughput sequencing technologies,
- to use the newly developed cDNA library to design a custom oligonucleotide DNA microarray and explore its potential for the development of other molecular markers,
- to validate the newly developed microarray by profiling functional differences in transcript expression between tissues, and
- to investigate the relationship between captive Atlantic bluefin tuna and digenean trematode *Didymosulcus katsuwonicola* at the transcriptomic and ultrastructural level.

## 2 Materials and Methods

### 2.1 Animal tissue collection

Atlantic bluefin tuna were reared in mid-Croatian offshore farm cages for two years. During the winter harvest of 2012, adult fish (curved fork length =  $177 \pm 9$  cm; weight =  $99 \pm 14$  Kg) were sacrificed by pithing and samples of kidney, spleen, liver, gonads, small intestine, heart (*apex ventriculi*), red and white skeletal muscle, skin scrapes, whole blood, and infected and uninfected gill filaments were dissected and preserved in RNAlater stabilization solution (Qiagen, UK) at  $-20^{\circ}\text{C}$ , after overnight storage at  $+4^{\circ}\text{C}$ . In addition, liver and kidney samples from juvenile moribund fish with clinical signs of septicaemia were available from another study (Lepen Pleić *et al.* 2013) and were included in a normalized cDNA library preparation to increase the diversity of the sequenced transcriptome. Phosphate-buffered (0,1 M PBS) 4% paraformaldehyde was used for fixation of gill samples destined for transmission electron microscopy (TEM).

### 2.2 RNA extraction

Between 30 - 40 mg of each of the tissues were separated for the analyses. A biopsy punch ( $\varnothing = 5$  mm, Stiefel, UK) was taken from gill filaments of healthy and infected animals (N = 7 in each group). The area surrounding the parasitic cyst was targeted and didymozoids removed under the dissecting microscope. Samples were homogenized in 1 mL of TRI Reagent (Sigma-Aldrich, UK) by 2 x 35 second disruption runs on a Mini-Beadbeater-24 (BioSpec Products, Inc, USA) and total RNA was extracted according to manufacturer's instructions. Two total RNA extracts were also prepared from removed parasites, to assess the potential for heterologous cross-hybridization to host microarray during the experiment.

Homogenates were incubated at room temperature (RT) for 5 minutes (min) and 100  $\mu\text{l}$  of 1-bromo-3-chloropropane (BCP) were added to achieve phase separation. Samples were shaken, incubated at RT for 15 min and centrifuged ( $20,000 \times g$  for 15 min at  $4^{\circ}\text{C}$ ). Aqueous (upper) phase was transferred into a new tube and RNA precipitated with the addition of equal volumes of isopropanol and RNA precipitation solution (1.2 M Sodium Chloride and 0.8 M Sodium Citrate Sesquihydrate) (10 min incubation at RT followed by centrifuge at  $20,000 \times g$  for 10 min at  $4^{\circ}\text{C}$ ). The use of

a high salt solution during precipitation is recommended for polysaccharide- and proteoglycan-rich sources (Chomczynski & Mackey 1995), as it selectively favours precipitation of the RNA. The RNA precipitate (gel-like pellet on the bottom of the tube) was subsequently washed with 1 mL of 75 % ethanol and centrifuged at  $20,000 \times g$  for 5 min at RT. Supernatant was removed, the RNA pellet air dried and dissolved in RNase-free water. Integrity of total RNA extracts was assessed by ethidium bromide agarose gel electrophoresis and purity and concentration by spectrophotometry (NanoDrop ND-1000, Thermo Scientific, USA).

During electrophoresis, differences between total RNA composition between *T. thynnus* ovaries and other tissues were observed (Figure 2.1). Small RNA fraction comprising tRNA and 5S RNA prevailed over typically observed 18 S and 28 S in eukaryotes, as previously found in amphibians (Picard & Wegnez 1979; Van den Eynde *et al.* 1989) and several other teleosts (Mazabraud *et al.* 1975; Diaz de Cerio *et al.* 2012).

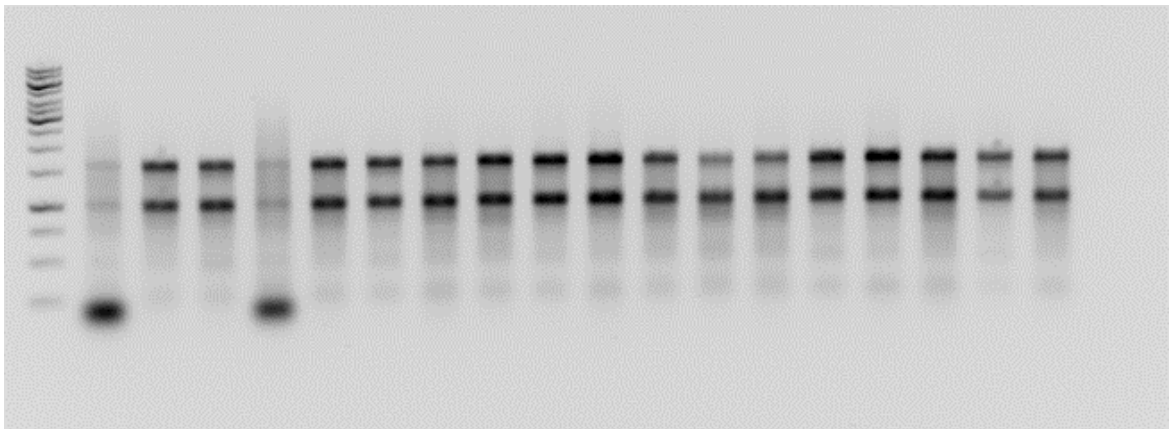


**Figure 2.1** Agarose gel (1 %) after electrophoresis of total RNA extracted from *T. thynnus* tissues. Samples in lanes 2 and 5 (on left, after the ladder DNA marker in lane 1) represent ovarian RNA with predominant small RNA fraction, different from all other samples inspected.

### 2.3 Normalized cDNA library preparation

A mixed RNA sample comprising equal amounts (5  $\mu\text{g}$ ) derived from all sampled tissues, except ovaries, was created from one female, one male and one moribund juvenile specimen and purified using RNeasy columns (Qiagen, UK). Due to differences in ovarian RNA composition, poly(A)<sup>+</sup> RNA was first isolated from the ovarian total RNA population using a Poly(A) Purist kit (Ambion, UK) and

subsequently 200 ng of the isolated mRNA were included in the pool. The MINT kit (Evrogen, Russia) was used to construct a full-length-enriched double stranded complementary DNA (cDNA) library, according to manufacturer's protocol. The workflow to prepare cDNA using the MINT kit is shown in Figure 2.2. First strand cDNA synthesis was started with 1.5 µg of the tissue RNA mixture (1.6 µl), 1 µl of 3' primer (5'- AAGCAGTGGTATCAACGC AGAGTAC(T)<sub>30</sub>VN - 3') provided with the kit, 1 µl of PlugOligo adapter and sterile water in total volume of 5 µl. The mix was incubated at 70 °C for 2 min. Reverse transcription mix was subsequently added consisting of 2 µl of 5 × First-Strand Buffer, 1 µl of dithiothreitol (DTT), 1 µl of dNTP mix, 1 µl of Mint Reverse transcriptase and incubated at 42 °C for 2 hours (hr), with the supplementation of 5 µl of IP-solution after 30 min. Evaluative PCR using 1 µl of first-strand cDNA as a template was performed in order to determine optimal number of cycles needed to achieve sufficient amplification without reaching the reaction plateau, by removing aliquots of reaction mixture during cycling and comparing them by agarose gel electrophoresis. Finally, the first-strand cDNA was amplified over 19 cycles (initial denaturation at 95 °C for 1 min, 19 cycles at 95 °C for 15 s, 66 °C for 20 s, 72 °C for 3 min and final extension at 66 °C for 15 s and 72 °C for 3 min). The reaction mixture included 40 µl of sterile water, 5 µl of 10 × Encyclo PCR Buffer, 1 µl of dNTP mix, 2 µl of PCR Primer M1 and 1 µl of 50 × Encyclo Polymerase Mix.

The TRIMMER kit (Evrogen, Russia) was then used to perform normalization procedure on 1 µg of cDNA starting material applying duplex-specific nuclease (DSN) method (Zhulidov *et al.* 2004). The principle is described in Figure 2.3. Hybridization reaction contained 9.8 µl of ds cDNA, 4 µl of 4 × Hybridization buffer and 2.2 µl of water, split into for 4 tubes each receiving 4 µl of the mixture. The reactions were overlaid with mineral oil, centrifuged at 14,000 rpm for 2 min, incubated in a thermal cycler at 98 °C for 2 min, followed by a 5 hours long incubation at 68 °C. Five µl of preheated DSN master buffer (100 mM Tris-HCl, pH = 8, 10 mM MgCl<sub>2</sub>, 2 mM DTT) were added to each tube and incubated at 68 °C for 10 min. Different dilutions (1, 1/2, 1/4 and no enzyme control) of DSN enzyme in DSN storage buffer (50 mM Tris-HCl, pH = 8) were subsequently added to different tubes and incubated at 68 °C for 25 min. This step is performed with the purpose of determining the best enzyme concentration for the normalization. Reactions were interrupted by adding 10 µl of DSN stop solution (5 mM EDTA), incubated at 68 °C for 5 min, supplemented with 20 µl of water and placed on ice. Control reactions (no DSN treatment) were subjected

to evaluate PCR amplification as previously described. Finally, it was determined that optimal normalization of the library was achieved with 1/2 DSN mixture followed by first amplification with standard Evrogen's M1 primer over 19 cycles. Second amplification, recommended to obtain best results, was performed with M2 primer (annealing temperature at 64°C) in doubled reaction volume over 12 cycles. Normalized and amplified cDNA library was purified with MinElute PCR Purification Kit (Qiagen, UK) and ranged in size from 0.25 to 3 kb as inspected on a 1.5% agarose/ethidium bromide gel (Figure 2.4).

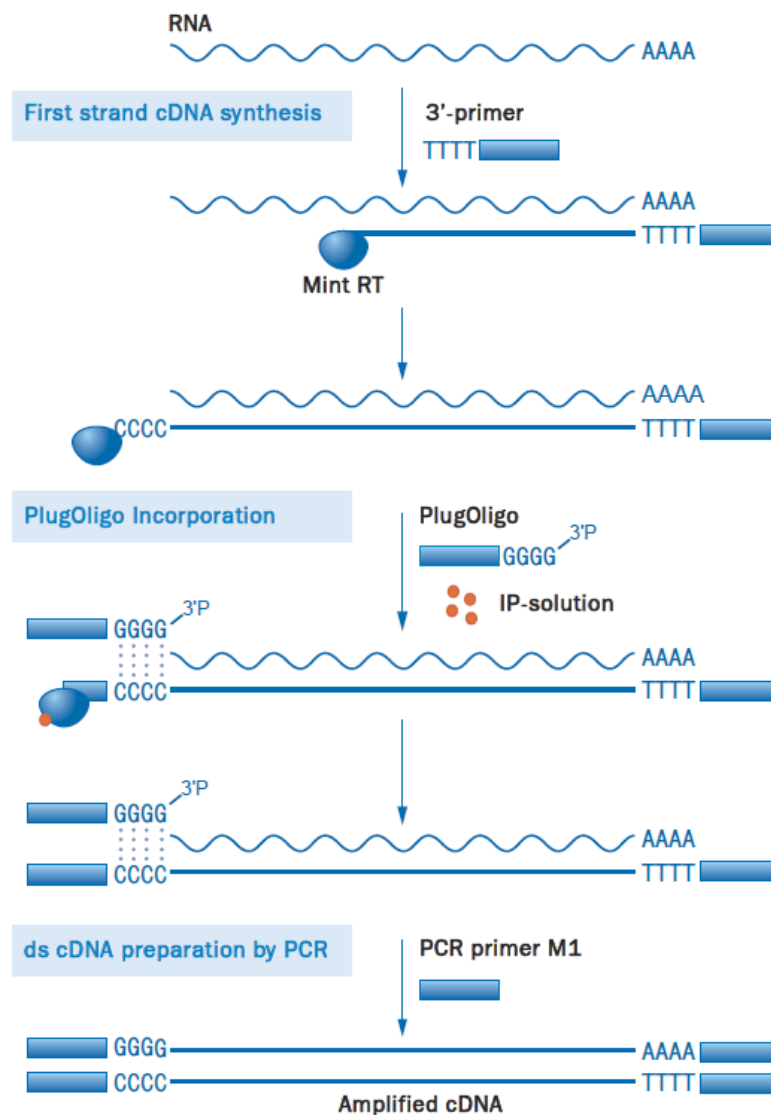


**Figure 2.2** Overview of the cDNA preparation using the MINT kit, as described in the User manual. The synthesis is primed with 3' primer. When reverse transcriptase reaches the 5' end of the mRNA it adds several deoxycytidines to the first cDNA strand, complementary to PlugOligo adapter that gets incorporated into 5' end of cDNA. Manufacturer's proprietary IP-solution allows the reverse transcriptase to use terminator PlugOligo as a template. At the third step, full-length-enriched double stranded cDNA synthesis is performed using PCR amplification. Amplified cDNA comprises same adapter sequences at both 3' and 5' ends.

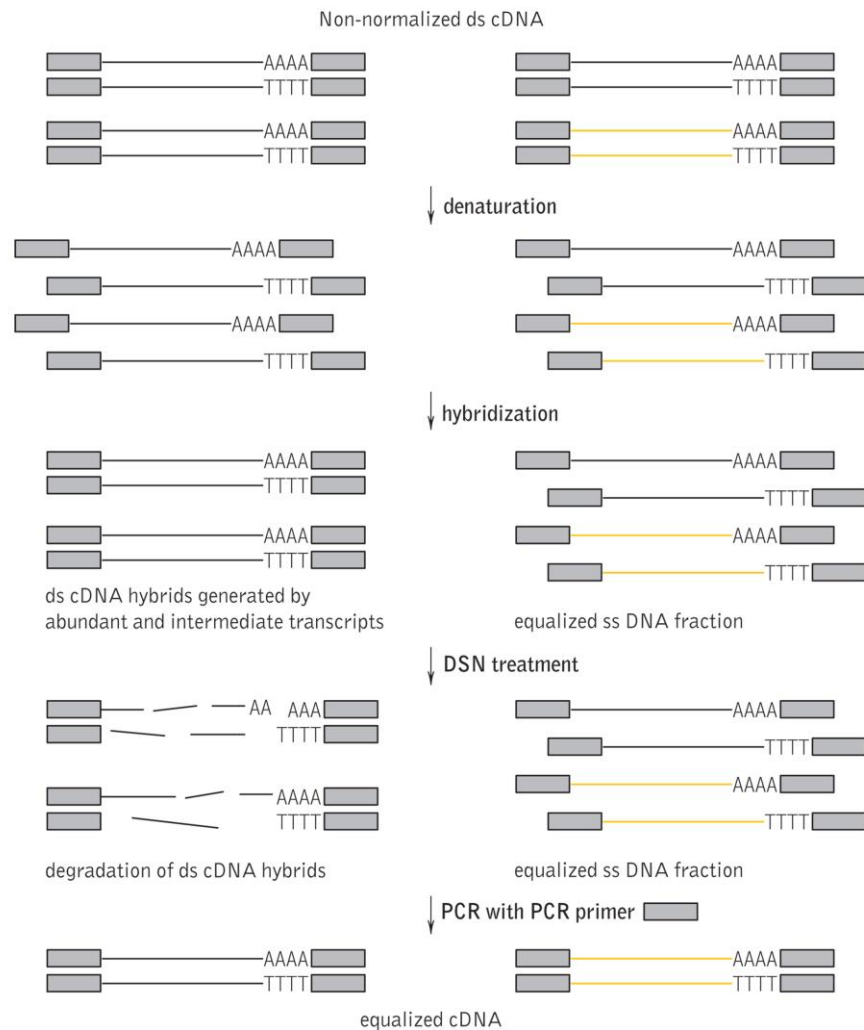


**Figure 2.3** Overview of the cDNA library normalization using the TRIMMER kit, as described in the User manual. Black lines represent abundant transcripts and orange lines rare transcripts. The method involves denaturation-reassociation of cDNA, where abundant transcripts reanneal quicker than rare sequences. Double-stranded fraction is degraded by duplex-specific nuclease (DSN) and the equalized single-stranded DNA fraction is amplified by polymerase chain reaction (PCR).

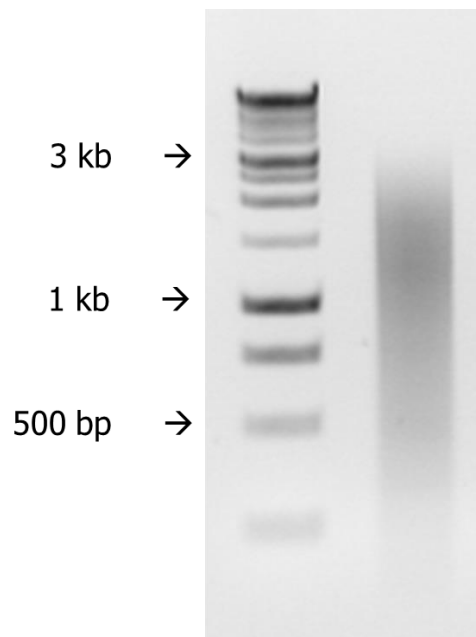


**Figure 2.4** Full-length enriched double stranded normalized cDNA library of *T. thynnus* after agarose gel electrophoresis (1.5 % gel). Successful normalization is evident as a consistent smear without visible bands corresponding to abundant transcripts.

## 2.4 Pyrosequencing

GS FLX Titanium library preparation and sequencing were performed by the Edinburgh Genomics facility (University of Edinburgh, UK). Approximately 5  $\mu$ g of normalized cDNA were used for generating a 454 sequencing library using the GS FLX Titanium Rapid Library Preparation kit (Roche Applied Science, UK), following manufacturer's instructions. Sequencing was performed using The Genome Sequencer™ (GS) Titanium FLX instrument (Roche Applied Science, UK). Bases were called with 454 software and reads trimmed to remove adapter sequences. The principle of 454 sequencing is described in Figure 2.5.

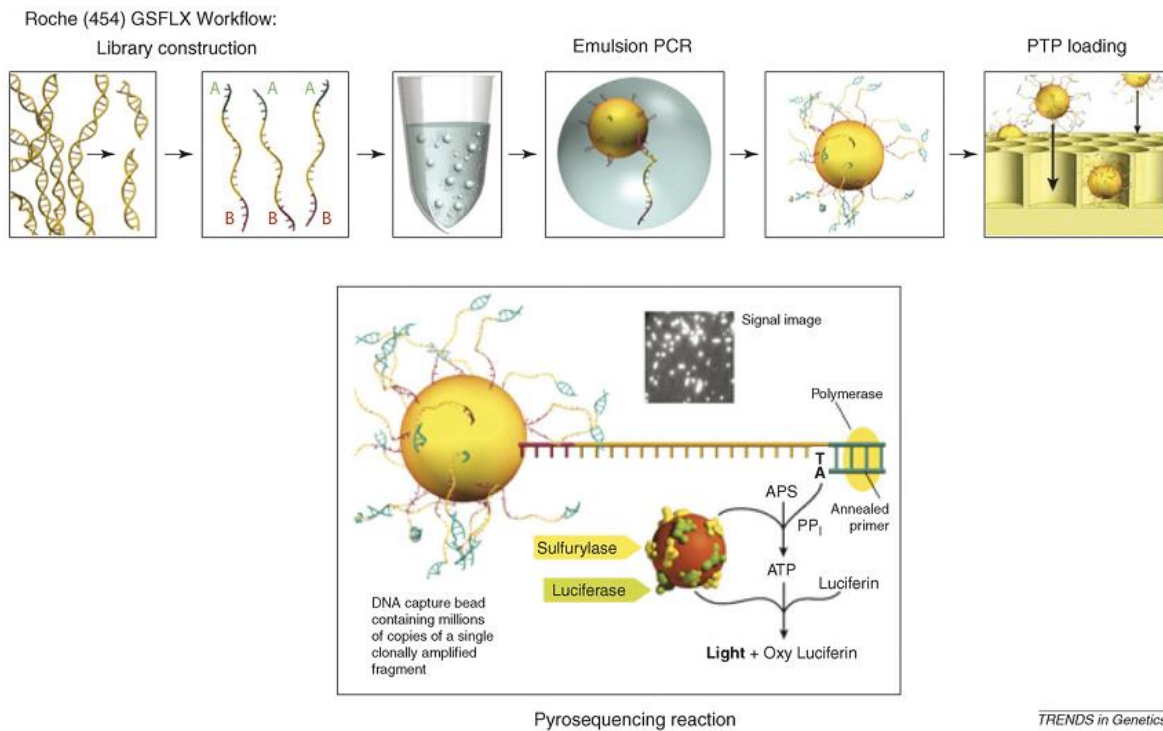


**Figure 2.5** 454 pyrosequencing workflow: library construction ligates 454-specific adapters to DNA fragments and couples amplification beads with DNA in an emulsion PCR to amplify fragments before sequencing. The beads are loaded into the picotiter plate (PTP). The bottom panel illustrates the pyrosequencing reaction, which uses the pyrophosphate molecule released on nucleotide incorporation by DNA polymerase to fuel a set of light producing reactions from the cleavage of oxyluciferin by luciferase. Light signals are recorded as synthesis proceeds. Reused from Mardis (2008).

## 2.5 Data filtering and assemblies

Sequences were filtered to remove low-quality reads (Phred score < 30) and PRINSEQ v0.20 (Schmieder & Edwards 2011) was used to remove PCR duplicates and low complexity sequences. Two complementary sequence read assembly methods were chosen for this study; WGS-assembler 7.0 (Celera assembler; Myers *et al.* 2000) and Mosaik-aligner v2.1 (Lee *et al.* 2014) were used to assemble the contigs based on *T. thynnus* EST sequences (2013/10/06 release). Subsequently, to lower the redundancy resulting from *de-novo* assemblies, Tandem repeats finder TRF 4.07b (Benson 1999) was used to remove all transcripts shorter than 500 bp or exhibiting repetition, with entropy above 1.

## 2.6 Sequence annotation and functional assignments

A sequence similarity search using the BLAST algorithm (Altschul *et al.* 1990) was performed for sequence annotation. The longest coding DNA sequences were determined for each transcript using the command-line program getorf from the EMBOSS v6.6.0 package (Rice *et al.* 2000). ESTScan v2 (Iseli *et al.* 1999; Lottaz *et al.* 2003) was then used to confirm transcript coding regions and determine sequence orientation. The coding sequences of the predicted transcripts were annotated using BLASTp searches against the GenBank Reference Proteins database (RefSeq Proteins; 2013/10/06 release, NCBI), with an expectation value (e-value) cut-off of  $10^{-4}$  and minimum alignment length of 33 amino acids being considered significant. Additionally, the transcripts were annotated using BLASTn searches against the EST (*T. thynnus* datasets, 2013/10/06 release) database. The inferred annotations were used to retrieve Gene Ontology (GO) annotation for molecular function, biological process and cellular component (Ashburner *et al.* 2000). To avoid redundant functional assignments, the best-rated similarity hit with at least one GO annotation was chosen. A custom pipeline converted GO terms to GO Slim terms, using the Protein Information resource and Generic GO Slim files (Bekaert 2013). Kyoto Encyclopedia of Genes and Genomes (KEGG) database (Kanehisa & Goto 2000) was used to infer functional annotation of the sequences through KEGG Automatic Annotation Server (KAAS) (Moriya *et al.* 2007) using single-directional best hit method for ESTs. Sequences with assigned KEGG orthology (KO) identifiers were categorized into functional groups according to the KEGG BRITE hierarchy files.

## 2.7 Genome mapping

Generated sequence data was compared with two perciform fish genomes that have been publicly released: *Thunnus orientalis* (Pacific bluefin tuna; NCBI Assembly GCA\_000418415.1; Nakamura *et al.* 2013), and *Oreochromis niloticus* (Nile tilapia, NCBI Assembly GCA\_000188235.2). The 133,062 contigs (684,497,465 bp) of *T. orientalis* and the 77,755 (927,696,114 bp) of *O. niloticus* genomes were downloaded and BLASTn (Altschul *et al.* 1990) was used to search for similar transcripts. The following parameters were used: minimum alignment size 80 nucleotides, minimum percentage of sequence identity 0.25, maximum e-value 0.001 and low complexity mask on, with all other parameters using default values to

account for the divergence and shortness for the sequences used. Results were displayed using a hive plot (Krzywinski *et al.* 2012).

## **2.8 *In silico* mining of EST-associated SSRs (EST-SSRs)**

In order to inspect the potential of assembled transcripts for the future development of other molecular markers, like Simple Sequence Repeats (SSRs), or more familiarly known as microsatellites, annotated sequences were searched with MICROSATELLITE identification Perl tool script (MISA), using default parameters. This tool allows for the identification and localization of perfect (mono-, di-, tri-, tetra-, penta-, -hexa- repeats) as well as compound microsatellites which are interrupted by a certain number of bases and have complex motifs. It also includes an integration module as interface with Primer 3 (Untergasser *et al.* 2012) for automatic modelling of primers flanking microsatellite regions. MISA is available at <http://pgrc.ipk-gatersleben.de/misa/>.

## **2.9 *Thunnus thynnus* microarray design**

Transcripts with a significant match to a referent protein were chosen for microarray probe design. In addition, fifty-seven publicly available full mRNA sequences from the *T. thynnus* nucleotide (NCBI) database were also included. 60-mer oligonucleotide probes were designed using the eArray (Agilent Technologies, UK) online probe design tool with Base Composition and Best Probe Methodologies, 3'bias and sense orientation. Two probes were designed for each target transcript. After initial screening, unique probes showing no cross-hybridization potential were selected to produce an 8 x 15 K Agilent custom oligonucleotide DNA microarray design format (Agilent Design ID = 038391), comprising 15,208 user defined features and 536 Agilent positive and negative controls. Target transcripts (N = 6,439) with best annotation were represented with two probes on the array and the remainder (N = 2,190) with a single probe. For calculation of the multiplicative detrending step implemented within the Agilent Feature extraction software 35 probes were replicated five times.

## 2.10 Microarray experiments

Two microarray experiments were performed in total, one for microarray validation including different tissues from adult *T. thynnus* and another comparing *D. katsuwonicola*-infected and uninfected gills. Common reference pool design was used in both experiments, where individual experimental samples are hybridized against the common reference comprising a contribution from each biological sample included in the experiment.

Five metabolically distinct tissues were chosen from adult *T. thynnus*: gill, heart, liver, testes and ovaries (4 biological replicates per tissue) for the first experiment. A total of 20 arrays were employed in the final design. Seven *D. katsuwonicola*-infected and uninfected gills each were analysed in the second experiment, with extra 2 samples each comprising a pool from 4 (two pairs) excised parasites. In total, 16 arrays were used for the second experiment and parasite RNA was not included in the common reference. The experimental designs are outlined in Table 2.1.

**Table 2.1** The outline of samples used for two *T. thynnus* microarray experiments.

<b>First experiment – comparison of metabolically different tissues</b>			
Sample	N (samples)	Common reference	N ( <i>T. thynnus</i> microarrays used)
Gill	4	Yes	20
Heart	4	Yes	
Liver	4	Yes	
Ovary	4	Yes	
Testis	4	Yes	
<b>Second experiment – transcriptional profiling of digenean infection</b>			
Sample	N (samples)	Common reference	N ( <i>T. thynnus</i> microarrays used)
Infected gills	7	Yes	14
Uninfected gills	7	Yes	
<i>D. katsuwonicola</i>	2 (parasite pools)	No	2

### 2.10.1 Preparation of total RNA samples for hybridization

Amplified and fluorescently labelled cRNA (complimentary RNA) for microarray hybridizations was prepared in accordance with the Two-Colour Microarray-Based Gene Expression Analysis - Low Input Quick Amp Labelling Protocol v6.6 (Agilent Technologies, USA) for both experiments. The principle is outlined in Figure 2.6. One hundred and fifty nanograms of total RNA from each sample were employed to initiate the cDNA synthesis, this being primed with an Oligo dT – T7 RNA polymerase promoter (total RNA was mixed with 0.8 µl of primer and water in total volume of 5.3 µl). The primer and the template were denatured by incubation at 65 °C for 10 min and subsequently placed in ice. cDNA mix was prepared by combining 2 µl of 5 × First Strand Buffer, 1 µl of 0.1 M DTT, 0.5 µl of 10 mM dNTP mix and 1.2 µl of Affinity Script RNase Block Mix after which 4.7 µl of the mix were added to reaction and incubated at 40 °C for 2 hr with final inactivation achieved by incubation at 70 °C for 15 min. Subsequently, T7 RNA polymerase incorporated Cyanine 3 (Cy3) or Cyanine 5 (Cy5) – CTPs, for the experimental or reference samples respectively, into a growing chain of antisense cRNAs. Six µl of the mix containing 0.75 µl of nuclease-free water, 3.2 µl of 5 × Transcription Buffer, 0.6 µl of 0.1 M DTT, 1 µl of NTP mix, 0.21 µl of T7 RNA polymerase Blend and 0.24 µl of Cyanine 3-CTP or Cyanine 5-CTP, were added to the tubes and incubated for another 2 hr at 40 °C. Amplified cRNA was purified using the GeneJET RNA Purification Kit (Thermo Scientific, UK) following the manufacturer's RNA Clean-up Protocol and was further quality-checked by spectrophotometry (NanoDrop ND-1000, Thermo Scientific, USA) and agarose gel electrophoresis. Three hundred nanograms of each Cy3 labelled test and 300 ng of Cy5 labelled reference pool cRNA were mixed together and incubated with 5 µl of 10 × Gene Expression Blocking Agent, 1 µl of 25 × Fragmentation Buffer and sterile water to reach total reaction volume of 25 µl. Samples were incubated at 60 °C for 30 min in the dark to fragment the RNA and cooled on ice for 1 min. Twenty-five µl of 2 × Hi-RPM Hybridization Buffer pre-warmed at 37 °C were added to reactions. Tubes were centrifuged at 13,000 × g for 1 min at RT, placed on ice and immediately loaded on the arrays. Competitive hybridizations were carried out in a rotary oven (Agilent Technologies, UK) over 17 hours at 65°C and 10 rpm. Following Agilent standard protocols the slides were subsequently washed in Wash Buffer 1 (at RT and 10 s at 31 °C), Wash Buffer 2 (1 min at 31 °C), acetonitrile (10 s) and Agilent Stabilization and Drying solution (30 s), the latter to reduce ozone-induced decay of Cy5 signal.

Slides were stored in light proof box and scanned within 1 hr of washing.

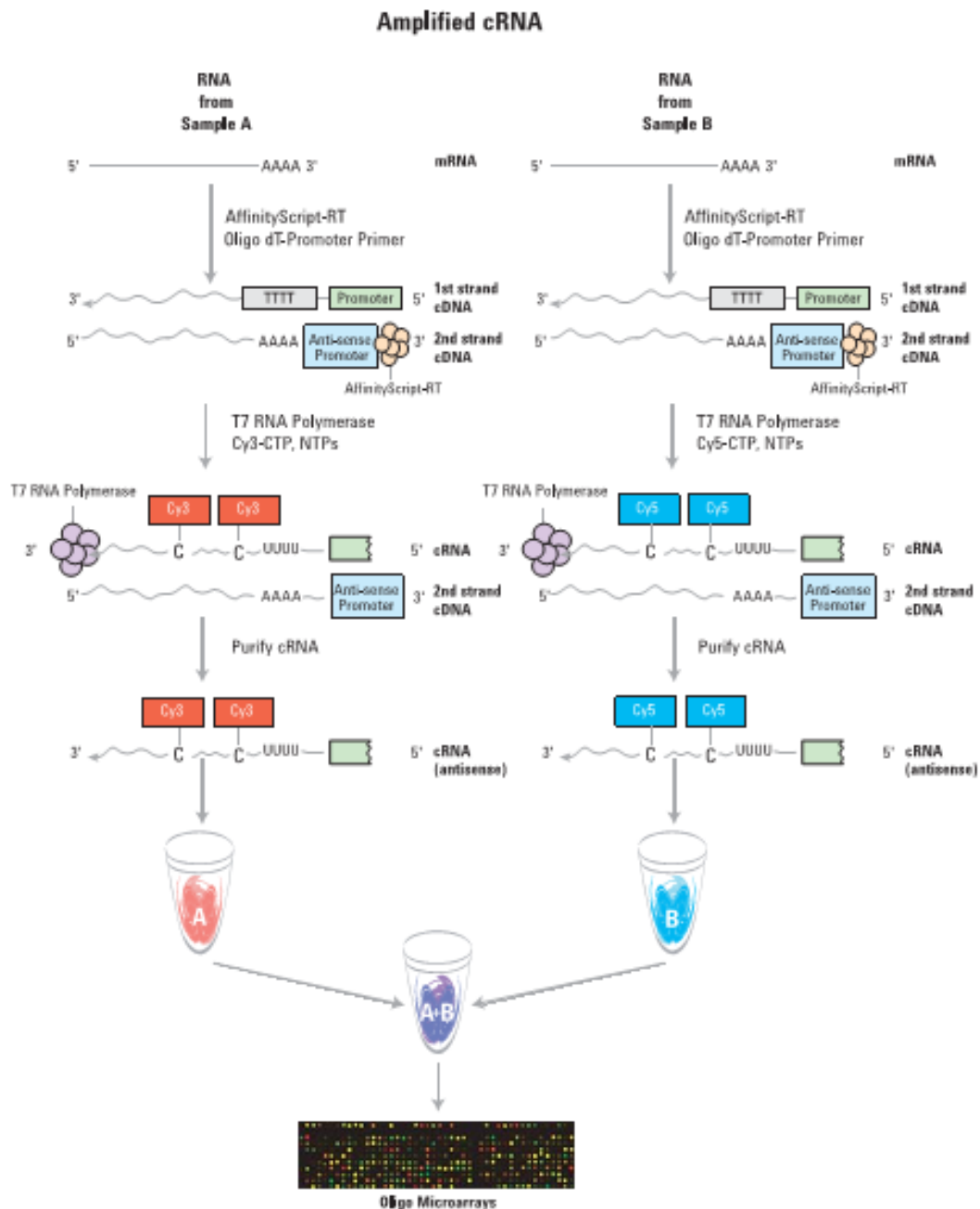


**Figure 2.6** Schematic diagram of amplified cRNA procedure according to Agilent User manual. Generation of cRNA for a two-colour microarray experiment is shown, primed with Oligo dT – T7 RNA polymerase promoter. After second strand synthesis T7 RNA polymerase incorporates Cyanine 3 or Cyanine 5 labelled CTPs into a growing chain of antisense cRNA, amplifying it in the procedure.

## 2.11 Microarray data analyses

Scanning was conducted using an Axon Genepix 4200A scanner with Genepix Pro 6.1 image acquisition software (Molecular Devices, UK) with 60 % red and 90 % green laser power and 5  $\mu\text{m}$  resolution. Saturation tolerance was set to 0.05 % and automatic photo-multiplier tube (auto-PMT) gain used to achieve similar mean intensities of Cy3 and Cy5 signals. Acquired data were exported and processed using the Agilent Feature Extraction software (v9.5.3.1) to obtain background-subtracted signals, as well as other spot statistics and quality metrics. Scan data were analysed using GeneSpring GX v12 (Agilent Technologies, UK). Baseline transformation was not employed and data were normalized using a Lowess model. Principal Component Analysis (PCA) was conducted to visually inspect the distribution of gene expression variance among arrays within and between experimental conditions. Following removal of Agilent control features, stringent quality filtering involved removal of saturated and non-uniform features, population outliers and features that were not significantly positive with respect to the local background intensity. This same initial screening procedure was applied for both experiments; however subsequent statistical analyses of gene expression profiles differed and were adjusted for each experiment.

### 2.11.1 Profiling of tissue-specific gene expression signatures

Considering the low number of replicates in each group, one-way ANOVA unequal variance (Welch) ( $P < 0.05$ ) was applied to preselect features showing potential differences in gene expression between tissues. Unsupervised network analysis was conducted on identified features using Biolayout Express 3D (Theocharidis *et al.* 2009), using a Pearson coefficient of correlation as a similarity measure and threshold over 0.94. The network graph was clustered into distinct patterns of gene expression using a Markov clustering algorithm (MCL) with inflation value set to 2.0 and smallest cluster allowed being 10. Functional gene set analyses were performed on the entire list of quality filtered entities based on KEGG Orthology (KO) identifiers. During the analyses, expression profiles were collapsed into 3,222 unique KOs using the median method. Tests were run to identify significantly up- and down- regulated pathways for each tissue and their pairwise combinations against all other samples using Generally Applicable Gene-set Enrichment (GAGE) analyses (Luo *et al.* 2009),

implemented as R/Bioconductor package (Gentleman *et al.* 2004), which is robust to small datasets with different sample sizes. A default false discovery rate (FDR)  $q$ -value of 0.1 was used as a cut-off. Pathways were subsequently grouped into KEGG functional categories and the difference between the counts of up- and down-regulated pathways in each category hierarchically clustered and displayed as a heatmap.

### **2.11.2 Inference of transcriptomic changes between infected and uninfected gills**

Differentially expressed transcripts between *T. thynnus* infected and uninfected gills with *D. katsuwonocola* were determined using second-level significance testing approach, higher criticism (HC) (Donoho & Jin 2004), in combination with feature filtering based on variable importance of selection (VIP) for partial least squares (PLS) multivariate modelling (Wold *et al.* 2001), as implemented in BioMark package for R software (Wehrens & Franceschi 2012a). HC attempts to solve multiple testing problem by shifting focus from single test results to entire collection of tests and detect small fraction of non-null hypotheses among many null hypothesis (Donoho & Jin 2008). Data specific HC threshold corresponds to maximum deviation of HC statistic, described as “Z-score of the  $P$ -value”, indicating deviation from expected uniformity. VIP is a method of feature selection for partial least squares (PLS) multivariate modelling procedure measuring the contribution of each variable according to the variance explained by each PLS component (Mehmood *et al.* 2012). Since this feature selection step does not produce  $P$ -values, they were obtained by permuting class labels generating the VIP statistics distribution under the null hypotheses (Wehrens & Franceschi 2012b), as implemented in BioMark package. The HCalpha parameter for higher criticism thresholding, the proportion of data to consider as possible biomarkers, was set to 0.25, although the results are not sensitive to the exact setting of this parameter (Donoho & Jin 2008). Functional pathway analyses were performed using GAGE, as previously described. Data were filtered to contain transcripts with best  $P$ -value as unique KO representatives. Pathview package (Luo & Brouwer 2013) was used to visualize expressional regulation of individual genes on KEGG maps for selected pathways.

The two arrays where *D. katsuwonocola* Cy3 labelled RNA was competitively

hybridized with Cy5 labelled *T. thynnus* reference were inspected separately from tuna specific hybridizations. Background subtracted signals were quality filtered in both channels and those positive and significant in respect to the background retained. The distributions of non-normalized green (Cy3) and red (Cy5) signals from these nonspecific hybridizations were compared to those obtained from tuna specific hybridizations, as well as the inferred Cy3/Cy5 ratio. Results were visualized using a boxplot.

## 2.12 Quantitative reverse transcription PCR (RT-qPCR)

In total, 17 transcripts across two experiments showing different expression profiles and spanning a wide range of fold change (FC) values were chosen for RT-qPCR validation of microarray results. Four genes were tested to serve as internal controls (reference genes): two from the literature, elongation factor-1 $\alpha$  (Elf-1 $\alpha$ ) (Morais *et al.* 2011), beta-actin (Actb) (Lepen Pleić *et al.* 2013), and two transcripts from the microarray each showing a stable expression profile per microarray experiment, annotated as FtsJ methyltransferase domain containing 2 (Ftsjd2) and mitochondrial ribosomal protein S18B (Mrps18b). Primer3 (Untergasser *et al.* 2012) software was used to design primers for the selected sequences with at least one in the pair overlapping the target hybridization area of the microarray 60-mer probe. Thermodynamic properties of possible secondary structures for the selected primer pairs were investigated using Oligo Analyzer 1.5 (Gene Link, USA). Data describing selected transcripts and primer sequences are shown in Table 2.2.

Complementary DNA was synthesised from 2  $\mu$ g of the same total RNA extractions used for the microarray experiment employing High Capacity cDNA Reverse Transcription Kit (Applied Biosystems, UK). The synthesis was primed with 1.5  $\mu$ l of random hexamer primers supplied with the kit and 0.5  $\mu$ l of anchored-oligo (dT)<sub>20</sub> (Eurofins, Germany) per 20  $\mu$ l reaction (including 2  $\mu$ l of 10  $\times$  RT Buffer, 0.8  $\mu$ l of 100 mM dNTP Mix, 1  $\mu$ l of MultiScribe reverse transcriptase and nuclease-free water). Reactions were loaded into the thermal cycler and incubated at 25  $^{\circ}$ C for 10 min, 37  $^{\circ}$ C for 2 hr and 85  $^{\circ}$ C for 5 min. DNase treatment was not performed prior to cDNA synthesis as it may result in RNA degradation (Pfaffl 2004). Instead, minus RT (RT-) controls (reverse transcriptase replaced with water) were created to control for the presence of genomic DNA in the extractions.

Real-time PCR assays were performed on a Mastercycler ep realplex2 (Eppendorf, Germany) using Luminaris Colour HiGreen qPCR Master Mix (Thermo Scientific, UK), in duplicate with 25 × cDNA template dilutions, 0.3 μM of each primer, 10 μl of 2 × Master Mix and water to reach the final volume of 20 μl. Thermal cycling was performed according to the following profile: 50°C for 2 minutes (Uracil-DNA Glycosylase pre-treatment), 95°C for 10 minutes, followed by 40 cycles of denaturation at 95°C for 15 seconds, annealing at 60°C for 30 seconds and elongation at 72°C for 30 seconds. After amplification a melting curve analysis was performed from 55°C to 95°C at 0.5°C increments for 15 seconds each to verify single product amplification. The correct size of PCR products was also verified by agarose gel electrophoresis (2.4 % gel). Six point standard curves of a 4 × dilution series of a pool of all starting cDNAs were run with every assay to determine primer-specific efficiencies. BestKeeper (Pfaffl *et al.* 2004) was used for the inspection of the Cq (cycle quantification) stability of reference genes. Relative quantification profiles normalized by geometric averaging of the most stable reference genes (Vandesompele *et al.* 2002) were inferred through  $E^{-\Delta\Delta Cq}$  method (Pfaffl 2001).

To compare the fit between qPCR and microarray fold changes (FCs), the concordance correlation coefficient (CCC) was calculated based on tissue-specific expression profiles, as well as other regression metrics previously described by Miron *et al.* (2006). In order to inspect statistical significance of observed profiles, a combined data set was formed using both qPCR and microarray data for each transcript coded by their respective percentile ranks. Nonparametric Kruskal-Wallis test was performed as implemented in R software.

Ratios or fold changes exhibited for infected vs. uninfected gills were analysed using ratio ttest for unequal variances (Djira *et al.* 2012) for qPCR and microarray data separately and displayed using a point-range plot as implemented in ggplot2 package for R software (Wickham 2009).

**Table 2.2** Characteristics of primers used in the RT-qPCR validation of microarray experiments. Transcripts were chosen from first, second, or both microarray experiments, noted in column Exp.

PrimerID	Primer Sequence	Probe ID*	Description	Tm °C	GC %	Prod.size	Status	Exp.
angptl2_2F	GCAGTTACAAGCAAATGACGATG	scf2722_2	Angiopoietin-like 2	61.9	43.5	119	Target gene	2
angptl2_2R	GCAAGCCTGCAAATGTTCTT			62.6	50.0			
aqp3b_1F	GCCTCTTGTCGTTTGTATCTCG	scf0247_1	Aquaporin 3b	61.2	50.0	103	Target gene	1,2
aqp3b_1R	AAAAGCCTTTCCCCTCAACC			61.7	50.0			
atp2a2a_1F	TCCATGTCCCTCCACTTCCT	scf5010_1	ATPase, Ca++ transporting, cardiac muscle, slow twitch 2a	59.9	55.0	163	Target gene	1
atp2a2a_1R	ACCGAATAATTCCTGGCCATAAAC	scf5010_2		59.4	41.7			
blvr1b_1F	AAGTGCCAAACCTGTACTGCTG	deg075252_2	Biliverdin reductase B (flavin reductase (NADPH))	61.6	50.0	114	Target gene	1
blvr1b_1R	CGATGATGGGGAACAAATCC			62.4	50.0			
casp3b_2F	CAGGGCTCCACTTTAACTGTTCT	scf6175_2	Caspase 3, apoptosis-related cysteine protease b	60.5	47.8	179	Target gene	2
casp3b_2R	ACAGAAAGTGGTTAAGGTTTCCC			58.8	43.5			
f5_2F	AGACGACCAGATCACAGCAATCA	scf5580_2	Coagulation factor V	61.9	47.8	131	Target gene	1
f5_2R	GCTGAAAGTCCACCTGAATCCAAC			62.1	50.0			
col10a1_1F	CAACCAAACAGACAGGCAGTTC	deg083376_2	Collagen, type X, alpha 1	62.0	50.0	129	Target gene	2
col10a1_1R	TTCCCCATCCCTGATCTCC			62.2	57.9			
C4like_2F	TGAAACAGACTGCCACACACA	deg132539_1	Complement C4-like	60.3	47.6	122	Target gene	1,2
C4like_2R	AGATCACACCCATGCTGACA			59.0	50.0			
cybb_1F	CGCAACAGCAGCCTTCTTAC	deg093727_1	Cytochrome b-245, beta polypeptide (chronic granulomatous disease)	61.1	55.0	103	Target gene	2
cybb_1R	CGATGGTAGGGTTCGTCTCA	deg093727_2		61.1	55.0			
exosc2_1F	TGGAGGAGATTGTGATGCTGA	scf6497_2	Exosome component 2	61.8	47.6	105	Target gene	1,2
exosc2_1R	AGCTGCTGGTGTGATCTTGG			61.4	55.0			
jak3_1F	CCGTTACAGCAATAGAGCAA	scf1709_1	Janus kinase 3 (a protein tyrosine kinase, leukocyte)	61.3	47.6	100	Target gene	2
jak3_1R	CTCCAGAGTGGGAACTTTATGG	scf1709_2		61.2	47.8			

PrimerID	Primer Sequence	Probe ID*	Description	Tm °C	GC %	Prod.size	Status	Exp.																																																																																																																										
masp2_3F	CCTTCTGTGGACCCAAGCCA	deg098955_1	Mannan-binding lectin serine peptidase 2	62.1	60.0	53	Target gene	2																																																																																																																										
masp2_3R	CACCTGGTAACCTCCTGTGTCA	deg098955_2		61.6	54.6				med6_1F	TGTTGTGGCGACTTCAGAGG	scf6480_1	Mediator complex subunit 6	62.4	55.0	117	Target gene	1	med6_1R	ATAGGGGTGCTACGGTCAGG	scf6480_2	61.3	60.0	pes_1F	ACCTGCTTAAAGACATCCGCTT	deg134977_2	Pescadillo	60.3	45.5	145	Target gene	1	pes_1R	GCTGGCTTGTTCTCCCTCA		59.6	57.9	phb2_3F	AGCACATATCAGCCATATCTCCAC	scf5986_2	Prohibitin 2	60.3	45.8	67	Target gene	1	phb2_3R	TCCACACACATAACCAAACATCTG		59.5	41.7	somtl_1F	GGGAGTCAAACAGAGAGCAATC	TTncbi48_1	Somatolactin	59.0	50.0	177	Target gene	1	somtl_1R	ACTTCTTTCACGAGCACTCTACA	TTncbi48_2	59.7	43.5	tpm4_1F	AGCTTCTGTCTCTCTGTTCTTGGA	deg071918_1	Tropomyosin 4	61.2	45.8	174	Target gene	2	tpm4_1R	ACGGACTATGCACAGTAACAACC	deg071918_2	60.9	47.8	TactinF1	CAGGGAGTGATGGTGGGTATGG		Beta actin	69.5	0.0	261	Reference	1,2	TactinR1	GAAGGTCTCGAACATGATCTGGGTC		69.8	0.0	Tt-qEF1-F	CCCCTGGACACAGAGACTTC		Elongation factor-1 $\alpha$	60.0	0.0	119	Reference	1,2	Tt-qEF1-R	GCCGTTCTTGAGATACCAG		60.0	0.0	ftsjd2_1F	ACTGCTCCTCCTGTCATCGC	scf0469_1	FtsJ methyltransferase domain containing 2	62.0	60.0	102	Reference	1,2	ftsjd2_1R	GGGTCCAGCTACAGATTTGCAG	scf0469_2	61.3	54.6	mrps18b_2F	CGAAGTGGCTAAAGTCAAGAAGA	deg073036_2	Mitochondrial ribosomal protein S18B	58.7	43.5	92	Reference	2	mrps18b_2R
med6_1F	TGTTGTGGCGACTTCAGAGG	scf6480_1	Mediator complex subunit 6	62.4	55.0	117	Target gene	1																																																																																																																										
med6_1R	ATAGGGGTGCTACGGTCAGG	scf6480_2		61.3	60.0				pes_1F	ACCTGCTTAAAGACATCCGCTT	deg134977_2	Pescadillo	60.3	45.5	145	Target gene	1	pes_1R	GCTGGCTTGTTCTCCCTCA		59.6	57.9	phb2_3F	AGCACATATCAGCCATATCTCCAC	scf5986_2	Prohibitin 2	60.3	45.8	67	Target gene	1	phb2_3R	TCCACACACATAACCAAACATCTG		59.5	41.7	somtl_1F	GGGAGTCAAACAGAGAGCAATC	TTncbi48_1	Somatolactin	59.0	50.0	177	Target gene	1	somtl_1R	ACTTCTTTCACGAGCACTCTACA	TTncbi48_2	59.7	43.5	tpm4_1F	AGCTTCTGTCTCTCTGTTCTTGGA	deg071918_1	Tropomyosin 4	61.2	45.8	174	Target gene	2	tpm4_1R	ACGGACTATGCACAGTAACAACC	deg071918_2	60.9	47.8	TactinF1	CAGGGAGTGATGGTGGGTATGG		Beta actin	69.5	0.0	261	Reference	1,2	TactinR1	GAAGGTCTCGAACATGATCTGGGTC		69.8	0.0	Tt-qEF1-F	CCCCTGGACACAGAGACTTC		Elongation factor-1 $\alpha$	60.0	0.0	119	Reference	1,2	Tt-qEF1-R	GCCGTTCTTGAGATACCAG		60.0	0.0	ftsjd2_1F	ACTGCTCCTCCTGTCATCGC	scf0469_1	FtsJ methyltransferase domain containing 2	62.0	60.0	102	Reference	1,2	ftsjd2_1R	GGGTCCAGCTACAGATTTGCAG	scf0469_2	61.3	54.6	mrps18b_2F	CGAAGTGGCTAAAGTCAAGAAGA	deg073036_2	Mitochondrial ribosomal protein S18B	58.7	43.5	92	Reference	2	mrps18b_2R	TGACATCACCATCACAGCATG	Pdeg073036_1	58.6	47.6										
pes_1F	ACCTGCTTAAAGACATCCGCTT	deg134977_2	Pescadillo	60.3	45.5	145	Target gene	1																																																																																																																										
pes_1R	GCTGGCTTGTTCTCCCTCA			59.6	57.9				phb2_3F	AGCACATATCAGCCATATCTCCAC	scf5986_2	Prohibitin 2	60.3	45.8	67	Target gene	1	phb2_3R	TCCACACACATAACCAAACATCTG		59.5	41.7	somtl_1F	GGGAGTCAAACAGAGAGCAATC	TTncbi48_1	Somatolactin	59.0	50.0	177	Target gene	1	somtl_1R	ACTTCTTTCACGAGCACTCTACA	TTncbi48_2	59.7	43.5	tpm4_1F	AGCTTCTGTCTCTCTGTTCTTGGA	deg071918_1	Tropomyosin 4	61.2	45.8	174	Target gene	2	tpm4_1R	ACGGACTATGCACAGTAACAACC	deg071918_2	60.9	47.8	TactinF1	CAGGGAGTGATGGTGGGTATGG		Beta actin	69.5	0.0	261	Reference	1,2	TactinR1	GAAGGTCTCGAACATGATCTGGGTC		69.8	0.0	Tt-qEF1-F	CCCCTGGACACAGAGACTTC		Elongation factor-1 $\alpha$	60.0	0.0	119	Reference	1,2	Tt-qEF1-R	GCCGTTCTTGAGATACCAG		60.0	0.0	ftsjd2_1F	ACTGCTCCTCCTGTCATCGC	scf0469_1	FtsJ methyltransferase domain containing 2	62.0	60.0	102	Reference	1,2	ftsjd2_1R	GGGTCCAGCTACAGATTTGCAG	scf0469_2	61.3	54.6	mrps18b_2F	CGAAGTGGCTAAAGTCAAGAAGA	deg073036_2	Mitochondrial ribosomal protein S18B	58.7	43.5	92	Reference	2	mrps18b_2R	TGACATCACCATCACAGCATG	Pdeg073036_1	58.6	47.6																								
phb2_3F	AGCACATATCAGCCATATCTCCAC	scf5986_2	Prohibitin 2	60.3	45.8	67	Target gene	1																																																																																																																										
phb2_3R	TCCACACACATAACCAAACATCTG			59.5	41.7				somtl_1F	GGGAGTCAAACAGAGAGCAATC	TTncbi48_1	Somatolactin	59.0	50.0	177	Target gene	1	somtl_1R	ACTTCTTTCACGAGCACTCTACA	TTncbi48_2	59.7	43.5	tpm4_1F	AGCTTCTGTCTCTCTGTTCTTGGA	deg071918_1	Tropomyosin 4	61.2	45.8	174	Target gene	2	tpm4_1R	ACGGACTATGCACAGTAACAACC	deg071918_2	60.9	47.8	TactinF1	CAGGGAGTGATGGTGGGTATGG		Beta actin	69.5	0.0	261	Reference	1,2	TactinR1	GAAGGTCTCGAACATGATCTGGGTC		69.8	0.0	Tt-qEF1-F	CCCCTGGACACAGAGACTTC		Elongation factor-1 $\alpha$	60.0	0.0	119	Reference	1,2	Tt-qEF1-R	GCCGTTCTTGAGATACCAG		60.0	0.0	ftsjd2_1F	ACTGCTCCTCCTGTCATCGC	scf0469_1	FtsJ methyltransferase domain containing 2	62.0	60.0	102	Reference	1,2	ftsjd2_1R	GGGTCCAGCTACAGATTTGCAG	scf0469_2	61.3	54.6	mrps18b_2F	CGAAGTGGCTAAAGTCAAGAAGA	deg073036_2	Mitochondrial ribosomal protein S18B	58.7	43.5	92	Reference	2	mrps18b_2R	TGACATCACCATCACAGCATG	Pdeg073036_1	58.6	47.6																																						
somtl_1F	GGGAGTCAAACAGAGAGCAATC	TTncbi48_1	Somatolactin	59.0	50.0	177	Target gene	1																																																																																																																										
somtl_1R	ACTTCTTTCACGAGCACTCTACA	TTncbi48_2		59.7	43.5				tpm4_1F	AGCTTCTGTCTCTCTGTTCTTGGA	deg071918_1	Tropomyosin 4	61.2	45.8	174	Target gene	2	tpm4_1R	ACGGACTATGCACAGTAACAACC	deg071918_2	60.9	47.8	TactinF1	CAGGGAGTGATGGTGGGTATGG		Beta actin	69.5	0.0	261	Reference	1,2	TactinR1	GAAGGTCTCGAACATGATCTGGGTC		69.8	0.0	Tt-qEF1-F	CCCCTGGACACAGAGACTTC		Elongation factor-1 $\alpha$	60.0	0.0	119	Reference	1,2	Tt-qEF1-R	GCCGTTCTTGAGATACCAG		60.0	0.0	ftsjd2_1F	ACTGCTCCTCCTGTCATCGC	scf0469_1	FtsJ methyltransferase domain containing 2	62.0	60.0	102	Reference	1,2	ftsjd2_1R	GGGTCCAGCTACAGATTTGCAG	scf0469_2	61.3	54.6	mrps18b_2F	CGAAGTGGCTAAAGTCAAGAAGA	deg073036_2	Mitochondrial ribosomal protein S18B	58.7	43.5	92	Reference	2	mrps18b_2R	TGACATCACCATCACAGCATG	Pdeg073036_1	58.6	47.6																																																				
tpm4_1F	AGCTTCTGTCTCTCTGTTCTTGGA	deg071918_1	Tropomyosin 4	61.2	45.8	174	Target gene	2																																																																																																																										
tpm4_1R	ACGGACTATGCACAGTAACAACC	deg071918_2		60.9	47.8				TactinF1	CAGGGAGTGATGGTGGGTATGG		Beta actin	69.5	0.0	261	Reference	1,2	TactinR1	GAAGGTCTCGAACATGATCTGGGTC		69.8	0.0	Tt-qEF1-F	CCCCTGGACACAGAGACTTC		Elongation factor-1 $\alpha$	60.0	0.0	119	Reference	1,2	Tt-qEF1-R	GCCGTTCTTGAGATACCAG		60.0	0.0	ftsjd2_1F	ACTGCTCCTCCTGTCATCGC	scf0469_1	FtsJ methyltransferase domain containing 2	62.0	60.0	102	Reference	1,2	ftsjd2_1R	GGGTCCAGCTACAGATTTGCAG	scf0469_2	61.3	54.6	mrps18b_2F	CGAAGTGGCTAAAGTCAAGAAGA	deg073036_2	Mitochondrial ribosomal protein S18B	58.7	43.5	92	Reference	2	mrps18b_2R	TGACATCACCATCACAGCATG	Pdeg073036_1	58.6	47.6																																																																		
TactinF1	CAGGGAGTGATGGTGGGTATGG		Beta actin	69.5	0.0	261	Reference	1,2																																																																																																																										
TactinR1	GAAGGTCTCGAACATGATCTGGGTC			69.8	0.0				Tt-qEF1-F	CCCCTGGACACAGAGACTTC		Elongation factor-1 $\alpha$	60.0	0.0	119	Reference	1,2	Tt-qEF1-R	GCCGTTCTTGAGATACCAG		60.0	0.0	ftsjd2_1F	ACTGCTCCTCCTGTCATCGC	scf0469_1	FtsJ methyltransferase domain containing 2	62.0	60.0	102	Reference	1,2	ftsjd2_1R	GGGTCCAGCTACAGATTTGCAG	scf0469_2	61.3	54.6	mrps18b_2F	CGAAGTGGCTAAAGTCAAGAAGA	deg073036_2	Mitochondrial ribosomal protein S18B	58.7	43.5	92	Reference	2	mrps18b_2R	TGACATCACCATCACAGCATG	Pdeg073036_1	58.6	47.6																																																																																
Tt-qEF1-F	CCCCTGGACACAGAGACTTC		Elongation factor-1 $\alpha$	60.0	0.0	119	Reference	1,2																																																																																																																										
Tt-qEF1-R	GCCGTTCTTGAGATACCAG			60.0	0.0				ftsjd2_1F	ACTGCTCCTCCTGTCATCGC	scf0469_1	FtsJ methyltransferase domain containing 2	62.0	60.0	102	Reference	1,2	ftsjd2_1R	GGGTCCAGCTACAGATTTGCAG	scf0469_2	61.3	54.6	mrps18b_2F	CGAAGTGGCTAAAGTCAAGAAGA	deg073036_2	Mitochondrial ribosomal protein S18B	58.7	43.5	92	Reference	2	mrps18b_2R	TGACATCACCATCACAGCATG	Pdeg073036_1	58.6	47.6																																																																																														
ftsjd2_1F	ACTGCTCCTCCTGTCATCGC	scf0469_1	FtsJ methyltransferase domain containing 2	62.0	60.0	102	Reference	1,2																																																																																																																										
ftsjd2_1R	GGGTCCAGCTACAGATTTGCAG	scf0469_2		61.3	54.6				mrps18b_2F	CGAAGTGGCTAAAGTCAAGAAGA	deg073036_2	Mitochondrial ribosomal protein S18B	58.7	43.5	92	Reference	2	mrps18b_2R	TGACATCACCATCACAGCATG	Pdeg073036_1	58.6	47.6																																																																																																												
mrps18b_2F	CGAAGTGGCTAAAGTCAAGAAGA	deg073036_2	Mitochondrial ribosomal protein S18B	58.7	43.5	92	Reference	2																																																																																																																										
mrps18b_2R	TGACATCACCATCACAGCATG	Pdeg073036_1		58.6	47.6																																																																																																																													

\*For primers that overlap both microarray probes for the target transcript, averaged microarray profiles were used for all comparative analyses

### **2.13 Transmission electron microscopy**

Didymozoid cysts were measured and ruptured with fine needles under the stereomicroscope, and individuals were identified following Ishii (1935) and Yamaguti (1970). After overnight fixation in phosphate-buffered (0,1 M PBS) 4 % paraformaldehyde at 4 °C, didymozoid cysts and non-infected gill tissues were post-fixed in 1 % osmium tetroxide for 1 h, dehydrated in an ascending series of acetone and embedded in Durcopan resin. Semi-thin sections were stained with 1 % toluidine and examined under an Olympus BX 40 light microscope. Ultra-thin sections (0.05 µm) were made from the chosen area of interest and stained with uranyl acetate and lead citrate. Material was examined under LEO 912 AB transmission electron microscope.

### **2.14 Data access**

The raw sequence data have been submitted to the EBI Sequence Read Archive (SRA) study PRJEB7253. Microarray design is accessed under A-MTAB-553 and raw and normalized data for the first experiment are submitted under the accession number E-MTAB-3412 in the EBI ArrayExpress database ([www.ebi.ac.uk/arrayexpress](http://www.ebi.ac.uk/arrayexpress)). The data for the second experiment will also be submitted pending the preparation of the manuscript for publication.

### 3 Results

In this section, results pertaining to the sequencing of *T. thynnus* normalized library, read assembly and annotation, genome mapping, EST-SSRs mining and qPCR analyses will be presented and discussed simultaneously as they describe different aspects and utilities of the constructed library or serve to validate otherwise generated data. The discussion section will be solely dedicated to functional and biological interpretation of tissue-specific gene expression profiles and transcriptomic and ultrastructural differences induced by *D. katsuwonocola* presence on *T. thynnus* gills.

#### 3.1 Pyrosequencing and transcriptome assembly

A total of 976,904 raw sequence reads were generated, with a mean size of 347 bases (b), which is consistent with the sequencing technology used (Gilles *et al.* 2011). The reads that passed quality control filtering, were trimmed for sequencing primers and adaptors and used for the assembly process. WGS-assembler (Celera) generated a *de-novo* transcriptome assembly of 70,108 contigs and 52,452 singletons. Contigs and singleton were scaffolded using Mosaik based on the 10,163 available ESTs. Based on the high quality reads of over 500 b and of higher complexity, 33,105 unique transcripts were assembled, with a mean length of 893 b and an N50 of 870. Of these, 22.0% of the transcripts had a length more than 1,000 b with 22.8% having a full-length coding region. To evaluate the quality of the assembled transcripts, all the usable sequencing reads were realigned to the transcripts. Distribution of obtained reads and assembled transcripts are visualized in Figure 3.1 and related descriptive statistics are presented in Table 3.1.

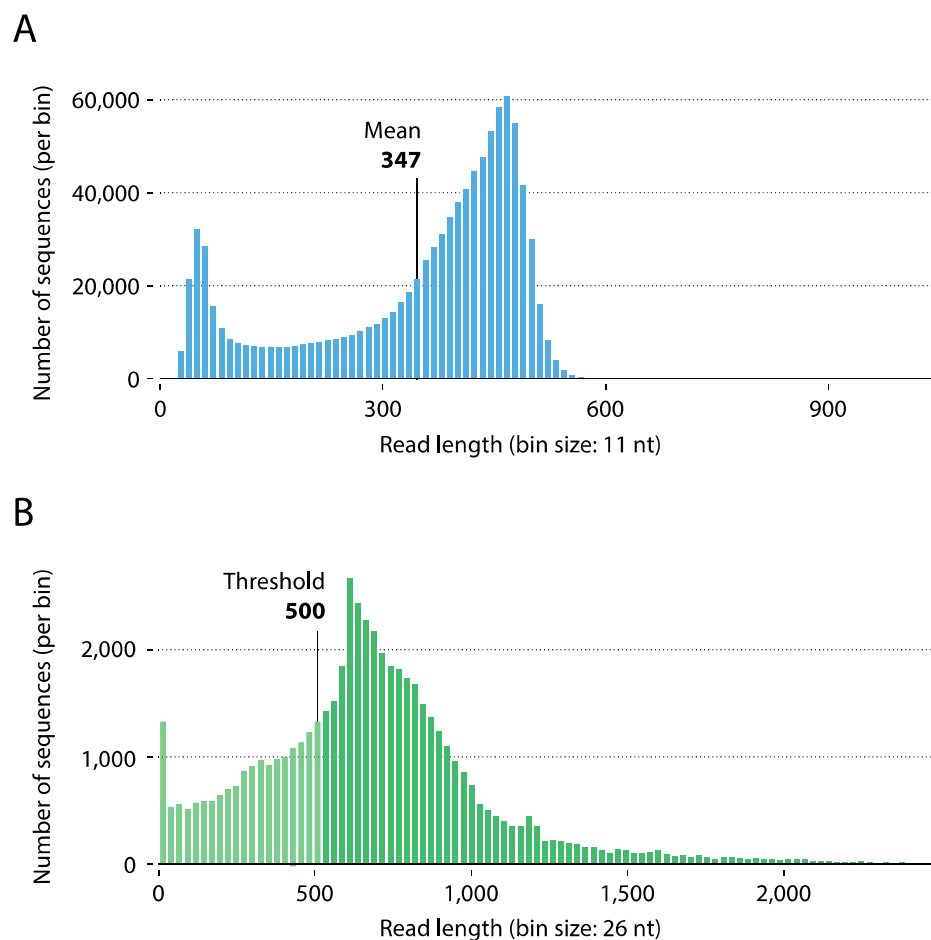


**Figure 3.1** Overview of the *T. thynnus* transcriptome sequencing and assembly. (A) Size distribution of 454 sequencing reads after removal of adaptor (mean 347 b, standard deviation 144 b). (B) Size distribution of assembled transcripts (no singletons). Cut-off at 500 b.

**Table 3.1** Statistics of the obtained reads and assembled sequences.

<b>Raw data</b>	
Number of reads	976,904
Mean read size	347
Total size of reads	338,522,590
<b>After assembly (no singletons)</b>	
Number of transcripts	70,108
Mean size	593
Total size of transcripts	41,564,882
<b>After assembly (singletons only)</b>	
Number of transcripts	52,452
Mean size	431
Total size of transcripts	22,601,482
<b>After filtering (&gt; 500 b)</b>	
Number of transcripts	33,105
N50	870
Total size of transcripts	29,512,631
Shortest transcript	500
Longest transcript	4,955
Mean size	893
Median size	799
Mean GC%	43.5%
N%	0.2%

### 3.2 Functional inference by searching against public databases

The assembled transcripts were annotated using BLASTp and BLASTn searches against the RefSeq Proteins and *T. thynnus* EST database respectively. The results indicated that out of 33,105 transcripts, 11,065 (33.4%) showed significant similarity to known proteins or gene transcripts in the RefSeq Proteins database. To evaluate the *T. thynnus* coverage of the assembled transcripts, the 10,163 EST available for *T. thynnus* were aligned to the 33,105 transcript sequences generated in this study and vice versa. In total, 4,939 (48.6%) of all *T. thynnus* ESTs aligned to at least one transcript, whereas 4,394 (13.3%) of the new transcripts had at least one corresponding *T. thynnus* EST. This demonstrates that the strategy employed captured some of the existing data and added new information to *T. thynnus* EST

database, by applying a different sequencing method across a larger span of functionally different tissues, compared to Chini *et al.* (2008).

Gene Ontology (GO) functional annotation was assigned to the assembled *T. thynnus* transcripts/genes on the basis of RefSeq Proteins annotation. Out of 11,065 transcripts that had similarity to known gene products, 8,384 (25.3% of total library) were assigned a GO annotation. Figure 3.2 shows that derived GO descriptions for *T. thynnus* transcripts cover a diverse set of molecular functions, cellular components and biological processes. Similarly, 8,334 (25.2%) out of the total 33,105 transcripts were assigned 4040 unique KEGG orthology (KO) identifiers and mapped to 262 different biochemical pathways in the KEGG BRITE functional hierarchy, excluding Human diseases. Pathways were categorized according to their functional groups and total transcript abundance with unique KO identifiers found in each group is outlined in Figure 3.3. The top five best represented categories were signal transduction, immune, endocrine, nervous system and cellular communication. Figure 3.3 also points to a substantial level of functional redundancy, as evident from lower number of unique KOs found in each group. This is an inherent feature of the KEGG classification as many pathways share the same genes, but some KOs are also assigned to different transcripts with similar functional motifs.

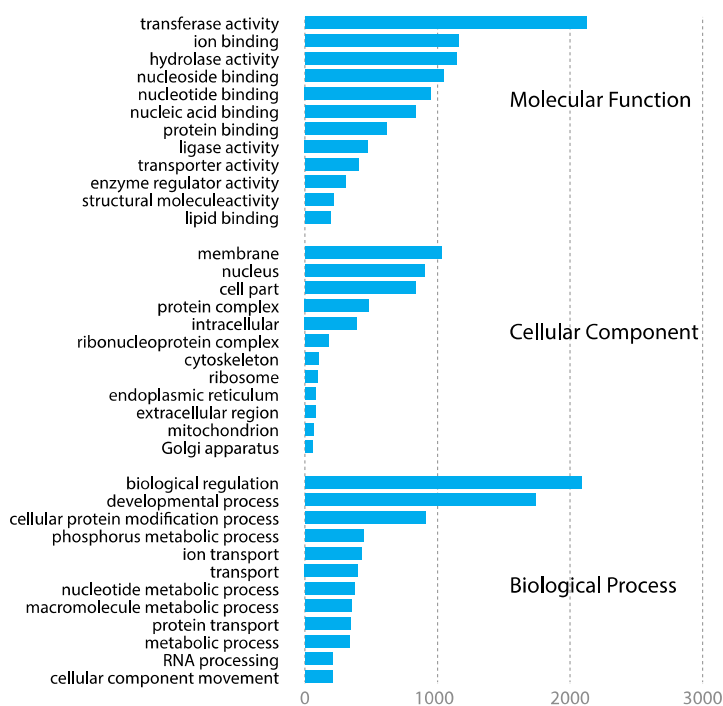


**Figure 3.2** Multilevel Gene Ontology categorization of the annotated *T. thynnus* transcripts. GO annotations were first converted to GO-Slim annotations and the multilevel chart shows the top twelve of each category to reduce the complexity of the chart.

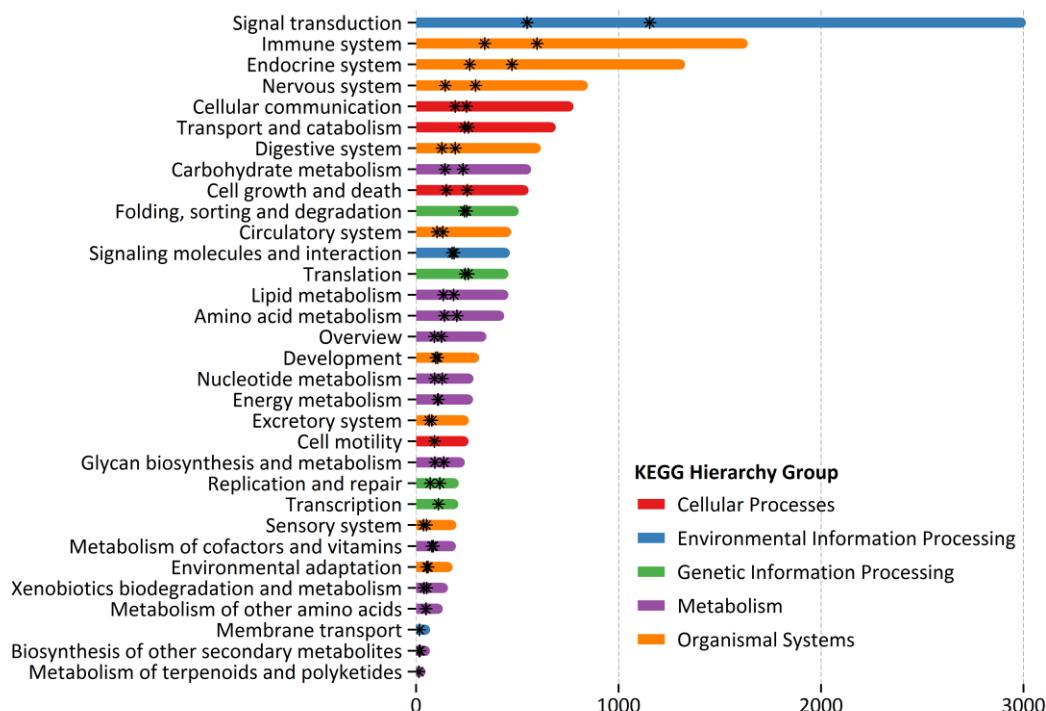


**Figure 3.3** KEGG functional annotation of *T. thynnus* transcripts based on BRITE hierarchy groups excluding Human diseases. Entire bars represent total count of transcripts per group and stars unique KOs per functional group and per pathway within each category in respective order from left to right.

### 3.3 Genome mapping

Mapping was performed to the two perciform genomic sequences: *T. orientalis* and *O. niloticus*. The genome assembly of *O. niloticus* is in a more advanced state, contigs being organized into linkage groups or chromosomes, while the *T. orientalis* genome is in its initial assembly release with sequences organized only into contigs. The results of the mapping to the two genomes were visualized using a hive plot where each genome is placed along a linear axis and hits are drawn as curved links connecting *T. thynnus* transcripts to respective target regions in each genome (Figure 3.4). As expected, more targets found a hit with the congeneric *T. orientalis* genome (28,678 or 86.6%) than the more distantly related *O. niloticus* genome (23,276 or 70.3%). *T. thynnus* and *T. orientalis* are considered to be very closely related and have been separated as sub-species until recently when molecular data, specifically mitochondrial DNA, corroborated their separate species status (Block & Stevens 2001; Chow *et al.* 2006). Our data also demonstrate their close connection and sequence

similarity which makes the *T. orientalis* genome an important resource for *T. thynnus* studies as well, with possible applications for exon-intron gene modelling or reference mapping in future sequencing studies. There was, however, a proportion of *T. thynnus* targets that did not find a match to *T. orientalis* genome, consisting mostly of non-annotated singletons showing an increased proportion of repetitive nucleotide stretches (data not shown). These sequences could be difficult to match, or may represent *T. thynnus*-specific diversification, or both.

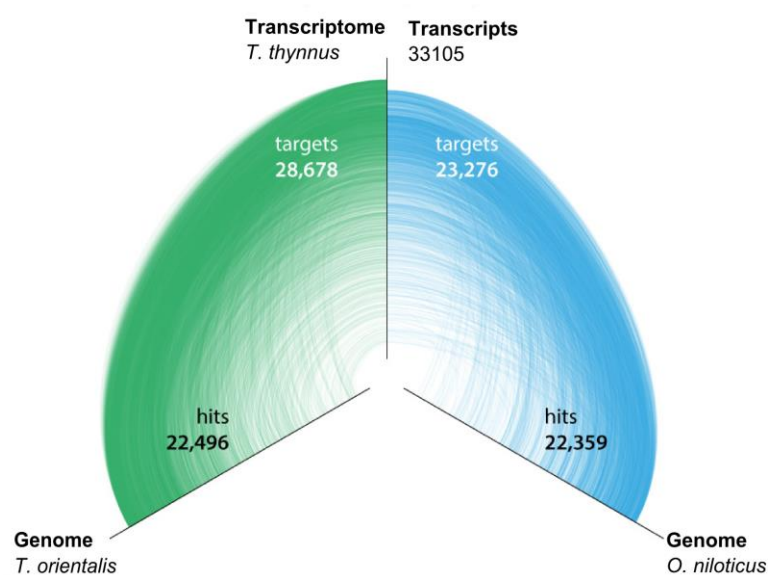


**Figure 3.4** Mapping of *T. thynnus* transcripts to *T. orientalis* and *O. niloticus* genomes. Hive plot of the BLASTn results. The number of transcripts (target) with a similar region (hit) is reported for each genome.

### 3.4 *In silico* EST-SSRs mining

Microsatellites or SSRs (also known as variable tandem number repeats, VNTRs, or short tandem repeats, STRs) are tandem repeats of 1 – 6 nucleotides found in nuclear genomes of many taxa (Selkoe & Toonen 2006). They are highly polymorphic, codominant markers and display inter-individual variability in length, or number of repeats, usually between 5 and 40. Due to this high allelic diversity and ease of amplification, they are regularly used for population and conservation genetics studies, genetic mapping, parentage assignment, marker-assisted selection with many application in the field of fisheries and aquaculture (Chistiakov *et al.* 2006). Although SSRs are considered selectively neutral, they are often functionally relevant,

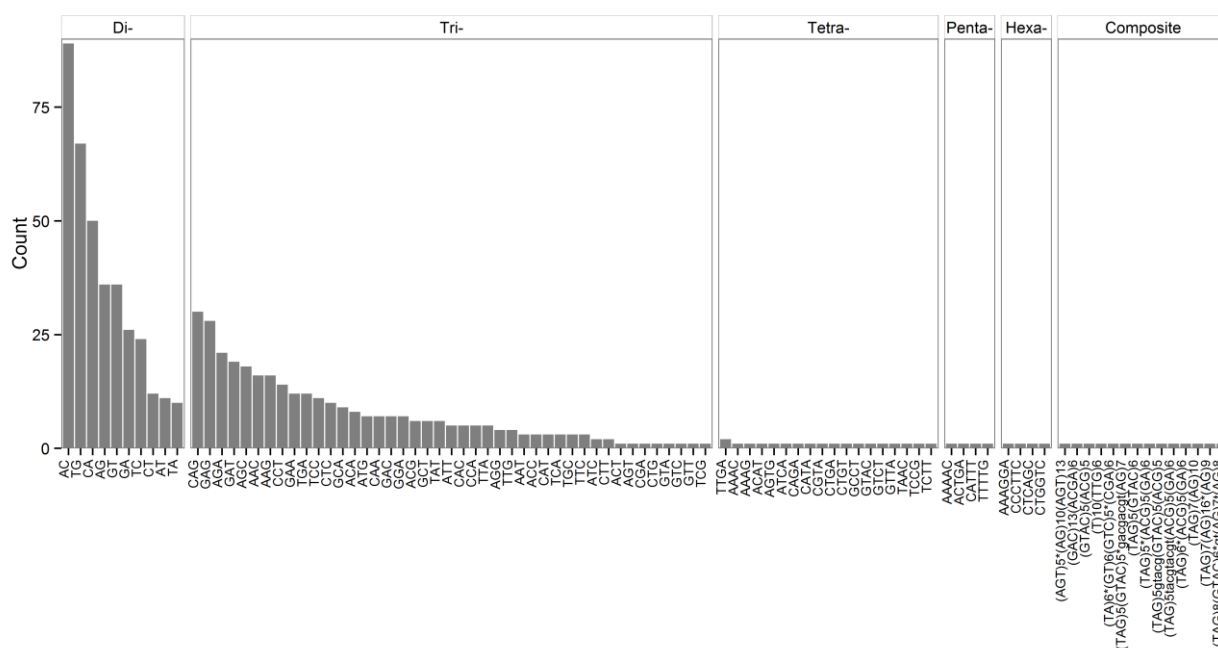
which particularly pertains to those located near transcribed sequences or in their coding regions. Availability of EST sequences from many organisms allows easy detection and development of such markers, with significant cross-species transferability as they are found in evolutionary more conserved genomic regions (Chistiakov *et al.* 2006; Selkoe & Toonen 2006). A marker closely linked to coding regions, such as EST-SSR, can be used to detect footprints of adaptive selection and associate it with potentially functionally related candidate genes (Vasemägi *et al.* 2005; Quéré *et al.* 2010).

In this study, *T. thynnus* assembled and annotated transcripts were searched for the presence of EST-SSRs. Mononucleotides mostly included poly A interspersed repeats and were excluded from the analyses. The results are summarized in Table 3.2. In total, 730 di-, tri-, tetra-, penta-, hexa- and composite repeats were detected, accounting for 6 % of the inspected sequences, with some redundancy, as several repeats were located on same sequences. This is evident in disparity between the counts of SSRs and targets, which are further reduced to unique proteins (Table 3.2). Di- and tri- nucleotide repeats accounted for almost all of the SSRs found. Here, the most commonly observed was AC motif (Figure 3.5), as generally found in vertebrates (Tóth *et al.* 2000) and other fish (Ju *et al.* 2005; Louro *et al.* 2010). The CG repeat was not detected, also consistent with findings in *Sparus aurata* (Louro *et al.* 2010). Here, the most frequently observed tri- nucleotide motif was CAG.

The data show the potential for development of new microsatellite markers with the application in future *T. thynnus* population and conservation studies as well as in genetic mapping of important traits.

**Table 3.2** Results of *in silico* search for EST-SSRs markers on annotated transcripts from *T. thynnus* cDNA library.

SSR type	Count	Frequency	Targets	Proteins
Di-	361	0.49	344	321
Tri-	328	0.45	315	288
Tetra-	19	0.03	19	19
Penta-	4	0.01	4	4
Hexa-	4	0.01	3	3
Composite	14	0.02	14	14
Total	730	0.06	699	649

**Figure 3.5** Counts of specific EST-SSR motifs found on annotated transcripts from *T. thynnus* cDNA library.

### 3.5 Results of microarray inference of tissue-specific gene expression profiles and qPCR validation

Principal component analyses (PCA) showed distinct separation of arrays into tissue-specific groups. The signals from one array deviated considerably from its biological replicates within the heart group, reflecting technical difficulties noted during hybridization and therefore this array was excluded from further analyses. From 15,068 *T. thynnus*-specific probes, 13,494 passed the quality filtering across the experiment and showed positive and significant signals above background in both channels. Most of these features, 12,306 (91.2%), were found to be differentially expressed (ANOVA,  $P < 0.05$ ) between at least two tissues, consistent with the expected low number of genes ubiquitously and constitutively expressed in an organism (Su *et al.* 2004). Network analyses based on these preselected features produced a complex graph with 8,836 nodes, further reduced into 87 clusters of discrete patterns of gene expression. Over half of the nodes were grouped within the first six clusters (Table 3.3), each corresponding to one tissue-specific up-regulated group of features, and an ovary and testis combination. The largest was an ovary-specific cluster while highest intensity values of expression were recorded for liver and heart transcripts, visualized in Figure 3.6. Other clusters not shown in this figure comprised entities with varying expression profiles across tissues. Full list of transcripts found in these main clusters will be omitted for clarity, however those mentioned in the final discussion can be found in Supplement 9.1.

**Table 3.3** Size and tissue specificity of the first six gene expression clusters of *T. thynnus* obtained by MCL algorithm in Biolayout Express 3D.

<b>MCL Clusters</b>	<b>Tissue specificity</b>	<b>N (nodes)</b>
Cluster 1	Ovary	1,598
Cluster 2	Heart	877
Cluster 3	Liver	654
Cluster 4	Gill	579
Cluster 5	Ovary/Testis	557
Cluster 6	Testis	253
Other	Mixed	2,018
No Class	/	2,300
Grand Total		8,836

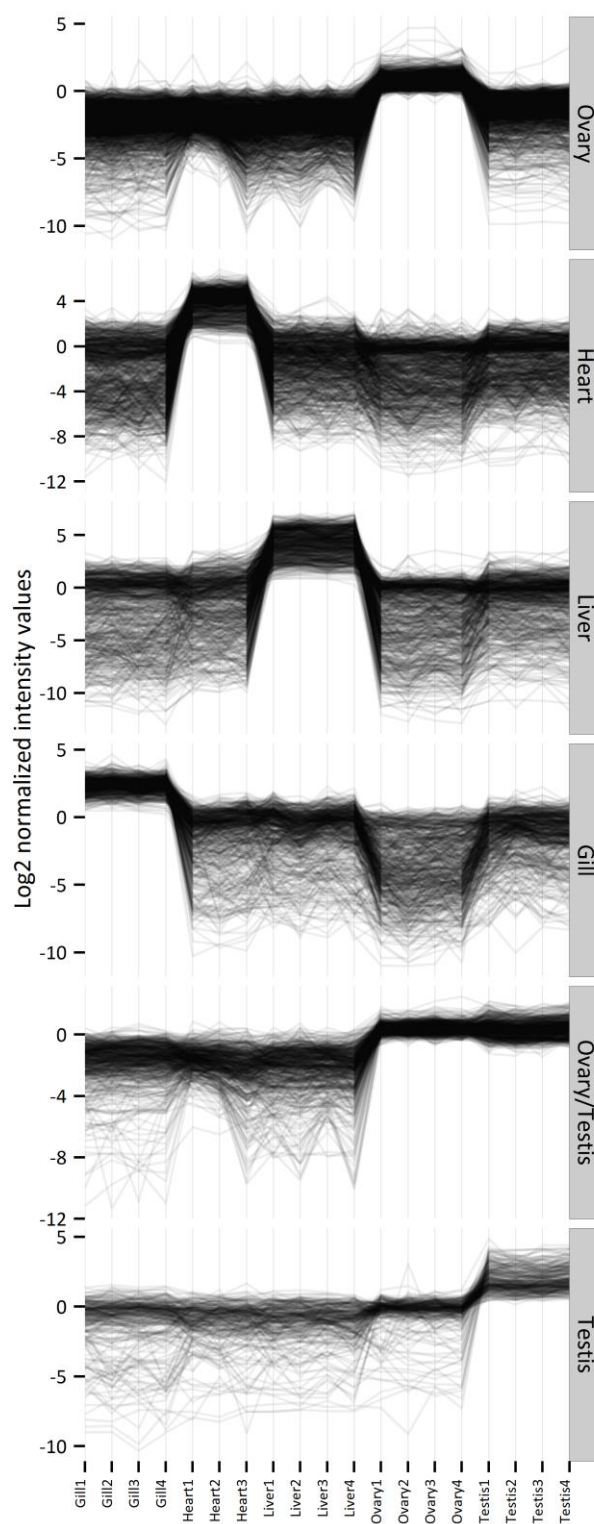


**Figure 3.6.** Clusters of tissue specific gene expression profiles of adult captive *T. thunnus* derived using Markov clustering algorithm in Biayout Express 3D, plotted in descending order according to number of features found in each cluster.

Functional contrasts between tissues, inferred through KEGG pathway categorization, into respective functional groups are visualized using a heatmap in Figure 3.7. There was strongest differentiation between gill and ovarian tissue, also reflecting the fact that the greatest number of up- and down-regulated pathways was found for these tissues respectively. The full list of pathways for each tissue and their pairwise combinations is available in Supplement 9.2.

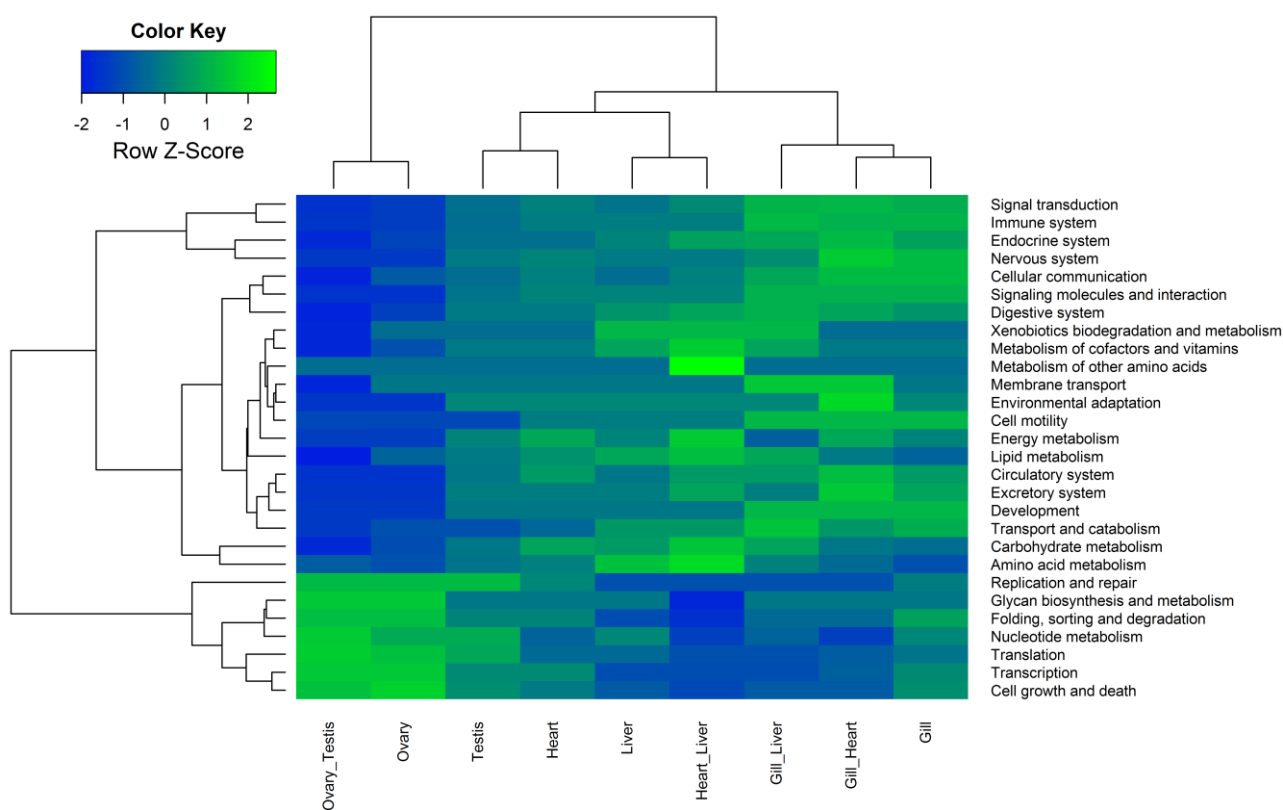


**Figure 3.7** Results of two-dimensional hierarchical clustering performed on difference between the counts of up- and down-regulated pathways in KEGG functional categories after GAGE gene set enrichment analyses on *T. thynnus* tissue expression profiles. Each tissue and their most informative pair-wise combinations are shown.

Eight transcripts representative of the six largest Biolayout clusters were chosen for the purpose of qPCR validation: aquaporin 3b - Aqp3b (Gill), sarcoplasmic reticulum calcium-ATPase 2 - Atp2a2a (Heart), complement C4-like - C4, coagulation factor V - F5 (Liver), exosome component 2 - Exosc2, pescadillo - Pes (Ovary), somatolactin - SL (Testis), mediator complex subunit 6 - Med6 (Ovary/Testis); and

two transcripts, biliverdin reductase B - Blvrb and prohibitin 2 - Phb2, showing varying expression profiles across tissues. Three reference genes were tested, Actb, Elf-1a, previously used in *T. thynnus* qPCR experiments (Morais *et al.* 2011; Gardner *et al.* 2012; Lepen Pleić *et al.* 2013), and a candidate from this microarray experiment, Ftsjd2, which subsequently did not show stable expression profiles according to BestKeeper tool, exceeding the recommended quantification cycle (Cq) standard deviation of 1 (Pfaffl *et al.* 2004). This was not unexpected as we were comparing different tissues of adult fish, however, the variation was systematically attributed only to ovarian tissue, which is characterized by a very different total RNA population as previously mentioned. Hence, non-normalized (normalized to total RNA used for cDNA synthesis) and normalized data (normalized to geometric mean of Actb, Elf-1a and Ftsjd2 = TEF) were further compared to microarray results.

Microarray and qPCR fold changes (FCs) among all five tissues for ten target genes were compared in  $\text{Log}_2$  space using the concordance correlation coefficient (CCC), proposed for global validation of microarray experiments (Miron *et al.* 2006). CCC is a product of a measure of precision (Pearson  $r$ ), describing linear correlation of the data, and accuracy, how close the least-squares regression line is to the identity line. It takes values from -1 (perfect inverse agreement) to 1 (perfect agreement). We evidenced a good agreement between microarray and qPCR data in this study, both in terms of precision and accuracy (Table 3.4, Figure 3.8). Due to the range enhancement artefact, Miron *et al.* (2006) suggested that up- and down-regulated genes should be inspected separately. Gene expression profiles were broken into positive and negative FCs, with former producing better scores (Table 3.4), which is sometimes observed in microarray and qPCR comparisons (Morey *et al.* 2006).

**Table 3.4** Correlation correspondence index (CCC) and other indices describing agreement of microarray and qPCR data (non-normalized (non) and normalized (TEF)) based on  $\text{Log}_2\text{FC}$  values for all data and up- and down-regulated values separately.

Indice	ALL DATA		UP		DOWN	
	non	TEF	non	TEF	non	TEF
Slope	0.91	0.99	0.88	1.05	0.82	1.05
Y intercept	-0.75	-0.24	-0.54	-0.59	-1.08	0.05
Precision (r)*	0.80	0.87	0.77	0.85	0.54	0.73
Accuracy	0.98	0.99	0.96	0.97	0.89	0.94
CCC	0.78	0.86	0.73	0.82	0.48	0.69

\*Correlation is significant at the 0.01 level (2-tailed).

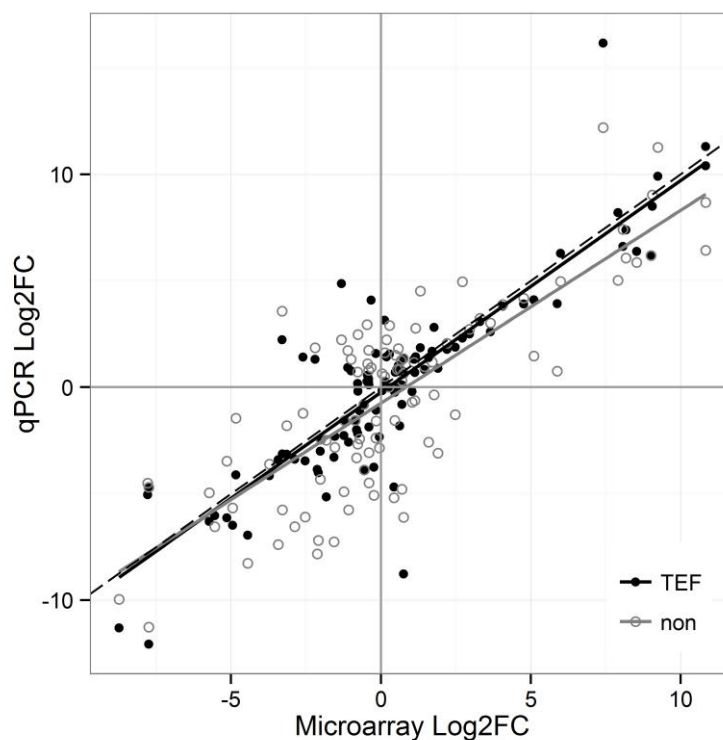


**Figure 3.8** Least-squares regression fit between microarray and qPCR (non-normalized (non) and normalized (TEF)) Log<sub>2</sub>FC in respect to the identity line (dashed) for the selected target genes of *T. thynnus*.

As there was better concurrence between normalized qPCR and microarray data with respect to non-normalized, only the normalized set was included in the joint qPCR and microarray statistical analyses, with data coded by respective percentile ranks. The goal was to maximize power to test differences between tissues by combining two outputs and increasing the number of replicates for each condition. Figure 3.9 shows derived expression profiles for target transcripts representatives of the six largest Biolayout clusters. Although there is some disagreement between qPCR and microarray data evidenced by increased interquartile ranges for certain transcripts and tissues, they both concur that the tissue, or its combination, suggested by the cluster assignment is the place of highest expression for selected transcripts. This assertion is statistically corroborated in most of the comparisons. Correlation of microarray and qPCR data is often affected by pitfalls and differences inherent to each technology, *i.e.* probe/primer properties and amplification kinetics (Chuaqui *et al.* 2002; Morey *et al.* 2006), which can differ from one transcript to another.

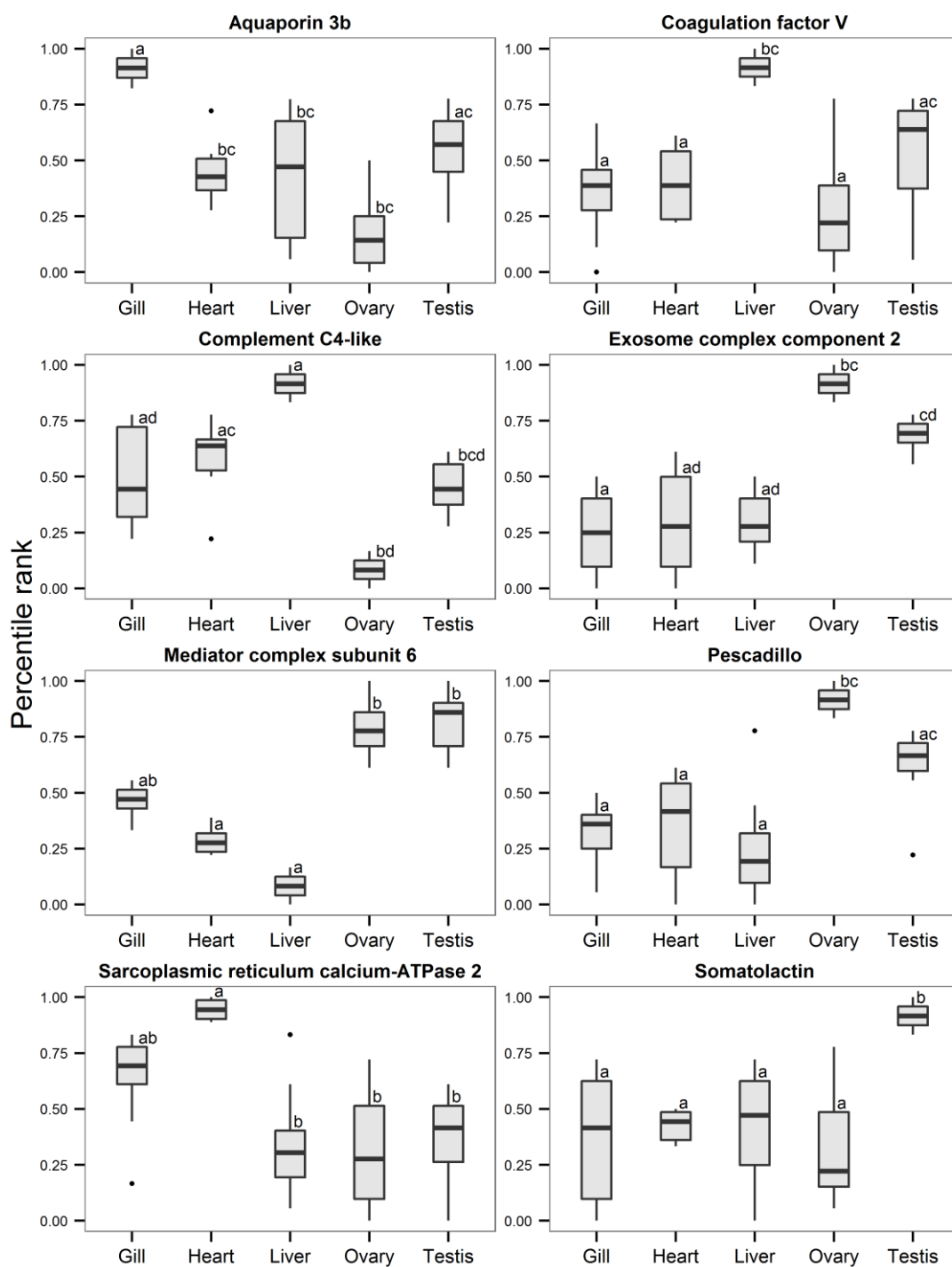


**Figure 3.9** Distribution of expression profiles derived by combining qPCR and microarray data using percentile ranks for target genes belonging to six largest *T. thynnus* tissue clusters. Statistical difference at  $P < 0.05$  between tissues is coded using different letters.

### 3.6 Microarray profiling of transcriptomic changes in gill epithelium induced by *D. katsuwonocola* infection and qPCR validation

Out of 12,381 positive and significant microarray features that passed quality filtering, 768 were selected by higher criticism (HC) thresholding as differentially expressed in *D. katsuwonocola*-infected gills in respect to uninfected, with permutational *P*-value cut-off of 0.038. No strong transcriptional biomarkers were noted and features showed consistent and moderate transcriptional regulation in both directions, with fold changes (FC) ranging from -10.38 to 4.56 (Table 3.5). The distinction of these features from all positive and significant probes is visualized using a volcano plot in Figure 3.10, with entities displaying FC > 2 plotted as triangles. The spread of values is slightly skewed towards down-regulated probes. Pathway enrichment analyses based on KEGG sets showed the down-regulation of metabolic and signalling groups functionally associated with endocrine, digestive and nervous system, with immunity related pathway Complement and coagulation cascades bidirectionally perturbed (Table 3.6 and Figure 3.11). Separate analyses of human diseases related KEGG pathways reports the resemblance of *D. katsuwonocola* presence on *T. thynnus* gills with infectious bacterial, immune and cardiovascular disorders. Finally, genes belonging to all significantly perturbed pathways and deemed differentially expressed by HC thresholding were selected as important molecular features of this host-parasite system. Characteristics of their expressional profiles are presented in Table 3.7.

**Table 3.5** Number and magnitude of fold change for differentially expressed transcripts selected after HC thresholding in *D. katsuwonocola* infected *T. thynnus* gills.

Regulation	N	Max (FC)	Min (FC)
UP	309	4.56	1.06
DOWN	459	-1.09	-10.38

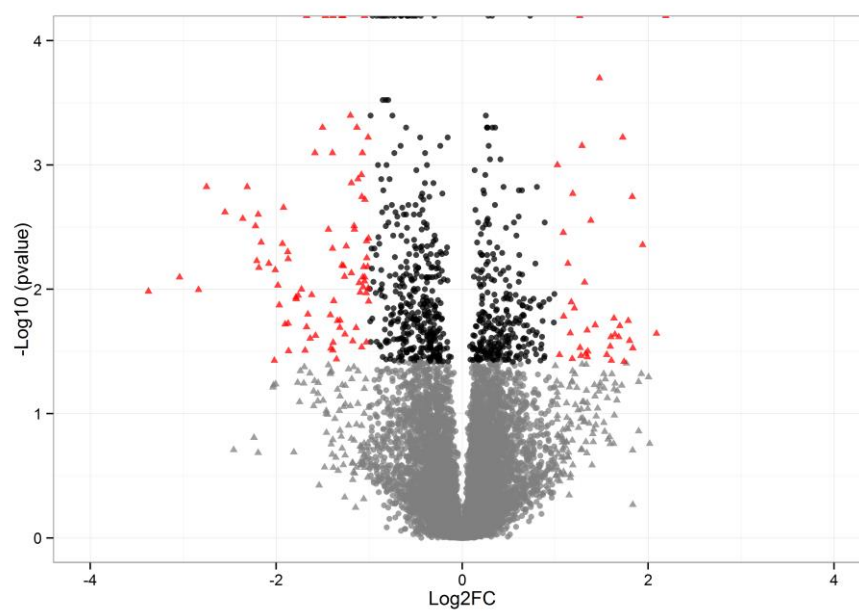


**Figure 3.10** Volcano plot of differentially regulated transcripts in *D. katsuwonica*-infected *T. thynnus* gills selected after HC thresholding (black). ▲ denotes fold change (FC) > 2. Red triangles denote significantly regulated transcripts with FC > 2.

**Table 3.6** Significantly perturbed KEGG pathways in *D. katsuwonica*-infected *T. thynnus* gills inferred through GAGE analyses of all positive and significant features on the microarray. Transcripts were collapsed to unique KO identifiers according to their best *P*-value.

	Regulation	Group	Pathway	p.geomean	stat.mean	p.val	q.val	set.size
METABOLIC AND SIGNALING SETS	BIDIRECTIONAL	Immune system	Complement and coagulation cascades	0.051	1.646	0.000	0.002	22
		Digestive system	Protein digestion and absorption	0.109	1.181	0.001	0.081	22
	DOWN	Circulatory system	Cardiac muscle contraction	0.076	-1.366	0.000	0.021	22
		Endocrine system	Insulin secretion	0.084	-1.342	0.000	0.021	17
		Digestive system	Fat digestion and absorption	0.121	-1.183	0.001	0.055	11
		Nervous system	Serotonergic synapse	0.103	-1.148	0.002	0.055	24
		Signalling molecules and interaction	ECM-receptor interaction	0.115	-1.117	0.002	0.058	21
		Endocrine system	Ovarian steroidogenesis	0.124	-1.094	0.003	0.065	12
		Environmental adaptation	Circadian entrainment	0.117	-1.032	0.004	0.080	23
		Nervous system	Retrograde endocannabinoid signaling	0.134	-1.025	0.004	0.080	14
		Digestive system	Protein digestion and absorption	0.135	-0.995	0.005	0.080	22
		Endocrine system	GnRH signaling pathway	0.152	-0.957	0.006	0.080	30
		Endocrine system	Estrogen signaling pathway	0.150	-0.957	0.006	0.080	26
		Lipid metabolism	Arachidonic acid metabolism	0.146	-0.985	0.006	0.080	11
		Cellular communication	Gap junction	0.161	-0.918	0.008	0.095	23
DISEASE SETS	BIDIRECTIONAL	Infectious diseases	<i>Staphylococcus aureus</i> infection	0.053	1.668	0.000	0.001	12
		Immune diseases	Systemic lupus erythematosus	0.083	1.401	0.000	0.006	13
		Infectious diseases	Pertussis	0.140	1.038	0.003	0.064	23
		Cardiovascular diseases	Hypertrophic cardiomyopathy	0.144	1.001	0.004	0.064	29
		Cardiovascular diseases	Arrhythmogenic right ventricular cardiomyopathy	0.159	0.928	0.008	0.079	23
		Cardiovascular diseases	Dilated cardiomyopathy	0.162	0.917	0.008	0.079	28

**Table 3.7** Transcripts showing statistically significant differential expression between uninfected and *D. katsuwonica*-infected gills belonging to different metabolic, signalling and disease related KEGG pathways. Asterisk (\*) next to fold change value indicates a probe with high non-specific or parasite associated cross-hybridization potential. Expression values are conditionally formatted to highlight patterns, with red denoting increased and blue decreased expression.

KO	Description	Gill	Infected gill	Fold change	Coeff. (P value)	Pathways
K07199	5'-AMP-activated protein kinase, regulatory beta subunit	-0.79 ± 0.28	-0.37 ± 0.24	1.33	2.25E-02	Hypertrophic cardiomyopathy (HCM)
K06736	cadherin 2, type 1, N-cadherin	-0.09 ± 0.12	-0.59 ± 0.47	-1.41	3.44E-02	Arrhythmogenic right ventricular cardiomyopathy (ARVC)
K02187	caspase 3	2.17 ± 0.22	2.5 ± 0.23	1.26	3.67E-02	Pertussis, Serotonergic synapse
K03914	coagulation factor II (thrombin) receptor	-0.78 ± 0.15	-1.28 ± 0.34	-1.42	6.50E-03	Complement and coagulation cascades
K06237	collagen, type IV, alpha	1.81 ± 0.15	1.19 ± 0.24	-1.54	0.00E+00	ECM-receptor interaction, Protein digestion and absorption
K06238	collagen, type VI, alpha	1.74 ± 0.26	0.54 ± 0.38	-2.30	4.00E-04	ECM-receptor interaction, Protein digestion and absorption
K06823	collagen, type XVIII, alpha	1.1 ± 0.3	0.03 ± 0.94	-2.09	9.60E-03	Protein digestion and absorption
K01332	complement component 2	-0.41 ± 0.4	1.32 ± 0.95	3.31	6.00E-04	Complement and coagulation cascades, Pertussis, <i>Staphylococcus aureus</i> infection, Systemic lupus erythematosus
K03989	complement component 4	-1.57 ± 0.49	0.61 ± 0.68	4.56	0.00E+00	Complement and coagulation cascades, Pertussis, <i>Staphylococcus aureus</i> infection, Systemic lupus erythematosus
K07418	cytochrome P450, family 2, subfamily J	0.25 ± 0.41	-0.91 ± 0.57	-2.23	3.30E-03	Arachidonic acid metabolism, Ovarian Steroidogenesis, Serotonergic synapse
K10381	desmoplakin	2.63 ± 0.52	1.44 ± 0.45	-2.28	1.40E-03	Arrhythmogenic right ventricular cardiomyopathy (ARVC)
K04361	epidermal growth factor receptor	2.17 ± 0.37	1.16 ± 0.45	-2.02	6.60E-03	Estrogen signaling pathway, Gap junction, GnRH signaling pathway
K08751	fatty acid-binding protein 2, intestinal	-0.26 ± 0.45	-2.58 ± 1.05	-4.97	1.50E-03	Fat digestion and absorption
K03903	fibrinogen alpha chain	-6.16 ± 0.18	-5.91 ± 0.14	1.19*	3.27E-02	Complement and coagulation cascades
K05717	fibronectin 1	1.13 ± 0.26	0.64 ± 0.25	-1.40	7.50E-03	ECM-receptor interaction
K05871	focal adhesion kinase 2	2.48 ± 0.18	2.09 ± 0.32	-1.31	1.16E-02	GnRH signaling pathway
K04634	guanine nucleotide-binding protein G(q) subunit alpha	1.53 ± 0.15	1.29 ± 0.18	-1.18	3.42E-02	Circadian entrainment, Estrogen signaling pathway, Gap junction, GnRH signaling pathway, Insulin secretion, Retrograde endocannabinoid signaling, Serotonergic synapse
K04527	insulin receptor	0.7 ± 0.12	0.38 ± 0.23	-1.25	1.03E-02	Ovarian Steroidogenesis
K05719	integrin beta 1	1.48 ± 0.24	0.76 ± 0.51	-1.65	2.40E-03	Arrhythmogenic right ventricular cardiomyopathy (ARVC), ECM-receptor interaction, Hypertrophic cardiomyopathy (HCM), Pertussis
K05636	laminin, beta 1	2.56 ± 0.22	2.13 ± 0.18	-1.35	2.30E-03	ECM-receptor interaction
K12473	low-density lipoprotein receptor	0.23 ± 0.32	-0.44 ± 0.4	-1.59	8.20E-03	Ovarian Steroidogenesis
K11090	lupus La protein	-0.52 ± 0.11	-0.25 ± 0.14	1.20	5.00E-04	Systemic lupus erythematosus
K04289	lysophosphatidic acid receptor 1	-1.15 ± 0.23	-1.53 ± 0.26	-1.30	2.38E-02	Gap junction

KO	Description	Gill	Infected gill	Fold change	Coeff. ( <i>P</i> value)	Pathways
K03992	mannan-binding lectin serine protease 1	-2.41 ± 0.91	-1.1 ± 0.57	2.49	8.80E-03	Complement and coagulation cascades, <i>Staphylococcus aureus</i> infection
K07763	matrix metalloproteinase-14 (membrane-inserted)	0.63 ± 0.31	1.38 ± 0.52	1.69	2.13E-02	GnRH signaling pathway
K01403	matrix metalloproteinase-9 (gelatinase B)	2.92 ± 0.2	2.57 ± 0.28	-1.27	1.34E-02	Estrogen signaling pathway
K07299	MFS transporter, SP family, solute carrier family 2 (facilitated glucose transporter), member 1	2.51 ± 0.43	1.92 ± 0.32	-1.51	1.76E-02	Insulin secretion
K04441	p38 MAP kinase	1.92 ± 0.31	1.27 ± 0.58	-1.58	6.60E-03	GnRH signaling pathway, Pertussis, Retrograde endocannabinoid signaling
K01283	peptidyl-dipeptidase A	2.65 ± 0.31	1.58 ± 0.63	-2.10	8.00E-04	Hypertrophic cardiomyopathy (HCM)
K03982	plasminogen activator inhibitor-1	2.87 ± 0.23	2 ± 0.29	-1.83	1.30E-03	Complement and coagulation cascades
K00509	prostaglandin-endoperoxide synthase 1	3.05 ± 0.25	2.34 ± 0.51	-1.64	7.60E-03	Arachidonic acid metabolism, Serotonergic synapse
K01830	prostaglandin-H2 D-isomerase	-5.68 ± 0.27	-6.76 ± 0.55	-2.11*	1.80E-03	Arachidonic acid metabolism
K07843	RAS, dexamethasone-induced Ras-related protein 1	1.18 ± 0.32	-0.12 ± 0.53	-2.45	0.00E+00	Circadian entrainment
K13885	scavenger receptor class B, member 1	-4.36 ± 0.42	-5.55 ± 1.04	-2.28	7.40E-03	Fat digestion and absorption, Ovarian Steroidogenesis
K13377	transforming growth factor beta-3	1.94 ± 0.17	1.54 ± 0.17	-1.32	8.00E-04	Hypertrophic cardiomyopathy (HCM)
K10373	tropomyosin 1	1.53 ± 0.21	1.03 ± 0.38	-1.41	5.30E-03	Cardiac muscle contraction, Hypertrophic cardiomyopathy (HCM)
K03156	tumor necrosis factor superfamily, member 2	2.15 ± 0.24	2.63 ± 0.36	1.40	2.65E-02	Hypertrophic cardiomyopathy (HCM), Pertussis, Systemic lupus erythematosus
K04850	voltage-dependent calcium channel L type alpha-1C	1.04 ± 0.92	-0.28 ± 0.71	-2.49	2.03E-02	Arrhythmogenic right ventricular cardiomyopathy (ARVC), Cardiac muscle contraction, Circadian entrainment, GnRH signaling pathway, Hypertrophic cardiomyopathy (HCM), Insulin secretion, Retrograde endocannabinoid signaling, Serotonergic synapse

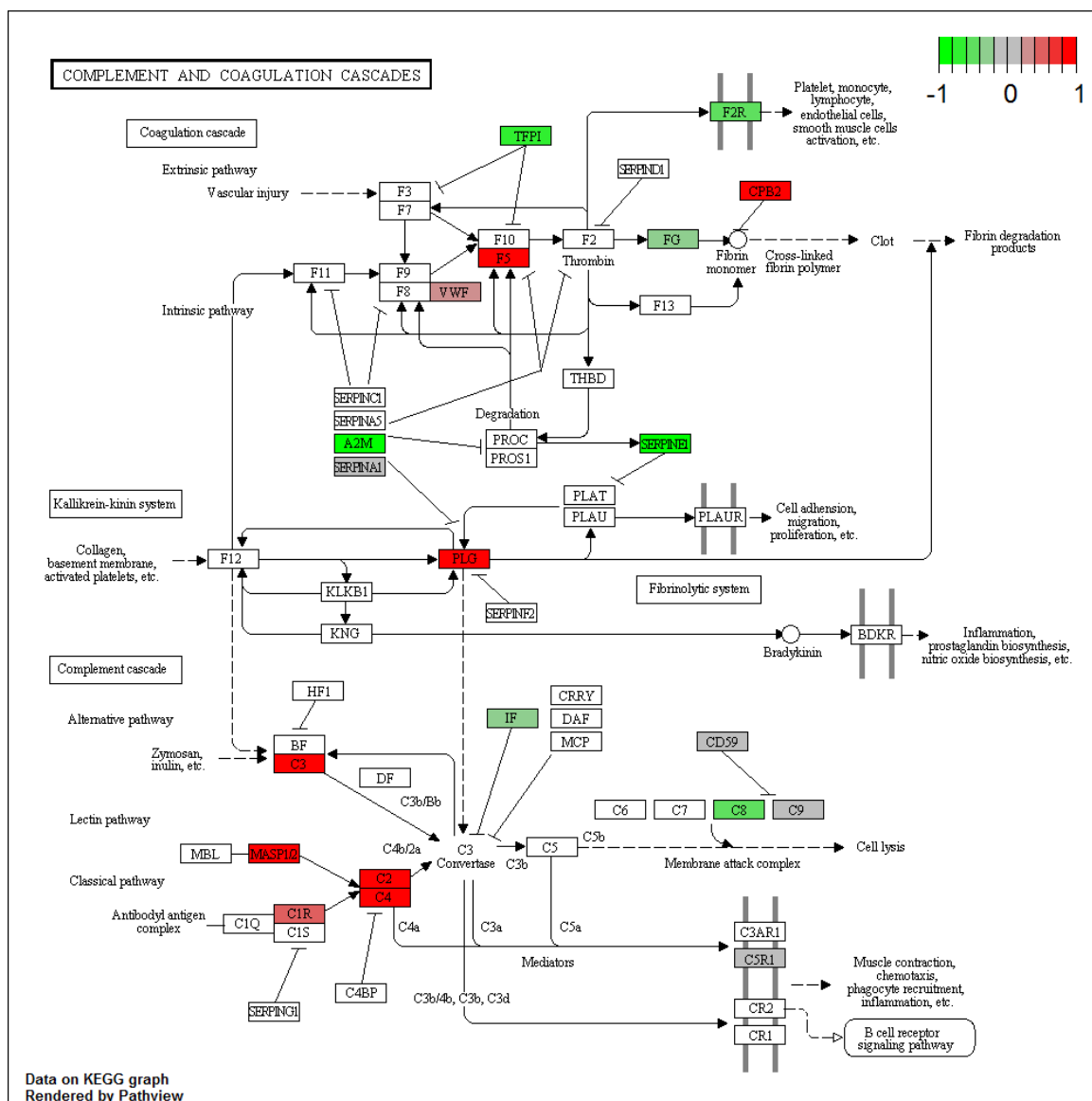


**Figure 3.11** Visualization of genes belonging to KEGG pathway Complement and coagulation cascades and differentially perturbed in *T. thynnus* gills infected with *D. katsuwanicola*, plotted using Pathview package for R/Bioconductor.

Ten transcripts validated by RT-qPCR were homologues of angiopoietin-like 2 (Angptl2), aquaporin 3b (Aqp3b), caspase 3 apoptosis-related cysteine protease b (Casp3), collagen, type X, alpha 1 (Col10a1), complement C4-like (C4), cytochrome b-245, beta polypeptide (Cybb), exosome component 2 (Exosc2), Janus kinase 3 (Jak3), mannan-binding lectin serine peptidase 2 (Masp2), tropomyosin 4 (Tpm4). They were all retrieved among 768 potential biomarkers after HC thresholding, selected based on their immunity related biological function and/or were included in the final gene list (Table 3.7). C4 and Tpm4 additionally were responsible for most extreme expressional changes noted on the microarray. All four potential reference genes (Actb, Elf-1 $\alpha$ , Ftsjd2 and Mrps18b) were stable according to the BestKeeper tool, however the normalizing index varied the least when beta-actin (Actb) was excluded from the calculation. Hence, the expression profiles of target genes, including Actb, were normalized to geometric average of Elf-1 $\alpha$ , Ftsjd2 and Mrps18b. Figure 3.12 shows regulation (fold change) of gene expression in infected vs. uninfected gills of *T. thynnus* for each transcript comparing qPCR and microarray results, both analysed with ratio ttest. There is good general agreement between the two sets of data and the direction of regulation for each transcript is univocal for both methods, with microarray data displaying somewhat larger expressional changes. According to ratio ttest 95 % confidence intervals not crossing no effect threshold of FC = 1, all transcripts, except for Actb, displayed significant ( $P < 0.05$ ) fold change in the microarray dataset, and only 3 in the qPCR set (Angptl2, Aqp3b, Col10a1). Linear fit of microarray and qPCR Log<sub>2</sub>FCs was significant (Figure 3.13). As previously mentioned, differences inherent to qPCR and microarray technology can affect the reproducibility of the data, especially when small fold changes (< 1.4) are evaluated (Morey *et al.* 2006). As identical trends in expression are observed between both technologies, the microarray data are considered to be valid, however, the exact size of observed changes might need further investigation.

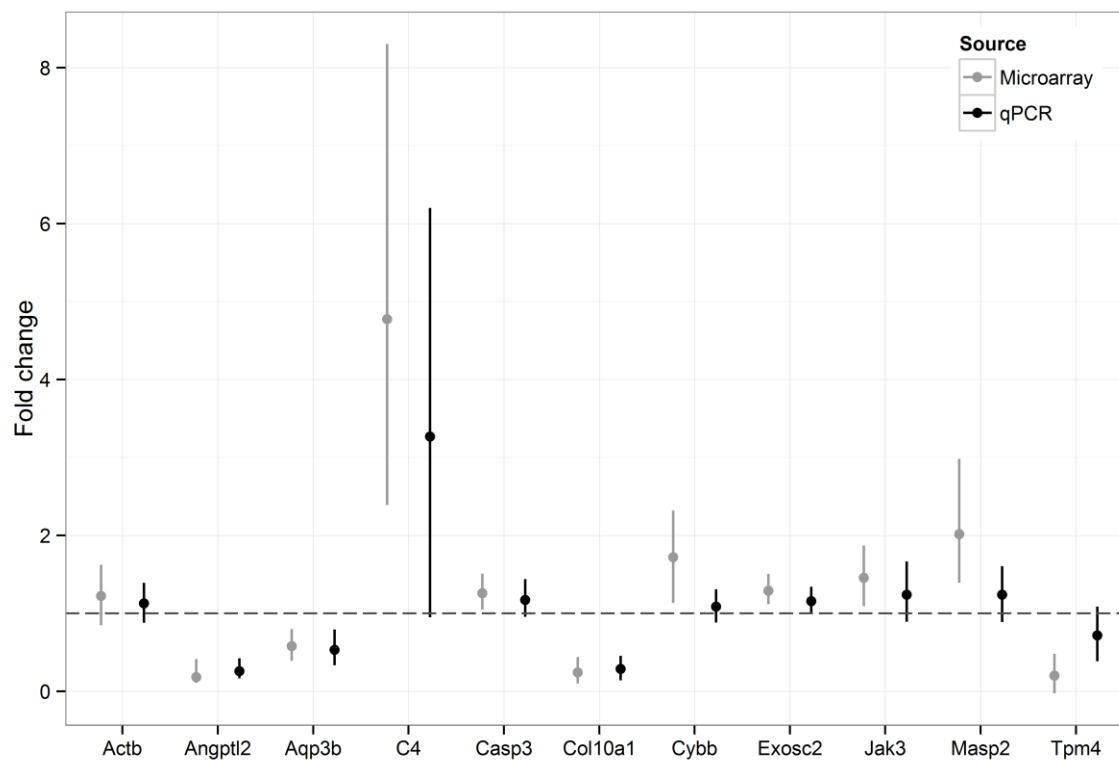


**Figure 3.12** Comparison of microarray and qPCR recorded fold change in expression for selected transcripts in *D. katsuwanicola* infected vs. uninfected *T. thynnus* gills (error bars = 95 % confidence interval of ratio ttest).

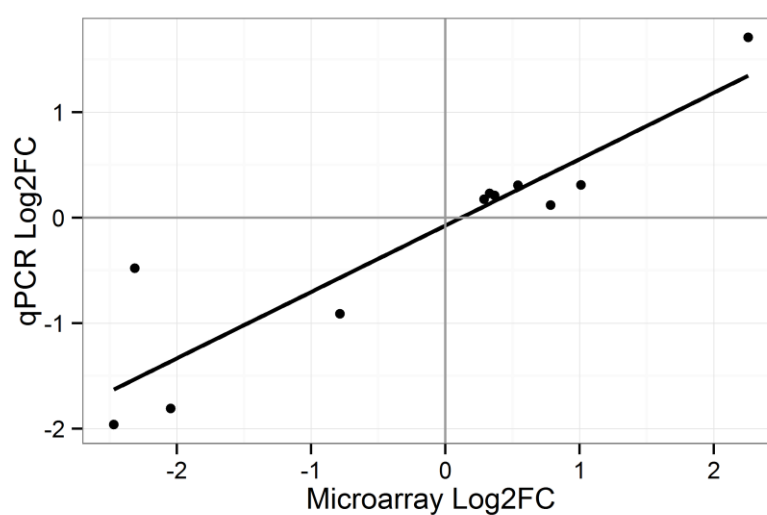


**Figure 3.13** Least squares regression line between microarray and qPCR Log2FC for validated transcripts (R-squared: 0.833, F-statistic: 45.03 on 1 and 9 df,  $P$ -value: 8.747e-05).

### 3.7 Heterologous hybridization of *D. katsuwnicola* to *T. thynnus* arrays

RGB (red, green, blue) overlay microarray images, showing Cy3 and Cy5 fluorescent signals as green and red spots respectively, were inspected visually during scanning and the absence of Cy3 signals was evident. Nevertheless, positive and significant Cy3 signals were recorded during feature extraction procedure. The distribution of green and red background subtracted signals for these probes was compared for *D. katsuwnicola* and *T. thynnus* hybridizations. Figure 3.14 shows that the signal retained from heterologous hybridizations is evidently lower than the one contained in tuna arrays, however in its upper quartile overlaps the majority of Cy3 signal contained in tuna specific hybridizations. This is equally valid for Cy3 to Cy5 ratio. Probes exhibiting this stronger signal were marked and require cautious interpretation as they could carry substantial non-specific cross-hybridization signal. The nature of this signal needs further exploration as its sources cannot be determined at this point. Transcripts with high non-specific cross-hybridization potential (included in the overlap percentile range and showing fluorescence well above background in non-specific hybridization according to Agilent feature extraction protocol) selected as molecular markers of the infection are marked with an asterisk (\*). Amongst transcripts showing the highest cross-hybridization signals, many basic functional maintenance genes are noted, like various ribosomal proteins, elongation factor 1 $\alpha$ , glyceraldehyde-3-phosphate dehydrogenase, cyclin, myoglobin, fibrinogen, heat shock protein 90.

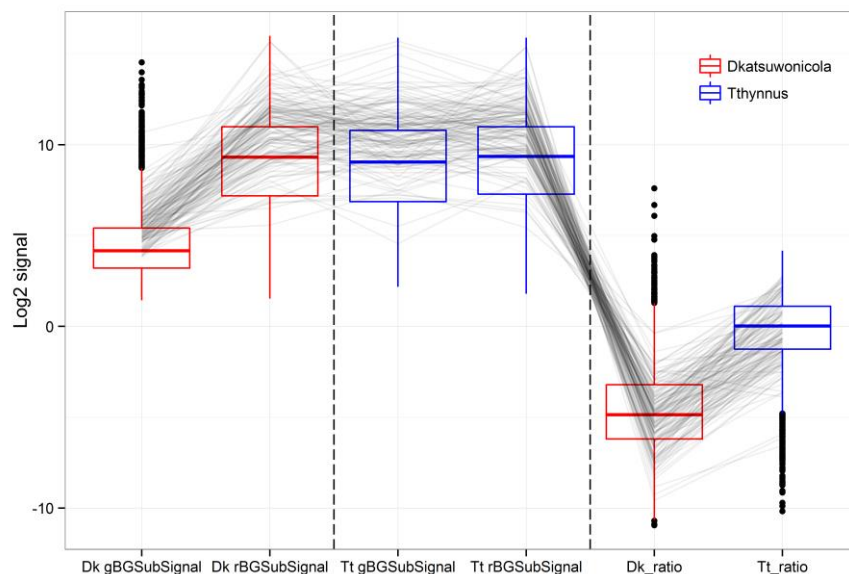


**Figure 3.14** Distribution of background subtracted signal (BGSubSignal) in green (g) and red (r) channel for *T. thynnus*-specific and heterologous hybridization of *D. katsuwonocola* to *T. thynnus* microarray, as well as green to red ratio. Lines indicate the position of transcripts showing significant differential expression between healthy and *D. katsuwonocola*-infected *T. thynnus* gills.

### 3.8 Ultrastructure of *Didymosulcus katsuwonocola* cysts

Two didymozoid individuals were encysted in a loose collagen capsule of varying thickness that encompassed a large afferent filament artery, lateral afferent lamellar arterioles and numerous small anastomosing capillaries. Basement membrane demarcated connective tissue capsule interspersed by fibroblast and fibrocytes from the multilayered squamous gill epithelium.

The cuticle of didymozoid hindbody was in direct contact with fibrocytes and collagen bundles and numerous vesicles with electron -dense or -translucent matrix were observed at their interface migrating towards digeneans (Figure 3.15). Approximately three cell layers distal to the didymozoid, collagen capsule contained numerous eosinophilic-granulated cell types, belonging to either mast cells or eosinophils. Capillaries in close contact with parasites were observed filled with electron-translucent vesicles, erythrocytes and few lymphocyte-like cells, while in their vicinity eosinophilic-granulated cell types were present. Clear distinction between mastocytes and eosinophils was in that the former contained spherical and large electron-dense granulae, while the later contained more irregular round-shaped

granulae were crystalloid body was observed (Figure 3.15). In some instances, degranulation of mast cells' granulae and small extracellular vesiculae were observed in the collagen capsule surrounding didymozoids. Although medially in the gill filament and distal from the didymozoid cyst, an axon encompassing bundles of nerve fibres was observed, a small axon with three nerve fibres was observed in collagen capsule in close vicinity to didymozoids cuticle (Figure 3.16). Squamous epithelial cells overlaid collagen capsule, varying in thickness in respect to cyst attachment point, being thicker proximally and feebler in distant parts. Epithelial cells were prismatic and interspaced with many eosinophilic-granulated cells and few plasma cells. Plasma cells had strikingly developed rough endoplasmic reticulum, few but large mitochondria, and heterochromatin eccentrically distributed beneath inner karyotheca (Figure 3.16). While few rodlet cells were present in sub-epithelial area, in distant part of squamous epithelium, many mucous goblet cells secreting electron-translucent substance, compartmentalised in granulae, were observed. Goblet cells had basally eccentric nucleus and basally situated many small mitochondria.

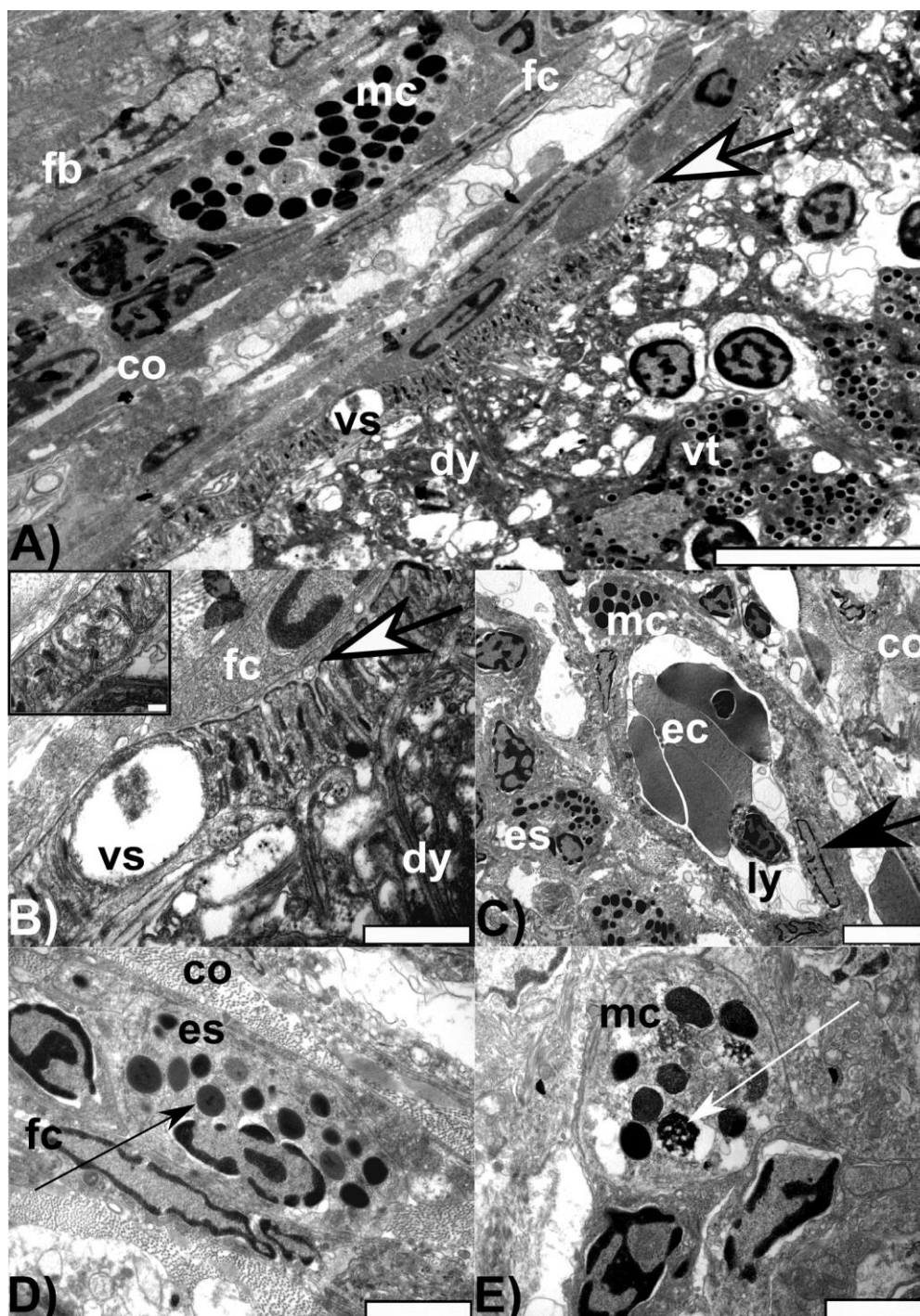


**Figure 3.15** *D. katsuwonocola* encysted in the Atlantic bluefin tuna (*T. thynnus*) gill tissues: A) Didymozoid's hindbody (dy), encompassing vitelline cells rich in vitelline granules (vt), is in direct contact with tuna connective tissue capsule by a tegument (white thick arrow) where transiting vesicles can be observed (vs). Host's connective tissue capsule is composed of collagen fibres (co), fibrocytes (fc), fibroblasts (fb) and dispersed mast cells (mc). Scale bar = 5  $\mu$ m; B) Tegument (white thick arrow) of the digenean (dy) shows abundant processes of transport of vesicles (vs) of varying size, and close contact to the fibrocyte (fc). Scale bar = 1  $\mu$ m. Insert: A detail of didymozoid tegument showing atypically desmosome-like connections between two cells. Scale bar = 0.2  $\mu$ m; C) One of numerous capillaries present in connective tissue capsule, surrounded by collagen fibres (co), mast cells (mc) and eosinophils (es). Note endothelial cell (thick black arrow) lining capillary wall, erythrocytes (ec) and a lymphocyte (ly). Scale bar = 5  $\mu$ m; D) Eosinophilic granulocyte (es) surrounded by collagen fibres (co) and fibrocyte (fc), contains typical granule with crystalloid body (thin black arrow). Scale bar = 2  $\mu$ m; E) Mast cell (mc) in process of degranulation (thin white arrow). Scale bar = 2  $\mu$ m.

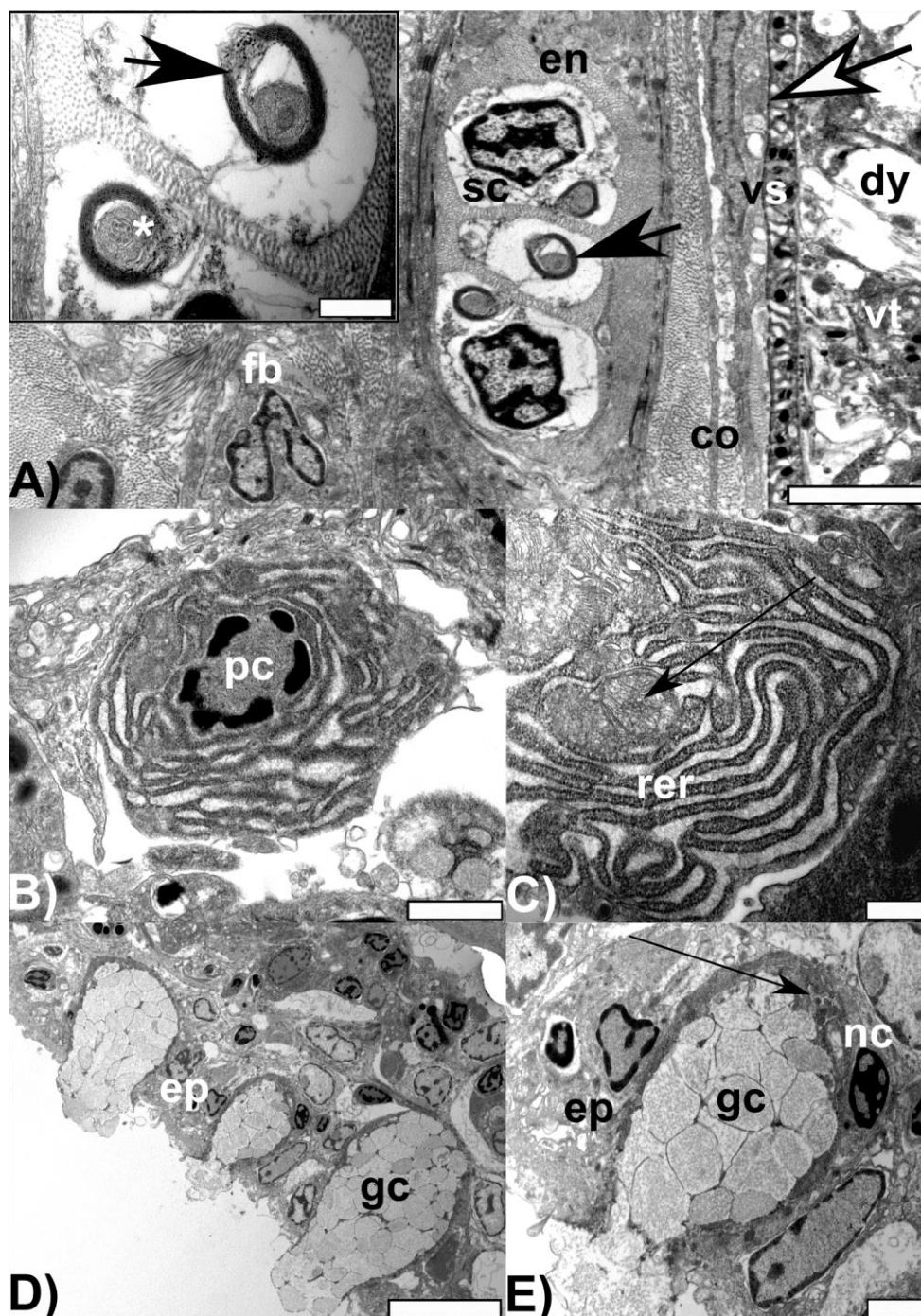


**Figure 3.16** *D. katsuwonocola* encysted in the Atlantic bluefin tuna (*T. thynnus*) gill tissues: A) Connective capsule surrounding didymozoid's hindbody (dy) encompasses a nerve composed of three neuronal axons. Each axon has thin myelinated sheaths (thick black arrow) of a Schwann cell (sc) showing large spherical nucleus, and bundles of endoneuric fibres (en). Fb - fibrocyte, co - collagen fibres, vs - vesicles transiting between host and didymozoid, vt - didymozoid vitelline granules, thick white arrow - interface between host and parasite. Scale bar = .2  $\mu\text{m}$ . Insert: Myelinated sheaths (thick black arrow) of a Schwann cell surrounding an axon. Note microtubules in the axon (white asterisk). Scale bar = 0.5  $\mu\text{m}$ ; B) A plasma cell (pc) observed in the connective tissue capsule. Note large spherical nucleus with peripheral heterochromatin. Scale bar = 1  $\mu\text{m}$ ; C) A detail of plasma cell with a highly developed rough endoplasmic reticulum (rer) and large mitochondria (thin black arrow). Scale bar = 0.5  $\mu\text{m}$ ; D) Multilayered squamous epithelium (ep) overlays connective tissue capsule that contains two didymozoids, and is abundant with mucous goblet cells (gc). Scale bar = 10  $\mu\text{m}$ ; E) Mucous goblet cell (gc) is surrounded by squamous epithelial cells (ep) and contains basally located small mitochondria (thin black arrow), fusiform nucleus (nc) and electron-translucent secretory granules. Scale bar = 2  $\mu\text{m}$ .

## 4 Discussion

### 4.1 Functional interpretation of tissue-specific expression profiles

As previously mentioned, functional contrasts, inferred through KEGG pathway categorization into respective functional groups (Figure 3.7), were strongest between gill and ovarian tissue. Gills were characterized by the largest diversity of functional categories, with immune system and signal transduction being the best-represented, followed by nervous, endocrine, digestive, excretory system and cellular communication *inter alia*. This is consistent with the multi-purpose role of the fish branchial tissue in maintaining systemic homeostasis. The gill provides a key barrier to the outer aquatic environment and serves as the major site of respiratory gas exchange, pH and ion balance, nitrogenous waste excretion and immune defence, being controlled and co-ordinated by a complex web of neural and endocrine pathways (Evans *et al.* 2005; Uribe *et al.* 2011). Tuna gills in particular have an unusually large surface area and thin blood-water barrier in respect to other active teleosts such as rainbow trout (Brill & Bushnell 2001) permitting extremely efficient oxygen extraction. It is considered that this entails a higher metabolic cost with respect to the maintenance of water and ion balance, explaining in part the increased metabolic rates of tunas (Bushnell & Brill 1992; Brill 1996). As a representative of gill-specific processes, aquaporin 3b (Aqp3b), a member of major intrinsic channel-forming proteins involved in teleost osmoregulation, water balance and nitrogen excretion (Cutler *et al.* 2007; Cerdà & Finn 2010), was found and confirmed in gill-specific Cluster 4 (Figure 3.9).

In contrast to the gills, the ovaries showed over-representation of glycan biosynthesis and metabolism, folding, sorting and degradation, as well as cell growth and death, nucleotide metabolism, transcription, translation, replication and repair. These processes are characteristic of developing oocytes (Babin *et al.* 2007). Transcripts found in ovary-specific Cluster 1 are functionally related to these processes (Supplement 9.1). For instance, ZP glycoprotein transcription has previously been detected and characterized for *T. thynnus* ovaries (Chini *et al.* 2008; Gardner *et al.* 2012). In the current study, ZP glycoprotein 3a.1 and ZP sperm-binding protein 4-like homologues were found in this cluster. ZP glycoproteins are incorporated in the acellular vitelline egg envelope (*zona pellucida* or *radiata*) during primary and secondary oocyte growth (Abascal & Medina 2005; Lubzens *et al.* 2010),

having an important role in the maintenance of oocyte viability and facilitation of fertilization. Primary oocyte growth is also characterized by intense transcriptional activity and the presence of abundant ribosomes in highly granulated ooplasm (Abascal & Medina 2005; Babin *et al.* 2007). Maternal factors, protein and RNA species, are produced at this time and serve to support embryo development until the zygotic genome is activated (Selman *et al.* 1993; Pelegri 2003; Babin *et al.* 2007). Our analyses also suggest these processes are coupled with RNA degradation and mRNA surveillance pathways, crucial for maintenance of the integrity of transcriptional activity. Expression of a pescadillo (Pes) homologue, important for early embryonic development in zebrafish (Allende *et al.* 1996), cell cycle progression and 60S ribosomal subunit synthesis (Kinoshita *et al.* 2001; Oeffinger *et al.* 2002), and a transcript corresponding to exosome component 2 (Exosc2) of the exosomal complex, comprising several 3'-5' exoribonucleases involved in mRNA, 5.8S rRNA and small RNA processing (van Hoof & Parker 1999; Allmang *et al.* 1999), were confirmed as ovary-specific in respect to other tested tissues (Figure 3.9). These processes could also reflect the fact that the specific total RNA population of *T. thynnus* ovary might be dominated by the 5S RNA fraction, thus resembling the oocyte RNA complement of African clawed frog *Xenopus laevis* (Picard & Wegnez 1979), Iberian ribbed newt *Pleurodeles waltl* (Van den Eynde *et al.* 1989) and a number of teleost species (Mazabraud *et al.* 1975; Diaz de Cerio *et al.* 2012). It is believed that the 5S fraction is stored with aminoacyl-tRNAs in 7S and/or 42S ribonucleoprotein particles in the ooplasm and is progressively transferred, starting with vitellogenesis, into ribosomes by the end of oocyte differentiation (Picard & Wegnez 1979). This observation concurs well with our samples being taken during winter when the most advanced oocyte stage found in *T. thynnus* ovaries is perinucleolar (Corriero *et al.* 2003). Other typical ovarian transcripts were also present in Cluster 1, including the aquaporin 1a homologue, previously detected in *T. thynnus* ovaries (Chini *et al.* 2008; Gardner *et al.* 2012) and involved in the process of oocyte hydration prior to ovulation, which is necessary for providing buoyancy in pelagic fish eggs (Fabra *et al.* 2005, 2006; Babin *et al.* 2007). A major driving force of this water influx is the osmotic pressure produced by oocyte yolk protein cleavage by lysosomal proteases termed cathepsins. Cathepsins B, D and L have been implicated in this process in fish (Carnevali *et al.* 1999; Babin *et al.* 2007). Gardner *et al.* (2012) found transcripts similar to cathepsin S, L and cathepsin Z precursor differentially expressed in ovarian relative to testis tissue in *T. thynnus* and postulated that the species likely uses

different cathepsin proteases for this purpose. In this study, expression profiles of different cathepsin-like transcripts (A, L, F, S, Z) were detected across tissue clusters with transcript similar to cathepsin S encompassed in the ovary-specific Cluster 1, therefore supporting this hypothesis (Supplement 9.1).

Testes appeared functionally similar to ovaries, characterized by nucleotide metabolism, replication, repair and translation; however, they were placed in a different cluster (Figure 3.7) and were more similar to other inspected tissues. Some of the transcriptional differences between ovary and testis have been identified for *T. thynnus* (Gardner *et al.* 2012). A similar transcript to one found differentially expressed in the previous study, is present here in the testes-specific Cluster 6; a component of t-complex Tcte1, important for molecular interaction between sperm and egg *zona pellucida* (Juneja *et al.* 1998). This was also identified as testis-specific in rainbow trout by Rolland *et al.* (2009), when compared to ovary, liver, muscle, gill and brain transcripts. Fatty acid binding protein 2, intestinal (Fabp2) suggested to play a role in sex dependent energy balance by Gardner *et al.* (2012) was found in heart-specific Cluster 2 with its expression markedly elevated in testes compared to ovaries. The presence of several typical pituitary hormone transcripts, growth hormone (GH) and somatolactin (SL), were also apparent in the testes-specific cluster. The expression profile for somatolactin was re-investigated with qPCR and joint analysis of both datasets statistically confirmed ( $P < 0.05$ ) this observation (Figure 3.9). Both hormones are members of the growth hormone/prolactin family and are implicated in pleiotropic functions such as somatic growth, osmoregulation, lipid metabolism and reproduction (Kaneko & Hirano 1993; Pérez-Sánchez 2000). Extra-pituitary expression of growth hormone has been demonstrated in mammals and chicken testes (Harvey *et al.* 2004), as well as fish (Filby & Tyler 2007; Miura *et al.* 2011) being localized to spermatogonia and primary spermatocytes in chicken and Sertoli cells surrounding the germ cells in Japanese eel. It has a paracrine role during spermatogenesis, stimulating proliferation of spermatogonia. This mitotic phase of spermatogenesis occurs in Mediterranean *T. thynnus* between October and January (Abascal *et al.* 2004), corresponding to the collection period for our samples. Accordingly, a germ cell line marker vasa homologue (Vasa), a putative RNA helicase found to be expressed in Pacific bluefin tuna spermatogonia (Kobayashi *et al.* 2002; Nagasawa *et al.* 2009), was also found to be up-regulated in testes of *T. thynnus* examined here. Primarily expressed in the pituitary gland, somatolactin mRNA has

been detected across various tissues, including gonads in fish (Yang *et al.* 1997; Lynn & Shepherd 2007). These findings suggest *T. thynnus* testes actively transcribe GH and SL, warranting further investigation, especially in the context of reproductive cycle in both gonads.

Functional analyses did not reveal any new additional pathways for the ovary/testis combination, referred to as gonad-specific, with respect to other tissues (Supplement 9.2). Gonad-specific Cluster 5 was characterized by the presence of transcripts generally important for germline development such as a subunit of mediator complex (Med6), transcriptional regulator of RNA polymerase II particularly important for expression of developmentally regulated genes (Kwon *et al.* 1999; Boube *et al.* 2002), and fanconi anaemia complementation group 1 (Fanci), part of the DNA repair mechanism during homologous recombination in meiosis (Titus *et al.* 2009). Piwi-like 2 (Piwil2) homologue, essential for the germline integrity via transposable element repression and gonad development (Zhou *et al.* 2012; Zhang *et al.* 2014), was also found in this cluster.

During their spawning migrations, tuna utilize perigonadal mesenteric fat deposits as a source of metabolic energy for reproductive maturation and active swimming, which are primarily processed by the liver (Mourente *et al.* 2002; Abascal *et al.* 2004). In this study the *T. thynnus* liver was functionally characterized by lipid, amino acid and carbohydrate metabolism, fat digestion and absorption, bile secretion, metabolism of cofactors and vitamins, xenobiotic biodegradation and immune system, consistent with the basic metabolic role of this organ (Wolf & Wolfe 2005) and agreeing with the previously generated EST library from *T. thynnus* (Chini *et al.* 2008). Among the transcripts showing predominant expression in the liver, members of a haem-containing superfamily of cytochrome P450 mono-oxygenases, involved in metabolic biotransformation of xenobiotics and lipids often associated with liver (Andersson & Förlin 1992; Olsvik *et al.* 2007), were found. The liver is also a key production site for coagulation and complement proteolytic cascade components, mediators of blood clotting and elements of the innate immune system. Two representative transcripts, homologues of blood coagulation factor V (F5), pivotal proteins in maintaining haemostasis with dual pro-coagulant and anti-coagulant activities in humans (Segers *et al.* 2007), and complement component C4 (C4), which plays a crucial role in the classical and lectin pathways of complement activation as a subunit of the C3 convertase (Boshra *et al.* 2006), were found to be significantly up-

regulated in the liver compared to other tissues (Figure 3.9).

Tuna cardiac function has been the subject of extensive investigation, as their hearts operate at ambient temperature while supporting high metabolic rates and endothermic physiology (Block & Stevens 2001). Tuna have large hearts that function at close to maximum stroke volumes and depend, more than other teleosts, on oxygen consuming fatty acid oxidation as a fuel source, similar to mammals (Bushnell & Brill 1992; Moyes 1996). Mitochondria isolated from skipjack tuna ventricles have a higher capacity to oxidize lactate than other metabolites, suggesting that lactate is also an alternative fuel source, especially during high intensity swimming when blood lactate is elevated (Moyes *et al.* 1992). These processes were well represented in the pathways and functional categories assigned to *T. thynnus* heart (*apex ventriculi*) compared to gill, liver and gonads in this study. Lipid (fatty acid degradation), energy (oxidative phosphorylation), carbohydrate metabolism (pyruvate metabolism, glycolysis/gluconeogenesis) and circulatory system (cardiac muscle contraction) were most prominent functional categories displayed for the heart (Figure 3.7). The ability to maintain cardiac performance during temperature acclimation, especially to cold, has been linked at the transcriptomic and functional level to Ca<sup>2+</sup>-dependent excitation-contraction coupling (EC) in *T. orientalis* (Shiels *et al.* 2011; Jayasundara *et al.* 2013). Up-regulation of sarcoplasmic reticulum calcium-ATPase 2 (Atp2a2a or Serca2) homologue, vital for Ca<sup>2+</sup> removal from cytosol into sarcoplasmic reticulum in vertebrates (Landeira-Fernandez *et al.* 2012), has been identified in *T. thynnus* heart-specific Cluster 2.

In respect to pairwise tissue combinations, comparisons where two tissues were tested against all others, those including gill, heart or liver resulted in the highest levels of new pathways not allocated to any of the individual tissue tests. This new information relates to transcripts showing similar levels of expression simultaneously in two tissues. The most pronounced feature in Figure 3.7 is the up-regulation of metabolism of other amino acids,  $\beta$ -alanine metabolism specifically (Supplement 9.2), found exclusively for the heart/liver combination.  $\beta$ -Alanine is produced in vertebrate liver and is used as a rate-limiting precursor for synthesis of histidine-containing dipeptides such as carnosine and anserine in skeletal muscle, heart and brain (Abe 2000; McCarty & DiNicolantonio 2014). These compounds are involved in intracellular pH buffering by tissues exhibiting high dependence on anaerobic glycolytic metabolism in which lactic acid is generated, such as fast-twitch white skeletal muscle

in fish (Abe 2000). High levels of histidine-containing dipeptides have been recorded for skipjack tuna white muscle, with anserine largely exceeding carnosine (Abe *et al.* 1986). Aside from strong buffering capacity, carnosine has also been found to exhibit antioxidant, pro-contractile, chelating and anti-glycating properties and it is considered that  $\beta$ -alanine diet supplementation can have protective cardiac effects due to increased levels of carnosine (McCarty & DiNicolantonio 2014). Other important pathways mediating environmental and physiological adaptation were also identified. HIF-1 (hypoxia inducible factor) signalling pathway was found to be up-regulated in gill/heart and heart/liver combinations. HIF is a transcriptional factor governing the physiological response to hypoxia that induces a wide range of changes in energy metabolism, red blood cell formation, vascularisation, oxygen transport and apoptosis (Nikinmaa & Rees 2005). Regulation of HIF-1 $\alpha$  has been reported in haematopoietic and gas-exchange organs in *T. orientalis* as a result of cold temperature acclimation (Mladineo & Block 2009). ABC transporter systems were found to be up-regulated in gill/heart and gill/liver combinations. The ATP-binding cassette (ABC-transporters) are trans-membrane spanning proteins involved in substrate translocation across membranes and form the basis of multi-xenobiotic resistance mechanism in aquatic animals, with high detoxification relevance. They also participate in transport of lipids, ions and other metabolites and have been attributed various tissue-specific roles (Luckenbach *et al.* 2014). Finally, insulin signalling pathway was found up-regulated in all pairwise combinations of gill, heart and liver, in contrast to reproductive tissues. Exerting its effect through insulin receptors and associated effector signalling cascade actively transcribed in various peripheral organs, insulin has been implicated in wide range of processes in fish, including vital carbohydrate and lipid metabolism, appetite regulation, growth and development (Caruso & Sheridan 2011).

## **4.2 Functional interpretation of transcriptomic and ultrastructural changes associated with *D. katsuwonicola* infection in *T. thynnus* gills**

Helminths comprise a phylogenetically diverse group of organisms: acanthocephalans, nematodes, trematodes and cestodes, many of which exhibit parasitic lifestyle associated with great economic and medical importance as they infect animals and humans and can provoke fatal diseases, like schistosomiasis or fascioliasis (Moreau & Chauvin 2010). Although relatively large in size and with complex life cycles that include active migration through the host tissue, helminthic infections tend to have chronic and subclinical character, the result of a long-term co-evolution of the host and the parasite.

Despite their diversity, helminths elicit consistent immune responses from mammalian hosts characterised by hypereosinophilia, considerable plasma cell IgE production, mucous mastocytosis, and goblet cells hyperplasia, accompanied by the production of the cytokines interleukin-4 (IL-4), IL-5, IL-9, IL-10, IL-13, collectively known as T-helper 2 (Th2) immune response (Anthony *et al.* 2007; Moreau & Chauvin 2010). Conversely, pro-inflammatory Th1 response is characterised by production of IL-2, IFN- $\gamma$ , lymphotoxin (LT- $\alpha$ ), TNF- $\alpha$  and other chemokines that stimulate phagocytosis, the oxidative burst, intracellular killing of microbes and antigen presentation to T cells by up-regulation of expression of class I and class II major histocompatibility complex (MHC) molecules on a variety of cells, reviewed in Spellberg & Edwards (2001) and Anthony *et al.* (2007). Th1 and Th2 immunity are interconnected as former also stimulates antibody production and latter actively suppresses IL-2 and IFN- $\gamma$  through the action of IL-4 and IL-10 inhibiting T cell differentiation. Th1 cell-mediated immune response is by default initiated in an attempt to clear and phagocytise intracellular and small pathogens, and automatically switched to humoral and antibody stimulating Th2 response over the course of infection in order to re-establish homeostasis (Spellberg & Edwards 2001). In contact with large extracellular invaders such as helminths, or overwhelming microbial burdens, adaptive Th2 response occurs immediately to avoid auto-inflammatory tissue destruction of the host. Polarization of the immune response, principally driven by CD4<sup>+</sup> T helper cells differentiation, into either phenotype, or a mixture of both, depends on various components, cytokine milieu being most important, hormones, antigen dose and antigen presenting cells, as well as systemic condition of the host and the parasite. Innate immune cells, phagocytes, make the decision to stimulate

type 1 or 2 response based on “danger signals” they encounter in the microenvironment. In addition to being adaptive from the perspective of the host, it is considered that helminths actively interfere and drive the initiation of more immune-tolerating type 2 response to create milieu in which they are allowed to successfully feed and propagate (Maizels *et al.* 2004). The host-parasite interaction can have different outcomes: in murine model of hookworm infection with *Heligmosomoides polygyrus* polarized type 2 response leads to expulsion of the parasite from the intestines, whereas type 2 response primarily down-regulates initial type 1 response during infection with a trematode *Schistosoma mansoni* and attenuates the advent of pathological granulomatous inflammation after egg deposition in the liver (Anthony *et al.* 2007).

Recently, innate immune cells, neutrophils and alternatively activated macrophages (AAMΦs), have been recognized as crucial effector cells of type 2 immune response. AAMΦs are characterized by arginase-1, IL-4 receptor α-chain (IL-4R $\alpha$ ), the mannose receptor CD206, the absence of inducible nitric oxide synthase (iNOS) expression and seem to exert tripartite function: control of type 1 immune response, wound healing and parasite expulsion (Anthony *et al.* 2007; Kreider *et al.* 2007). Bonne-Année *et al.* (2013) demonstrated that human and mouse AAMΦs collaborate with neutrophils and complement components to kill the parasite *Strongyloides stercoralis in vitro*. Accelerated tissue repair can be as important as parasite control when facing metazoan migration through the host tissue and there is significant overlap in cellular and molecular mechanisms that mediate both effects. Releasing toxic granules in the presence of the parasite and acting as antigen presenting cells, eosinophils participate in the pathogen elimination as well as AAMΦs. Both cell types can be a source of wound healing regulators, such as angiogenic RELMs (resistin-like molecules), transforming growth factors (TGF $\alpha$  and TGF $\beta$ ), fibroblast growth factors, and participate in collagen turnover by exerting transcriptional control over extracellular matrix degrading matrix metalloproteinases (MMPs) and their inhibitors (Allen & Sutherland 2014).

When teleost responses against helminthic infections are concerned, much can be learned from mammalian host models. Fish are the oldest vertebrate group and ancestor to the development of the adaptive immune response. Due to their evolutionary importance in the origin of adaptive immunity, their defence mechanisms and interactions with parasites, including helminths, have been well studied and

reviewed in literature (Secombes & Chappell 1996; Alvarez-Pellitero 2008; Sitjà-Bobadilla 2008; Buchmann 2012; Reyes-Cerpa *et al.* 2012; Zhu *et al.* 2013). Fish display greater variety and complexity of innate immune mechanisms combined with relatively incomplete adaptive immune responses comparing to higher vertebrates. Different pattern recognition receptors (PRRs) that recognize pathogen associated molecular patterns (PAMPs) have been found in fish, such as Toll-like receptors (TLRs), RIG-I like receptors (RLRs), NOD-like receptors (NLRs), and C-type lectin receptors (CLRs), some of which do not have counterparts in mammals (Laing *et al.* 2008; Palti 2011). Fish are equipped with fully developed enzymatic proteolytic cascades of the complement system (Boshra *et al.* 2006), various lectin family members and antimicrobial peptides that serve as first line of defence against microbial attack (Zhu *et al.* 2013). Numerous cytokines, cytokine receptors and suppressors of their signalling have been characterized from various fish species (Wang *et al.* 2011a), including markers of typical mammalian type 1 or type 2 response (Zou *et al.* 2005; Wang *et al.* 2011b; Reyes-Cerpa *et al.* 2012; Hammarén *et al.* 2014). With CD8<sup>+</sup> and CD4<sup>+</sup> T cells, immunoglobulin producing B cells, macrophages, polymorphonuclear leukocytes, and MHC class I and II interaction molecules present (Buchmann 2012; Zhu *et al.* 2013), it is reasonable to search for mammalian paradigm in fish responses against helminths. However, different teleost species may be employing different means to the same end. As it was recently discovered, MHC class II and CD4<sup>+</sup> genes are absent from Atlantic cod, *Gadus morhua* genome sequence, yet the species does not show increased susceptibility to disease in the natural environment (Star *et al.* 2011). Somatic-recombination class switch mechanism from IgM to IgE, a hallmark of mammalian type 2 response, is absent in fish (Stavnezer & Amemiya 2004). Fish have limited repertoire of immunoglobulins, most important antigen receptors and antibodies, compared to mammals, where IgE orthologue is completely absent, IgM tetramer predominates, but other tissue-related functional Igs have been discovered, such as IgD, IgZ, IgT, as well as unusual membrane IgM isoform in zebrafish (Hu *et al.* 2011) and a chimeric IgM-IgZ structure identified in common carp (Savan *et al.* 2005). Furthermore, alternatively activated macrophages have not been defined in fish, but genes encoding their molecular functions exist (Buchmann 2012). Fish macrophages have been found to elicit cytokine and specific antibodies assisted cytotoxic effects against helminths through reactive oxygen species production (Whyte *et al.* 1989; Secombes & Chappell 1996). There is much to be learned from fish interactions with

pathogens, especially considering the variability, flexibility and the origin of existing and well established immune responses encountered in higher vertebrates.

In this study we have used transcriptomic and ultrastructural approach to explore the interaction between Atlantic bluefin tuna *T. thynnus* and a digenean (Trematoda) parasite *Didymosulcus katsuwonicola*, the most abundant species of tuna parasite assemblages (Mladineo *et al.* 2011). The infection is manifested as the presence of fibrous cysts on the host gill filaments encapsulating two digeneans and the absence of gross pathological signs (Mladineo 2006). At the time of sampling, the cysts were already well established, visible and approximately 2 mm in diameter, indicating a chronic process. Encapsulation of different didymozoid parasites is commonly observed reaction in tuna and other scombrid hosts (Perera 1992a; b, 1994; Marino *et al.* 2003; Mladineo 2006; Justo *et al.* 2008, 2013; Di Maio & Mladineo 2008). Fibronnective capsule containing fibroblasts is infiltrated with different immune cell types, lymphocytes, macrophages or eosinophilic granulated cells (Perera 1994; Mladineo 2006; Justo *et al.* 2013) with varying degrees of vascularization, from almost absent (Di Maio & Mladineo 2008) to highly pronounced (Marino *et al.* 2003; Justo *et al.* 2008), correlating with the severity of associated inflammatory response and tissue damage caused. In our case, the ultrastructural analyses inferred through TEM revealed the abundant collagenous matrix of the capsule comprising fibrocytes, fibroblasts, eosinophilic-granulated mast cells, eosinophils, plasma cells with well-developed endoplasmic reticulum, few rodlet and numerous mucus-producing goblet cells, indicating the accumulation of cellular immune machinery around the parasite. Numerous transiting vesicles recorded in didymozoid's tegument in direct contact with the capsule, network of anastomosing capillaries and presence of nerve fibres point to the active molecular cross-talk between the host and the parasite.

Based on different neuropeptides identified in the heart of *Coregonus lavaretus* infected with *Ichthyocotylurus erraticus*, Dezfuli *et al.* (2005) suggested that innervation might serve to stimulate blood flow through the developing cyst. The mast cells/eosinophilic granule cells are, similarly to mammals, important innate mediators of inflammation in fish, degranulating vasoactive and pro-inflammatory mediators at the site of insult and associated with helminthic infections along with teleost specific rodlet cells (Ainsworth 1992; Reite & Evensen 2006). Strikingly developed rough endoplasmic reticulum of plasma cells is consistent with their role in active synthesis of immunoglobulins. The ability to mount a humoral specific

response has been demonstrated for Southern bluefin tuna *T. maccoyii* against blood fluke *Cardicola forsteri* in serum (Aiken *et al.* 2008) and elevated transcription of IgM in the gills of Pacific bluefin tuna *T. orientalis* against two *Cardicola* species (Polinski *et al.* 2014). Immunoglobulin transcription was not detected in our case, however the homologous sequences were not represented on the microarray. Further studies are necessary to establish if humoral response is initiated in *T. thynnus* against *D. katsuwonocola*, in which case it could provide the host with the protective immunity against reinfection, as observed for the eye fluke *Diplostomum spathaceum* in rainbow trout (Karvonen *et al.* 2005), and account in some part for the conspicuous decline of the parasite abundance during tuna rearing cycle. Aside from their crucial role in extracellular matrix (ECM) production and remodelling, fibroblasts, the only cell type consistently reported with all didymozoid infections, are powerful cytokine producing cells and can significantly contribute to shaping of local inflammatory reactions (Ingerslev *et al.* 2010; Mladineo & Block 2010).

Microarray analyses of associated transcriptome revealed moderate differences in gene expression when compared to the uninfected gill lamellae, with only 16.6 % of significant transcripts being regulated more than or at least twice. This is consistent with the chronic nature of the infection and its low pathogenic impact. Although various immune cells were recruited at the fibrous capsule surrounding the didymozoid, eosinophils, mast cells, plasma cells, consistent with the mammalian type 2 response, functional KEGG pathway analyses depicted primarily metabolic disorder with significant perturbation and loss of neuro-endocrine and signalling processes coupled with gap junction and extracellular matrix communication decline (Table 3.6). The only immune system significantly induced and bidirectionally perturbed was the complement and coagulation proteolytic cascade. Some of the cytokines noted indicate a rather pro-inflammatory state with moderate induction of TNF $\alpha$  and suppression of transforming growth factor TGF $\beta$  (Table 3.7). The status of other cytokines typically involved in type 2 response is currently unknown as they were not sequenced nor included on the microarray.

Similar moderate transcriptional stimulation compared to one registered here of acute phase cytokine TNF $\alpha$ , one of the first initiators of inflammatory reaction upon insult, was previously detected in congeneric host *T. orientalis* gill tissue surrounding the cysts of *D. katsuwonocola* (Mladineo & Block 2010). The authors did not find similar response in the spleen, kidney, liver nor skin mucus of *T. orientalis*, confirming

the local impact of the infection. A subsequent study in our laboratory showed that it is the TNF $\alpha$ 2 isoform that is most responsive to *D. katsuwonocola*, while treatment of tuna peripheral blood leukocytes (PBL) with *D. katsuwonocola* total antigen extract suppresses TNF $\alpha$ 1, indicating its possible role in later stages of infection (Lepen Pleić *et al.* 2015). TGF $\beta$  is a pleiotropic cytokine affecting various cellular processes such as proliferation, differentiation, migration, apoptosis, tissue and wound repair and is considered to have important immunosuppressive effects on Th1 type responses during helminthic infections (Anthony *et al.* 2007). TGF $\beta$ 1 induced peripheral blood leukocyte (PBL) proliferation while it significantly blocked phytohemagglutinin- or lipopolysaccharide-stimulated PBL proliferation in grass carp, suggesting its complex role in signalling network associated with leukocyte proliferation in fish (Yang & Zhou 2008). It is also one of the most potent profibrotic growth factors. Here, the down-regulation of TGF $\beta$ 3 seems to be indicated, an isoform also known to exert chondrogenetic properties (James *et al.* 2009; Cheah *et al.* 2010).

Reduced collagen mRNA production, although unexpected, was observed at this stage of infection and seems to be consistent with this cytokine profile. Human dermal and pulmonary fibroblasts have shown decrease in collagen mRNA expression level when incubated with TNF $\alpha$  (Lindner *et al.* 2012). Decreased transcription of other cytoskeletal components, such as tropomyosin, structural proteins of cellular adherens junctions, cadherin and desmoplakin, as well as components of extracellular matrix network, fibronectin and integrin, and basal lamina constituent laminin, was also observed. Degradation of tight junction proteins and paracellular barriers has been associated with increase in epithelial permeability and leakiness of intestinal mucosa in murine models of nematode infection with *Heligmosomoides polygyrus* (Su *et al.* 2011) and *Trichinella spiralis* (McDermott *et al.* 2003), mediated by mast cell specific protease in the latter case. This parasite expulsion mechanism also facilitates leukocyte transport through tissue matrix. Reduced expression of cytoskeletal and extracellular matrix (ECM) components seems to correlate with simultaneous impairment of cellular communication and signal transduction in our case, which might be beneficial for the digenean. Suppression of several pathways involved in neuro-endocrine mediation of cellular functions was noted, including serotonergic synapse and steroid signalling. The transcripts predominantly observed responsible for this pattern include different receptors and signal transducers functionally shared between different pathways, like epidermal growth factor receptor, insulin receptor, a

voltage-dependent calcium channel, p38 MAP kinase and guanine nucleotide-binding protein G(q) subunit alpha, or metabolic enzymes also participating in arachidonic acid metabolism (discussed later). This effect might be the result of immune related events. Evidence from human research indicate that inflammatory effects of TNF antagonise the natural GnRH response (MacEwan 2008), highlighting the immune-neuro-endocrine interface. Furthermore, differential expression of two homologues of matrix metalloproteinases (MMPs) was recorded, slight elevation of MMP-14 and suppression of MMP-9, also involved in steroid signalling pathways. MMPs are zinc-dependent endopeptidases involved in extracellular matrix degradation and remodelling, with important inflammatory role as they proteolytically facilitate macrophage and leucocyte migration, expose hidden epitopes and receptors and impact cytokine signalling (Zitka *et al.* 2010). Gelatinases MMP-2 and MMP-9, collagenase MMP-13 have mostly been involved in inflammatory responses associated with bacterial infections in different fish species and parasitic copepod *Lepeophtheirus salmonis* infection in Atlantic salmon (Pedersen *et al.* 2015). In a zymosan-induced peritonitis model for common carp *Cyprinus carpio*, MMP-9 induced expression was recorded twice, during the initial phase and during the process of termination of the inflammatory response (Chadzinska *et al.* 2008). It was also up-regulated during first several days of establishment a monogenean *Neoheterobothrium hirame* infection in Japanese flounder *Paralichthys olivaceus*, and subsequently declined (Matsuyama *et al.* 2007). Until the termination of infection ensues, it seems that in our digenean infection model suppression of MMP-9 might promote profibrotic state after the reduction in production and deposition of collagen. MMP-14 (or MT1-MMP) is a membrane metalloproteinase with decreased affinity for collagen degradation, however involved in other metalloproteinases zymogen activation and important for embryogenesis in zebrafish (Zhang *et al.* 2003). It was reported to provide malignant cells with protection mechanism against complement-mediated cytotoxicity by cleaving opsonizing components C3b and C4b and inhibiting the complement cascade (Rozanov *et al.* 2004). Up-regulation of C4 in our case, the transcript showing the highest increase in expression, could be compensatory response. Interestingly, the expression of MMP-9, MMP-14 and angiogenic factor angiopoietin 2 was found to be positively regulated by TNF $\alpha$  in a study of vascularization and turnover of mineralized cartilage associated with fracture healing (Lehmann *et al.* 2005). Reduction of MMP-9 and angiopoietin 2, suggesting the cessation of neovascularization processes, in our study reflect the specificities of

parasite and host interaction.

Complement system represents important effector of innate immunity in fish serum, skin, mucosal surfaces, facilitating opsonisation, phagocytosis of invaders, cytotoxic killing and antigen processing, linking the innate and adaptive immune response (Boshra *et al.* 2006), the only immune related pathway registered in our study. Complement can be activated *via* classical pathway, initiated by antibody-antigen complex, alternative pathway when C3 is activated upon direct binding to various microbial surfaces, and lectin pathway. The latter proceeds through a mannose-binding lectin (MBL) or ficolin interacting with carbohydrate moieties on pathogen surface which activates mannan-binding serine lectin proteases that cleave C2 and C4 components. Although classical and alternative pathways have been commonly associated with pathogen interactions in fish (Boshra *et al.* 2006; Alvarez-Pellitero 2008; Zhu *et al.* 2013), the up-regulation of latter components (Figure 3.11) implies that lectin-activated complement is involved in *T. thynnus* response to digenean infection. Binding of MBL has been associated with many pathogens, however best described in various bacteria (Jack *et al.* 1998), one of the reasons why this trematode infection was portrayed as a bacterial infectious disease in KEGG pathway analyses. Involvement of adventitious or indigenous bacteria in host interaction with *D. katsuwonicola* cannot be completely ruled out as it was previously known to exacerbate secondary bacterial infections in tuna (Mladineo 2006). Carbohydrate determinants can highly influence host-parasite relationships and helminthic N-glycans have a tendency for fucosylated side chains and high mannose content (Klabunde *et al.* 2000; Maizels *et al.* 2004), possibly explaining this complement activation pathway. Mannose-rich glycoproteins were determined to be major activators of complement alternative pathway in *Oncorhynchus mykiss* against monogenean *Gyrodactylus derjavini* (Buchmann 1998). Cytotoxic effects against helminths are known to be dependent on the activation of complement system (Hoole & Arme 1986; Whyte *et al.* 1989; Secombes & Chappell 1996; Bonne-Année *et al.* 2013). Complement can facilitate leukocyte adherence to parasite surface through their complement-receptors (Sher 1976; McLaren & Ramalho-Pinto 1979). In addition, complement anaphylatoxins can provide chemotactic gradient and orchestrate numerous responses from other cells, like mast cells and eosinophils, affecting degranulation, secretion of cytokines, matrix metalloproteinases (DiScipio & Schraufstatter 2007), or the release of reactive oxygen species (ROS), indicated here

by the up-regulation of NADPH oxidase (cytochrome b-245, Cybb) (Kazura *et al.* 1981; Secombes *et al.* 1992). The striking inter-individual variability in expression of some immune components was demonstrated for complement component C4 homologue, confirmed both by microarray and qPCR (Figure 3.12). This could result from high cellular diversity associated with the digenean capsule, not necessarily equally represented in all samples, pointing further to the variability of individual host-parasite interaction dependent on various factors, like size and age of the host, duration of infection, abiotic factors, and most importantly genetic background (Haase *et al.* 2014).

Interestingly, in a transcriptomic study by RNA sequencing of advanced enteromyxosis in turbot *Scophthalmus maximus*, the authors observed several features of host response in pyloric caeca that show similarity to patterns observed here, in *T. thynnus* gills, such as complement activation through lectin pathway and down-regulation of numerous genes encoding cytoskeletal and extracellular matrix proteins, like collagen (Robledo *et al.* 2014). It was suggested that starvation and intestinal damage induced by prolonged infection of *Enteromyxum scophthalmii* might compromise protein synthesis as it is an energy-demanding process. This could partially be applicable here as protein digestion and absorption were generally perturbed with tendency toward down-regulation. The suppression of facilitated glucose transporter GLUT1 (MFS transporter, SP family, solute carrier family 2, member 1) was evident (Table 3.7) and induction of 5'-AMP-activated protein kinase (AMPK) that plays a role in cellular energy homeostasis, which could be a compensatory response. Additionally, a homologue of intestinal fatty acid binding protein 2 (Fabp2) was significantly down-regulated. Fabp2 belongs to a group of molecules that act as intracellular lipid chaperones that reversibly bind hydrophobic ligands, such as saturated and unsaturated long-chain fatty acids and coordinate lipid responses in cells (Furuhashi & Hotamisligil 2008). Lipids participate in many vital cellular processes like energy metabolism, cell signalling, transcriptional regulation or inflammation. As mentioned in previous microarray experiment, it was found to be highly expressed in *T. thynnus* heart and suggested to play a role in sex dependent energy balance by Gardner *et al.* (2012). We have also observed the down-regulation of arachidonic acid metabolism pathway where arachidonic acid is released from membrane phospholipids in response to inflammatory stimuli, converted to prostaglandin H<sub>2</sub> by the cyclooxygenase enzymes COX-1 and COX-2 (also known as

prostaglandin endoperoxide synthases) after which numerous prostaglandins can be generated *via* their respective synthases. Prostaglandins are potent eicosanoid modulators of basic homeostatic physiological functions, such as mucus secretion, or contribute to the control of local immune response by suppressing type 1 cytokines, ROS production and promoting vasodilation (Harris *et al.* 2002; Lindenstrøm *et al.* 2004), in which case the observed down-regulation corresponds with generally pro-inflammatory fibrous environment in *D. katsuwonicola* cyst. Interestingly, parasites also produce prostaglandins and use them as immunomodulatory effectors to control host response and behaviour (Sitjà-Bobadilla 2008).

Helminths are generally known as masters of immunomodulation (Maizels *et al.* 2004). They produce various host-like antigens, homologues of host cytokine network, glycans, lipid molecules, lectins, protease inhibitors, antioxidants and neuropeptides in order to achieve molecular mimicry, inhibit or otherwise exploit host immune cell signalling or even change its behaviour. It has been suggested that, rather than exerting direct effects on the host nervous system, parasites could manipulate immune-neural connections instead, and act by diverting the immune system that they are in intimate contact with (Adamo 2002). For instance, the activation of innate immune system and up-regulation of head kidney leukocytes' respiratory burst activity in three-spined stickleback happens late during the infection with a cestode *Schistocephalus solidus*, when the parasite is ready for transmission to its final host (Scharsack *et al.* 2007). The authors suggested this might interfere with neuroendocrine signalling and promote reduced predation avoidance behaviour. Several helminths utilize hosts inflammatory reaction to secure their attachment to different predilection sites in gills, intestine, heart (Sitjà-Bobadilla 2008). *D. katsuwonicola* might be using the same strategy to create a shelter within fibrous capsule in tuna gills, where it manages to feed and procreate. It is foreseeable that, should the observed condition with reduced collagen synthesis and remodelling persist, the parasite growth might exert substantial pressure on the cyst wall resulting in parasite and egg expulsion into the environment, one of the possible ways this infection might be further propagated.

Finally, the data should be interpreted with some caution as the exact source of the significant signal observed during heterologous hybridizations of *D. katsuwonicola* transcripts to *T. thynnus* microarray cannot be ascertained. Molecular mimicry and the need to immunomodulate evolutionary reflect at helminth's nucleotide sequence level

as well. High degree of similarity was established between various parasite and mammalian genes for structural, regulatory proteins, enzymes and growth factors, reviewed in Salzet *et al.* (2000). Using comparative genomics, Yu *et al.* (2008) identified several extremely similar homologues between *Schistosoma japonicum* and its human host, with some of them displaying human codon usage bias suggesting horizontal gene transfer as probable mode of acquisition. This implies that conspicuous cross-hybridizational signal observed could be biologically relevant. Nonspecific hybridization, faulty probes, accidental transfer from the host during sample handling and cyst separation, evolutionary conserved nature of certain genes (like ribosomal proteins) probably all contribute to the observed phenomenon. However, in a more appropriate experimental design this type of microarray application could be used to determine transcripts with physiological and evolutionary relevance in host-parasite systems.

## 5 Conclusions

Newly sequenced cDNA library, built from different adult captive *T. thynnus* tissues, captured both existing and novel knowledge with respect to the EST archive for this species. It provides an important transcriptomic resource that can be further deployed for study of various aspects of *T. thynnus* ecology and genomics with strong application in aquaculture. New and flexible gene expression profiling tool, in the form of a 15K oligonucleotide DNA microarray, was successfully developed and validated. The inferred expression profiles for gill, heart, liver and gonads provide a useful starting point for exploring gene expression patterns in *T. thynnus* and for planning new transcriptomic studies. The oligo-microarray can also be further expanded to include un-annotated transcripts from the generated library with the aim of extending their functional characterization through correlation with annotated entities. It is important to keep in mind that even tissue specific profiles can be population dependent (Whitehead & Crawford 2005), and that environmental pressures can shape transcriptional signatures over phylogenetic distance (Malenke *et al.* 2013), warranting further research on captive and wild tuna populations.

Cellular and molecular components of the interaction of Atlantic bluefin tuna *T. thynnus* with the digenean trematode *Didymosulcus katsuwonicola* have been investigated. Various immune cell types, such as eosinophils, mast cells, plasma cells, rodlet and goblet cells, and fibroblasts have been observed in the fibronnective capsule encysting the parasite exerting moderate transcriptional regulation. At this stage, mild pro-inflammatory environment is indicated, with the activation of complement system, dampened collagen, extracellular matrix synthesis as well as neuro-endocrine signalling. In order to put these findings in the correct context, further studies will have to be conducted to investigate the parasite side of the story, as immunomodulation is common among helminths, also addressing the possible sequence similarity between the tuna and the digenean observed in this study.

## 6 References

- Abascal FJ, Medina A (2005) Ultrastructure of oogenesis in the bluefin tuna, *Thunnus thynnus*. *Journal of Morphology*, **264**, 149–160.
- Abascal F, Megina C, Medina A (2004) Testicular development in migrant and spawning bluefin tuna (*Thunnus thynnus* (L.)) from the eastern Atlantic and Mediterranean. *Fishery Bulletin*, **102**, 407–417.
- Abe H (2000) Role of histidine-related compounds as intracellular proton buffering constituents in vertebrate muscle. *Biochemistry (Moscow)*, **65**, 757–765.
- Abe H, Brill R, Hochachka P (1986) Metabolism of L-histidine, carnosine, and anserine in skipjack tuna. *Physiological Zoology*, **59**, 439–450.
- Adamo SA (2002) Modulating the modulators: Parasites, neuromodulators and host behavioral change. *Brain, Behavior and Evolution*, **60**, 370–377.
- Aiken HM, Hayward CJ, Crosbie P, Watts M, Nowak BF (2008) Serological evidence of an antibody response in farmed southern bluefin tuna naturally infected with the blood fluke *Cardicola forsteri*. *Fish & Shellfish Immunology*, **25**, 66–75.
- Ainsworth AJ (1992) Fish granulocytes: Morphology, distribution, and function. *Annual Review of Fish Diseases*, **2**, 123–148.
- Allen JE, Sutherland TE (2014) Host protective roles of type 2 immunity: Parasite killing and tissue repair, flip sides of the same coin. *Seminars in Immunology*, **26**, 329–340.
- Allende ML, Amsterdam A, Becker T *et al.* (1996) Insertional mutagenesis in zebrafish identifies two novel genes, pescadillo and dead eye, essential for embryonic development. *Genes & Development*, **10**, 3141–3155.
- Allmang C, Kufel J, Chanfreau G *et al.* (1999) Functions of the exosome in rRNA, snoRNA and snRNA synthesis. *The EMBO Journal*, **18**, 5399–5410.
- Altschul S, Gish W, Miller W, Myers E, Lipman D (1990) Basic local alignment search tool. *Journal of Molecular Biology*, **215**, 403–410.
- Alvarez-Pellitero P (2008) Fish immunity and parasite infections: from innate immunity to immunoprophylactic prospects. *Veterinary Immunology and Immunopathology*, **126**, 171–198.
- Andersson T, Förlin L (1992) Regulation of the cytochrome P450 enzyme system in fish. *Aquatic Toxicology*, **24**, 1–20.
- Anthony RM, Rutitzky LI, Urban JF, Stadecker MJ, Gause WC (2007) Protective immune mechanisms in helminth infection. *Nature Reviews Immunology*, **7**, 975–987.
- Ashburner M, Ball C, Blake J *et al.* (2000) Gene ontology: tool for the unification of biology. The Gene Ontology Consortium. *Nature Genetics*, **25**, 25–29.

- Babin PJ, Cerdà J, Lubzens E (Eds.) (2007) *The Fish Oocyte From Basic Studies to Biotechnological Applications*. Springer Netherlands.
- Bekaert M (2013) SlimIt. <http://www.isalmon.eu/slimit/>.
- Benson G (1999) Tandem repeats finder: a program to analyze DNA sequences. *Nucleic Acids Research*, **27**, 573–580.
- Bicskei B, Bron JE, Glover KA, Taggart JB (2014) A comparison of gene transcription profiles of domesticated and wild Atlantic salmon (*Salmo salar* L.) at early life stages, reared under controlled conditions. *BMC Genomics*, **15**, 884.
- Block BA, Dewar H, Blackwell SB *et al.* (2001) Migratory movements, depth preferences, and thermal biology of Atlantic bluefin tuna. *Science*, **293**, 1310–1314.
- Block BA, Finnerty JR (1994) Endothermy in fishes: a phylogenetic analysis of constraints, predispositions, and selection pressures. *Environmental Biology of Fishes*, **40**, 283–302.
- Block BA, Finnerty JR, Stewart AF, Kidd J (1993) Evolution of endothermy in fish: mapping physiological traits on a molecular phylogeny. *Science*, **260**, 210–214.
- Block BA, Stevens ED (Eds.) (2001) *Tuna: Physiology, Ecology, and Evolution*. Academic Press, San Diego, California, USA.
- Block BA, Teo SL, Walli A *et al.* (2005) Electronic tagging and population structure of Atlantic bluefin tuna. *Nature*, **434**, 1121–1127.
- Bonne-Année S, Kerepesi LA, Hess JA *et al.* (2013) Human and mouse macrophages collaborate with neutrophils to kill larval *Strongyloides stercoralis*. *Infection and Immunity*, **81**, 3346–3355.
- Boshra H, Li J, Sunyer JO (2006) Recent advances on the complement system of teleost fish. *Fish & Shellfish Immunology*, **20**, 239–262.
- Boube M, Joulia L, Cribbs DL, Bourbon H-M (2002) Evidence for a mediator of RNA polymerase II transcriptional regulation conserved from yeast to man. *Cell*, **110**, 143–151.
- Bouck A, Vision T (2007) The molecular ecologist's guide to expressed sequence tags. *Molecular Ecology*, **16**, 907–924.
- Boustany AM, Reeb CA, Block BA (2008) Mitochondrial DNA and electronic tracking reveal population structure of Atlantic bluefin tuna (*Thunnus thynnus*). *Marine Biology*, **156**, 13–24.
- Brill RW (1996) Selective advantages conferred by the high performance physiology of tunas, billfishes, and dolphin fish. *Comparative Biochemistry and Physiology Part A: Physiology*, **113**, 3–15.

- Brill RW, Bushnell PG (2001) The cardiovascular system of tunas. In: *Tuna: Physiology, Ecology, and Evolution* Fish Physiology. (eds Block BA, Stevens ED), pp. 79–120. Academic Press, San Diego, California, USA.
- Buchmann K (1998) Binding and lethal effect of complement from *Oncorhynchus mykiss* on *Gyrodactylus derjavini* (Platyhelminthes: Monogenea). *Diseases of Aquatic Organisms*, **32**, 195–200.
- Buchmann K (2012) Fish immune responses against endoparasitic nematodes - experimental models. *Journal of Fish Diseases*, **35**, 623–635.
- Bushnell PG, Brill RW (1992) Oxygen transport and cardiovascular responses in skipjack tuna (*Katsuwonus pelamis*) and yellowfin tuna (*Thunnus albacares*) exposed to acute hypoxia. *Journal of Comparative Physiology B*, **162**, 131–143.
- Carlsson J, McDowell JR, Carlsson JEL, Graves JE (2007) Genetic identity of YOY bluefin tuna from the eastern and western Atlantic spawning areas. *The Journal of Heredity*, **98**, 23–28.
- Carnevali O, Carletta R, Cambi A, Vita A, Bromage N (1999) Yolk formation and degradation during oocyte maturation in seabream *Sparus aurata*: involvement of two lysosomal proteinases. *Biology of Reproduction*, **60**, 140–146.
- Caruso MA, Sheridan MA (2011) New insights into the signaling system and function of insulin in fish. *General and Comparative Endocrinology*, **173**, 227–247.
- Cerdà J, Finn RN (2010) Piscine aquaporins: an overview of recent advances. *Journal of Experimental Zoology Part A: Ecological Genetics and Physiology*, **313A**, 623–650.
- Chadzinska M, Baginski P, Kolaczowska E, Savelkoul HFJ, Verburg-Van Kemenade L (2008) Expression profiles of matrix metalloproteinase 9 in teleost fish provide evidence for its active role in initiation and resolution of inflammation. *Immunology*, **125**, 601–610.
- Cheah FSH, Winkler C, Jabs EW, Chong SS (2010) Tgf $\beta$ 3 regulation of chondrogenesis and osteogenesis in zebrafish is mediated through formation and survival of a subpopulation of the cranial neural crest. *Mechanisms of Development*, **127**, 329–344.
- Chini V, Cattaneo AG, Rossi F *et al.* (2008) Genes expressed in Blue Fin Tuna (*Thunnus thynnus*) liver and gonads. *Gene*, **410**, 207–213.
- Chistiakov DA, Hellems B, Volckaert FAM (2006) Microsatellites and their genomic distribution, evolution, function and applications: A review with special reference to fish genetics. *Aquaculture*, **255**, 1–29.
- Chomczynski P, Mackey K (1995) Short technical reports. Modification of the TRI reagent procedure for isolation of RNA from polysaccharide- and proteoglycan-rich sources. *Biotechniques*, **19**, 942–945.

- Chow S, Nakagawa T, Suzuki N, Takeyama H, Matsunaga T (2006) Phylogenetic relationships among *Thunnus* species inferred from rDNA ITS1 sequence. *Journal of Fish Biology*, **68**, 24–35.
- Chuaqui R, Bonner R, Best C *et al.* (2002) Post-analysis follow-up and validation of microarray experiments. *Nature Genetics*, **Supplement**, 509 – 514.
- Corriero A, Desantis S, Deflorio M *et al.* (2003) Histological investigation on the ovarian cycle of the bluefin tuna in the western and central Mediterranean. *Journal of Fish Biology*, **63**, 108–119.
- Corriero A, Medina A, Mylonas CC *et al.* (2007) Histological study of the effects of treatment with gonadotropin-releasing hormone agonist (GnRHa) on the reproductive maturation of captive-reared Atlantic bluefin tuna (*Thunnus thynnus* L.). *Aquaculture*, **272**, 675–686.
- Culurgioni J, Mele S, Merella P *et al.* (2014) Metazoan gill parasites of the Atlantic bluefin tuna *Thunnus Thynnus* (Linnaeus) (Osteichthyes: Scombridae) from the Mediterranean and their possible use as biological tags. *Folia Parasitologica*, **61**, 148–156.
- Cutler CP, Martinez A-S, Cramb G (2007) The role of aquaporin 3 in teleost fish. *Comparative Biochemistry and Physiology Part A: Molecular & Integrative Physiology*, **148**, 82–91.
- Dezfuli BS, Giari L, Simoni E *et al.* (2005) Histopathology, ultrastructure and immunohistochemistry of *Coregonus lavaretus* hearts naturally infected with *Ichthyocotylurus erraticus* (Trematoda). *Diseases of Aquatic Organisms*, **66**, 245–254.
- Diaz de Cerio O, Rojo-Bartolomé I, Bizarro C, Ortiz-Zarragoitia M, Cancio I (2012) 5S rRNA and accompanying proteins in gonads: powerful markers to identify sex and reproductive endocrine disruption in fish. *Environmental Science & Technology*, **46**, 7763–7771.
- DiScipio RG, Schraufstatter IU (2007) The role of the complement anaphylatoxins in the recruitment of eosinophils. *International Immunopharmacology*, **7**, 1909–1923.
- Djira GD, Mario H, Gerhard D, Schaarschmidt F (2012) mratios: Inferences for ratios of coefficients in the general linear model. *R package version 1.3.17*, <http://CRAN.R-project.org/package=mratio>.
- Donoho D, Jin J (2004) Higher criticism for detecting sparse heterogeneous mixtures. *The Annals of Statistics*, **32**, 962–994.
- Donoho D, Jin J (2008) Higher criticism thresholding: Optimal feature selection when useful features are rare and weak. *Proceedings of the National Academy of Sciences of the United States of America*, **105**, 14790–14795.

- Douglas SE, Knickle LC, Williams J, Flight RM, Reith ME (2008) A first generation Atlantic halibut *Hippoglossus hippoglossus* (L.) microarray: application to developmental studies. *Journal of Fish Biology*, **72**, 2391–2406.
- Ekblom R, Galindo J (2011) Applications of next generation sequencing in molecular ecology of non-model organisms. *Heredity*, **107**, 1–15.
- Evans DH, Piermarini PM, Choe KP (2005) The multifunctional fish gill: dominant site of gas exchange, osmoregulation, acid-base regulation, and excretion of nitrogenous waste. *Physiological Reviews*, **85**, 97–177.
- Van den Eynde H, Mazabraud A, Denis H (1989) Biochemical research on oogenesis. RNA accumulation in the oocytes of the newt *Pleurodeles waltl*. *Development*, **106**, 11–6.
- Fabra M, Raldúa D, Bozzo MG *et al.* (2006) Yolk proteolysis and aquaporin-1 $\alpha$  play essential roles to regulate fish oocyte hydration during meiosis resumption. *Developmental Biology*, **295**, 250–262.
- Fabra M, Raldúa D, Power DM, Deen PMT, Cerdà J (2005) Marine fish egg hydration is aquaporin-mediated. *Science*, **307**, 545.
- Ferraresso S, Milan M, Pellizzari C *et al.* (2010) Development of an oligo DNA microarray for the European sea bass and its application to expression profiling of jaw deformity. *BMC Genomics*, **11**, 354.
- Filby AL, Tyler CR (2007) Cloning and characterization of cDNAs for hormones and/or receptors of growth hormone, insulin-like growth factor-I, thyroid hormone, and corticosteroid and the gender-, tissue-, and developmental-specific expression of their mRNA transcripts in fathead minnow (*Pimephales promelas*). *General and Comparative Endocrinology*, **150**, 151–163.
- Froese R, Pauly D (2014) FishBase. World Wide Web electronic publication.
- Fromentin J-M, Powers JE (2005) Atlantic bluefin tuna: population dynamics, ecology, fisheries and management. *Fish and Fisheries*, **6**, 281–306.
- Furuhashi M, Hotamisligil G (2008) Fatty acid-binding proteins: role in metabolic diseases and potential as drug targets. *Nature Reviews Drug Discovery*, **7**, 489.
- Galaktionov KV, Dobrovolskij A. (2003) *The biology and evolution of Trematodes. An Essay on the Biology, Morphology, Life Cycles, Transmissions, and Evolution of Digenetic Trematodes.* (B Fried, T Graczyk, Eds.). Kluwer Academic Publishers, Dordrecht, The Netherlands.
- Gardner LD, Jayasundara N, Castilho PC, Block B (2012) Microarray gene expression profiles from mature gonad tissues of Atlantic bluefin tuna, *Thunnus thynnus* in the Gulf of Mexico. *BMC Genomics*, **13**, 530.
- Gentleman RC, Carey VJ, Bates DM *et al.* (2004) Bioconductor: open software development for computational biology and bioinformatics. *Genome Biology*, **5**, R80.

- Gilles A, Megléc E, Pech N *et al.* (2011) Accuracy and quality assessment of 454 GS-FLX Titanium pyrosequencing. *BMC Genomics*, **12**, 245.
- Ginetsinskaya TA (1988) *Trematodes, their life cycle, biology and evolution*. Originally published: Leningrad : Nauka publishers, 1968. Translated by Amerind Publ., New Delhi.
- Grubišić L, Šegvić-Bubić T, Lepen Pleić I *et al.* (2013) Morphological and genetic identification of spontaneously spawned larvae of captive Bluefin Tuna *Thunnus thynnus* in the Adriatic Sea. *Fisheries*, **38**, 410–417.
- Haase D, Rieger JK, Witten A *et al.* (2014) Specific gene expression responses to parasite genotypes reveal redundancy of innate immunity in vertebrates. *PLoS One*, **9**, e108001.
- Hammarén MM, Oksanen KE, Nisula HM *et al.* (2014) Adequate Th2-Type Response Associates with Restricted Bacterial Growth in Latent Mycobacterial Infection of Zebrafish. *PLoS Pathogens*, **10**, e1004190.
- Harris SG, Padilla J, Koumas L, Ray D, Phipps RP (2002) Prostaglandins as modulators of immunity. *Trends in Immunology*, **23**, 144–150.
- Harvey S, Baudet M-L, Murphy A *et al.* (2004) Testicular growth hormone (GH): GH expression in spermatogonia and primary spermatocytes. *General and Comparative Endocrinology*, **139**, 158–167.
- Hayward CJ, Ellis D, Foote D *et al.* (2010) Concurrent epizootic hyperinfections of sea lice (predominantly *Caligus chiastos*) and blood flukes (*Cardicola forsteri*) in ranched Southern Bluefin tuna. *Veterinary Parasitology*, **173**, 107–115.
- Van Hoof A, Parker R (1999) The exosome: a proteasome for RNA? *Cell*, **99**, 347–350.
- Hoole P, Arme C (1986) The role of serum in leucocyte adherence to the plerocercoid of *Ligula intestinalis* (Cestoda: Pseudophyllidea). *Parasitology*, **92**, 413–424.
- Hu YL, Zhu LY, Xiang LX, Shao JZ (2011) Discovery of an unusual alternative splicing pathway of the immunoglobulin heavy chain in a teleost fish, *Danio rerio*. *Developmental and Comparative Immunology*, **35**, 253–257.
- Hughes TR, Mao M, Jones AR *et al.* (2001) Expression profiling using microarrays fabricated by an ink-jet oligonucleotide synthesizer. *Nature Biotechnology*, **19**, 342–347.
- ICCAT (2014) Report of The Standing Committee on Research and Statistics (SCRS). ICCAT, Madrid, Spain.
- Ingerslev HC, Ossum CG, Lindenstrøm T, Engelbrecht Nielsen M (2010) Fibroblasts express immune relevant genes and are important sentinel cells during tissue damage in Rainbow trout (*Oncorhynchus mykiss*). *PLoS ONE*, **5**, e9304.

- Iseli C, Jongeneel C, Bucher P (1999) ESTScan: a program for detecting, evaluating, and reconstructing potential coding regions in EST sequences. *Proceedings / International Conference on Intelligent Systems for Molecular Biology; ISMB*, 138–148.
- Ishii N (1935) Studies on the family Didymozoidae (Monticelli 1888). *Japanese Journal of Zoology*, **6**, 279–335.
- Jack DL, Dodds AW, Anwar N *et al.* (1998) Activation of complement by mannose-binding lectin on isogenic mutants of *Neisseria meningitidis* serogroup B. *The Journal of Immunology*, **160**, 1346–1353.
- James AW, Xu Y, Lee JK, Wang R, Longaker M (2009) Differential Effects of Transforming Growth Factor-beta1 and - beta3 on Chondrogenesis in Posterofrontal Cranial Suture- Derived Mesenchymal Cells *in Vitro*. *Plastic and Reconstructive Surgery*, **123**, 31–43.
- Jayasundara N, Gardner LD, Block BA (2013) Effects of temperature acclimation on Pacific bluefin tuna (*Thunnus orientalis*) cardiac transcriptome. *American Journal of Physiology. Regulatory, Integrative and Comparative Physiology*, **305**, R1010–R1020.
- Ju Z, Wells MC, Martinez A, Hazlewood L, Walter RB (2005) An *in silico* mining for simple sequence repeats from expressed sequence tags of zebrafish, medaka, *Fundulus*, and *Xiphophorus*. *In Silico Biology*, **5**, 439–463.
- Juneja R, Agulnik SI, Silver LM (1998) Sequence divergence within the sperm-specific polypeptide TCTE1 is correlated with species-specific differences in sperm binding to zona-intact eggs. *Journal of Andrology*, **19**, 183–188.
- Justo MCN, Kohn A, Pereira CDS, Flores-lobes F (2013) Histopathology and autoecology of *Didymocylindrus simplex* (Digenea : Didymozoidae), parasite of *Katsuwonus pelamis* (Scombridae) in the Southwestern Atlantic Ocean, off South America. *Zoologia*, **30**, 312–316.
- Justo MCN, Tortelly R, Menezes RC, Kohn A (2008) First record in South America of *Didymosulcus palati* and *Didymosulcus philobranchiarca* (Digenea, Didymozoidae) with new hosts records and pathological alterations. *Memorias do Instituto Oswaldo Cruz*, **103**, 207–210.
- Kanehisa M, Goto S (2000) KEGG: Kyoto Encyclopedia of Genes and Genomes. *Nucleic Acids Research*, **28**, 27–30.
- Kaneko T, Hirano T (1993) Role of prolactin and somatolactin in calcium regulation in fish. *The Journal of Experimental Biology*, **184**, 31–45.
- Karvonen A, Pauku S, Seppälä O, Valtonen ET (2005) Resistance against eye flukes: naïve versus previously infected fish. *Parasitology Research*, **95**, 55–59.

- Katavic I, Ticina V, Franicevic V (2003) Bluefin tuna (*Thunnus thynnus* L.) farming on the Croatian coast of the Adriatic Sea — present stage and future plans. *Cahiers Options Méditerranéennes*, **60**, 101–106.
- Kazura JW, Fanning MM, Blumer JL, Mahmoud AAF (1981) Role of cell-generated hydrogen peroxide in granulocyte-mediated killing of schistosomula of *Schistosoma mansoni* *in vitro*. *Journal of Clinical Investigation*, **67**, 93–102.
- Kinoshita Y, Jarell AD, Flaman JM *et al.* (2001) Pescadillo, a novel cell cycle regulatory protein abnormally expressed in malignant cells. *The Journal of Biological Chemistry*, **276**, 6656–6665.
- Klabunde J, Berger J, Jensenius JC *et al.* (2000) *Schistosoma mansoni*: adhesion of mannan-binding lectin to surface glycoproteins of cercariae and adult worms. *Experimental Parasitology*, **95**, 231–239.
- Knapp JM, Aranda G, Medina A, Lutcavage M (2014) Comparative assessment of the reproductive status of female Atlantic bluefin tuna from the Gulf of Mexico and the Mediterranean Sea. *PloS ONE*, **9**, e98233.
- Kobayashi T, Kajiura-Kobayashi H, Nagahama Y (2002) Two isoforms of *vasa* homologs in a teleost fish: their differential expression during germ cell differentiation. *Mechanisms of Development*, **111**, 167–171.
- Kreider T, Anthony RM, Urban JF, Gause WC (2007) Alternatively activated macrophages in helminth infections. *Current Opinion in Immunology*, **19**, 448–453.
- Kružić P, Vojvodić V, Bura-Nakić E (2014) Inshore capture-based tuna aquaculture impact on *Posidonia oceanica* meadows in the eastern part of the Adriatic Sea. *Marine Pollution Bulletin*, **86**, 174–185.
- Krzywinski M, Birol I, Jones SJ, Marra MA (2012) Hive plots-rational approach to visualizing networks. *Briefings in Bioinformatics*, **13**, 627–644.
- Kuo WP, Liu F, Trimarchi J *et al.* (2006) A sequence-oriented comparison of gene expression measurements across different hybridization-based technologies. *Nature Biotechnology*, **24**, 832–840.
- Kwon JY, Park JM, Gim BS *et al.* (1999) *Caenorhabditis elegans* mediator complexes are required for developmental-specific transcriptional activation. *Proceedings of the National Academy of Sciences of the United States of America*, **96**, 14990–14995.
- Laing KJ, Purcell MK, Winton JR, Hansen JD (2008) A genomic view of the NOD-like receptor family in teleost fish: identification of a novel NLR subfamily in zebrafish. *BMC Evolutionary Biology*, **8**, 42.
- Landeira-Fernandez AM, Castilho PC, Block BA (2012) Thermal dependence of cardiac SR Ca<sup>2+</sup>-ATPase from fish and mammals. *Journal of Thermal Biology*, **37**, 217–223.

- Lee W-P, Stromberg MP, Ward A *et al.* (2014) MOSAIK: a hash-based algorithm for accurate next-generation sequencing short-read mapping. (CK Hsiao, Ed,). *PLoS ONE*, **9**, e90581.
- Lehmann W, Edgar CM, Wang K *et al.* (2005) Tumor necrosis factor alpha (TNF-alpha) coordinately regulates the expression of specific matrix metalloproteinases (MMPS) and angiogenic factors during fracture healing. *Bone*, **36**, 300–310.
- Lepen Pleić I, Bušelić I, Trumbić Ž *et al.* (2015) Expression analysis of the Atlantic bluefin tuna (*Thunnus thynnus*) pro-inflammatory cytokines, IL-1 $\beta$ , TNF $\alpha$ 1 and TNF $\alpha$ 2 in response to parasites *Pseudocycnus appendiculatus* (Copepoda) and *Didymosulcus katsuwanicola* (Digenea). *Fish & Shellfish Immunology*, **45**, 946–954.
- Lepen Pleić I, Secombes CJ, Bird S, Mladineo I (2013) Characterization of three pro-inflammatory cytokines, TNF $\alpha$ 1, TNF $\alpha$ 2 and IL-1 $\beta$ , in cage-reared Atlantic bluefin tuna *Thunnus thynnus*. *Fish & Shellfish Immunology*, **36**, 98–112.
- Lester RJG, Newman LJ (1986) First Rediae and Cercariae to Be Described from Heteropods. *The Journal of Parasitology*, **72**, 195–197.
- Lindenstrøm T, Secombes CJ, Buchmann K (2004) Expression of immune response genes in rainbow trout skin induced by *Gyrodactylus derjavini* infections. *Veterinary Immunology and Immunopathology*, **97**, 137–148.
- Lindner D, Zietsch C, Becher PM *et al.* (2012) Differential expression of matrix metalloproteases in human fibroblasts with different origins. *Biochemistry Research International*, **2012**, 10 pages.
- Liu Z, Li RW, Waldbieser GC (2008) Utilization of microarray technology for functional genomics in ictalurid catfish. *Journal of Fish Biology*, **72**, 2377–2390.
- Lottaz C, Iseli C, Jongeneel C, Bucher P (2003) Modeling sequencing errors by combining Hidden Markov models. *Bioinformatics*, **19 Suppl 2**, ii103–ii112.
- Louro B, Passos ALS, Souche EL *et al.* (2010) Gilthead sea bream (*Sparus auratus*) and European sea bass (*Dicentrarchus labrax*) expressed sequence tags: Characterization, tissue-specific expression and gene markers. *Marine Genomics*, **3**, 179–191.
- Lubzens E, Young G, Bobe J, Cerdà J (2010) Oogenesis in teleosts: how eggs are formed. *General and Comparative Endocrinology*, **165**, 367–389.
- Luckenbach T, Fischer S, Sturm A (2014) Current advances on ABC drug transporters in fish. *Comparative Biochemistry and Physiology Part C: Toxicology and Pharmacology*, **165**, 28–52.
- Luo W, Brouwer C (2013) Pathview: An R/Bioconductor package for pathway-based data integration and visualization. *Bioinformatics*, **29**, 1830–1831.
- Luo W, Friedman MS, Shedden K, Hankenson KD, Woolf PJ (2009) GAGE: generally applicable gene set enrichment for pathway analysis. *BMC Bioinformatics*, **10**, 161.

- Lynn SG, Shepherd BS (2007) Molecular characterization and sex-specific tissue expression of prolactin, somatolactin and insulin-like growth factor-I in yellow perch (*Perca flavescens*). *Comparative Biochemistry and Physiology Part B: Biochemistry and Molecular Biology*, **147**, 412–427.
- MacEwan DJ (2008) Interactions between TNF and GnRH. *Neurochemical Research*, **33**, 678–682.
- MacKenzie BR, Mosegaard H, Rosenberg AA (2009) Impending collapse of bluefin tuna in the northeast Atlantic and Mediterranean. *Conservation Letters*, **2**, 25–34.
- Di Maio A, Mladineo I (2008) Ultrastructure of *Didymocystis semiglobularis* (Didymozoidae, Digenea) cysts in the gills of Pacific bluefin tuna (*Thunnus orientalis*). *Parasitology Research*, **103**, 641–647.
- Maizels RM, Balic A, Gomez-Escobar N *et al.* (2004) Helminth parasites - masters of regulation. *Immunological Reviews*, **201**, 89–116.
- Malenke JR, Milash B, Miller AW, Dearing MD (2013) Transcriptome sequencing and microarray development for the woodrat (*Neotoma* spp.): custom genetic tools for exploring herbivore ecology. *Molecular Ecology Resources*, **13**, 674–687.
- Mardis ER (2008) The impact of next-generation sequencing technology on genetics. *Trends in Genetics*, **24**, 133–141.
- Margulies M, Egholm M, Altman W *et al.* (2005) Genome sequencing in open microfabricated high density picoliter reactors. *Nature*, **437**, 376–380.
- Marino F, Giannetto S, Cavallaro M *et al.* (2003) *Unitubulotestis sardae* (Trematoda: Didymozoidae) infection in Atlantic bonito *Sarda sarda* (Perciformes: Scomberomoridae) in the Ionian and Tyrrhenian Seas: histopathological and SEM investigations. *Journal of Submicroscopic Cytology and Pathology*, **35**, 215–220.
- Matijević S, Bilić J, Ribičić D, Dunatov J (2012) Distribution of phosphorus species in below-cage sediments at the tuna farms in the middle Adriatic Sea (Croatia). *Acta Adriatica*, **53**, 399–412.
- Matsuyama T, Fujiwara A, Nakayasu C *et al.* (2007) Microarray analyses of gene expression in Japanese flounder *Paralichthys olivaceus* leucocytes during monogenean parasite *Neoheterobothrium hirame* infection. *Diseases of Aquatic Organisms*, **75**, 79–83.
- Mazabraud A, Wegnez M, Denis H (1975) Biochemical research on oogenesis. RNA accumulation in the oocytes of teleosts. *Developmental Biology*, **44**, 326–332.
- McCarty MF, DiNicolantonio JJ (2014)  $\beta$ -Alanine and orotate as supplements for cardiac protection. *Open Heart*, **1**, e000119.
- McDermott JR, Bartram RE, Knight P a *et al.* (2003) Mast cells disrupt epithelial barrier function during enteric nematode infection. *Proceedings of the National Academy of Sciences of the United States of America*, **100**, 7761–7766.

- McLaren DJ, Ramalho-Pinto FJ (1979) Eosinophil-mediated killing of schistosomula of *Schistosoma mansoni in vitro*: synergistic effect of antibody and complement. *The Journal of Immunology*, **123**, 1431–1438.
- Mehmood T, Liland KH, Snipen L, Sæbø S (2012) A review of variable selection methods in Partial Least Squares Regression. *Chemometrics and Intelligent Laboratory Systems*, **118**, 62–69.
- Melamed P, Gong Z, Fletcher G, Hew CL (2002) The potential impact of modern biotechnology on fish aquaculture. *Aquaculture*, **204**, 255–269.
- Miller KM, Maclean N (2008) Teleost microarrays: development in a broad phylogenetic range reflecting diverse applications. *Journal of Fish Biology*, **72**, 2039–2050.
- Miron M, Woody OZ, Marcil A *et al.* (2006) A methodology for global validation of microarray experiments. *BMC Bioinformatics*, **7**, 333.
- Mišlov Jelavić K, Stepanowska K, Grubišić L, Šegvić Bubić T, Katavić I (2012) Reduced feeding effects to the blood and muscle chemistry of farmed juvenile bluefin tuna in the Adriatic Sea. *Aquaculture Research*, **43**, 317–320.
- Miura C, Shimizu Y, Uehara M *et al.* (2011) Gh is produced by the testis of Japanese eel and stimulates proliferation of spermatogonia. *Reproduction*, **142**, 869–877.
- Miyake PM, Serna JMD la, Natale A Di *et al.* (2003) General review of bluefin tuna farming in the Mediterranean area. *Collective Volume of Scientific Papers ICCAT*, **55**, 114–124.
- Mladineo I (2006) Histopathology of five species of *Didymocystis* spp. (Digenea: Didymozoidae) in cage-reared Atlantic bluefin tuna (*Thunnus thynnus thynnus*). *Veterinary Research Communications*, **30**, 475–484.
- Mladineo I, Block BA (2009) Expression of Hsp70, Na<sup>+</sup>/K<sup>+</sup> ATP-ase, HIF-1 $\alpha$ , IL-1 $\beta$  and TNF- $\alpha$  in captive Pacific bluefin tuna (*Thunnus orientalis*) after chronic warm and cold exposure. *Journal of Experimental Marine Biology and Ecology*, **374**, 51–57.
- Mladineo I, Block BA (2010) Expression of cytokines IL-1 $\beta$  and TNF- $\alpha$  in tissues and cysts surrounding *Didymocystis wedli* (Digenea, Didymozoidae) in the Pacific bluefin tuna (*Thunnus orientalis*). *Fish & Shellfish Immunology*, **29**, 487–493.
- Mladineo I, Bočina I (2009) Type and ultrastructure of *Didymocystis wedli* and *Koellikerioides intestinalis* (Digenea, Didymozoidae) cysts in captive Atlantic bluefin tuna (*Thunnus thynnus* Linnaeus, 1758). *Journal of Applied Ichthyology*, **25**, 762–765.
- Mladineo I, Miletić I, Bočina I (2006) *Photobacterium damsela* subsp. *piscicida* Outbreak in Cage-Reared Atlantic Bluefin Tuna *Thunnus thynnus*. *Journal of Aquatic Animal Health*, **18**, 51–54.

- Mladineo I, Šegvić T, Petrić M (2011) Do captive conditions favor shedding of parasites in the reared Atlantic bluefin tuna (*Thunnus thynnus*)? *Parasitology International*, **60**, 25–33.
- Mladineo I, Tudor M (2004) Digenea of Adriatic cage-reared northern bluefin tuna (*Thunnus thynnus thynnus*). *Bulletin of the European Association of Fish Pathologists*, **24**, 144–152.
- Mladineo I, Žilić J, Čanković M (2008) Health survey of Atlantic Bluefin Tuna, *Thunnus thynnus* (Linnaeus, 1758), Reared in Adriatic Cages from 2003 to 2006. *Journal of the World Aquaculture Society*, **39**, 281–289.
- Mommens M, Fernandes JM, Tollefsen K, Johnston IA, Babiak I (2014) Profiling of the embryonic Atlantic halibut (*Hippoglossus hippoglossus* L.) transcriptome reveals maternal transcripts as potential markers of embryo quality. *BMC Genomics*, **15**, 829.
- Morais S, Mourente G, Ortega A, Tocher JA, Tocher DR (2011) Expression of fatty acyl desaturase and elongase genes, and evolution of DHA:EPA ratio during development of unfed larvae of Atlantic bluefin tuna (*Thunnus thynnus* L.). *Aquaculture*, **313**, 129–139.
- Moreau E, Chauvin A (2010) Immunity against helminths: Interactions with the host and the intercurrent infections. *Journal of Biomedicine and Biotechnology*, **2010**, Article ID 428593.
- Morey JS, Ryan JC, Van Dolah FM (2006) Microarray validation: factors influencing correlation between oligonucleotide microarrays and real-time PCR. *Biological Procedures Online*, **8**, 175–193.
- Moriya Y, Itoh M, Okuda S, Yoshizawa AC, Kanehisa M (2007) KAAS: an automatic genome annotation and pathway reconstruction server. *Nucleic Acids Research*, **35**, W182–W185.
- Mourente G, Megina C, Díaz-Salvago E (2002) Lipids in female northern bluefin tuna (*Thunnus thynnus thynnus* L.) during sexual maturation. *Fish Physiology and Biochemistry*, **24**, 351–363.
- Moyes CD (1996) Cardiac metabolism in high performance fish. *Comparative Biochemistry and Physiology Part A: Physiology*, **113**, 69–75.
- Moyes C, Mathieu-Costello OA, Brill RW, Hochachka PW (1992) Mitochondrial metabolism of cardiac and skeletal muscles from a fast (*Katsuwonus pelamis*) and a slow (*Cyprinus carpio*) fish. *Canadian Journal of Zoology*, **70**, 1246–1253.
- Munday BL, O'Donoghue PJ, Watts M, Rough K, Hawkesford T (1997) Fatal encephalitis due to the scuticociliate *Uronema nigricans* in sea-caged, southern bluefin tuna *Thunnus maccoyii*. *Diseases of Aquatic Organisms*, **30**, 17–25.
- Munday BL, Sawada Y, Cribb T, Hayward CJ (2003) Diseases of tunas, *Thunnus* spp. *Journal of Fish Diseases*, **26**, 187–206.

- Myers E, Sutton G, Delcher A *et al.* (2000) A whole-genome assembly of *Drosophila*. *Science*, **287**, 2196–2204.
- Mylonas CC, De La Gándara F, Corriero A, Ríos AB (2010) Atlantic Bluefin Tuna (*Thunnus Thynnus*) Farming and Fattening in the Mediterranean Sea. *Reviews in Fisheries Science*, **18**, 266–280.
- Nagasawa K, Takeuchi Y, Miwa M *et al.* (2009) cDNA cloning and expression analysis of a *vasa*-like gene in Pacific bluefin tuna *Thunnus orientalis*. *Fisheries Science*, **75**, 71–79.
- Nakamura Y, Mori K, Saitoh K *et al.* (2013) Evolutionary changes of multiple visual pigment genes in the complete genome of Pacific bluefin tuna. *Proceedings of the National Academy of Sciences of the United States of America*, **110**, 11061–11066.
- Nielsen J, Pavey S (2010) Perspectives: gene expression in fisheries management. *Current Zoology*, **56**, 157–174.
- Nikinmaa M, Rees BB (2005) Oxygen-dependent gene expression in fishes. *American Journal of Physiology. Regulatory, Integrative and Comparative Physiology*, **288**, R1079–R1090.
- Oeffinger M, Leung A, Lamond A, Tollervey D (2002) Yeast Pescadillo is required for multiple activities during 60S ribosomal subunit synthesis. *RNA*, **8**, 626–636.
- Olsvik PA, Lie KK, Saele Ø, Sanden M (2007) Spatial transcription of CYP1A in fish liver. *BMC Physiology*, **7**, 12.
- Ottolenghi F (2008) Capture-based aquaculture of bluefin tuna. In: *Capture-based aquaculture. Global overview*. (eds Lovatelli A, Holthus P), pp. 169–182. FAO Fisheries Technical Paper, Rome, Italy.
- Palti Y (2011) Toll-like receptors in bony fish: From genomics to function. *Developmental and Comparative Immunology*, **35**, 1263–1272.
- Pedersen ME, Vuong TT, Rønning SB, Kolset SO (2015) Matrix metalloproteinases in fish biology and matrix turnover. *Matrix Biology*, **In press**, doi:10.1016/j.matbio.2015.01.009.
- Pelegri F (2003) Maternal factors in zebrafish development. *Developmental Dynamics*, **228**, 535–554.
- Perera K (1992a) Light microscopic study of the pathology of a species of didymozoan, *Nematobothriinae* gen. sp. from the gills of slimy mackerel *Scomber australasicus*. *Diseases of Aquatic Organisms*, **13**, 103–109.
- Perera K (1992b) Ultrastructure of the primary gill lamellae of *Scomber australasicus* infected by a didymozoid parasite. *Diseases of Aquatic Organisms*, **13**, 111–121.

- Perera K (1994) Light and electron microscopic study of the pathology of a species of didymozoid (Trematoda, Digenea) infecting the gill arches of *Scomber australasicus* (Teleostei, Scombridae). *Diseases of Aquatic Organisms*, **18**, 119–127.
- Pérez-Sánchez J (2000) The involvement of growth hormone in growth regulation, energy homeostasis and immune function in the gilthead sea bream (*Sparus aurata*): a short review. *Fish Physiology and Biochemistry*, **22**, 135–144.
- Pfaffl MW (2001) A new mathematical model for relative quantification in real-time RT-PCR. *Nucleic Acids Research*, **29**, e45.
- Pfaffl MW (2004) Quantification Strategies in Real-Time PCR. In: *A-Z of Quantitative PCR* (ed Bustin SA), p. 882. International University Line, La Jolla, CA, USA.
- Pfaffl MW, Tichopad A, Prgomet C, Neuvians TP (2004) Determination of stable housekeeping genes, differentially regulated target genes and sample integrity: BestKeeper - Excel-based tool using pair-wise correlations. *Biotechnology Letters*, **26**, 509–515.
- Picard B, Wegnez M (1979) Isolation of a 7S particle from *Xenopus laevis* oocytes: a 5S RNA-protein complex. *Proceedings of the National Academy of Sciences of the United States of America*, **76**, 241–245.
- Polinski M, Shirakashi S, Bridle A, Nowak B (2014) Transcriptional immune response of cage-cultured Pacific bluefin tuna during infection by two *Cardicola* blood fluke species. *Fish & Shellfish Immunology*, **36**, 61–67.
- Pozdnyakov SE (1996) *Trematode suborder Didymozoata*. Tikhookeanskii Nauchno-Issledovatel'skii Rybokhozyaistvennyi Tsent, Vladivostok.
- Pozdnyakov SE, Gibson DI (2008) Family Didymozoidae Monticelli, 1888. In: *Keys to the Trematoda Volume 3* (eds Bray R, Gibson D, Jones A), pp. 631 – 734. CABI Publishing, Wallingford.
- Quéré N, Guinand B, Kuhl H *et al.* (2010) Genomic sequences and genetic differentiation at associated tandem repeat markers in growth hormone, somatolactin and insulin-like growth factor-1 genes of the sea bass, *Dicentrarchus labrax*. *Aquatic Living Resources*, **23**, 285–296.
- Reite OB, Evensen Ø (2006) Inflammatory cells of teleostean fish: A review focusing on mast cells/eosinophilic granule cells and rodlet cells. *Fish & Shellfish Immunology*, **20**, 192–208.
- Reyes-Cerpa S, Maisey K, Reyes-López F *et al.* (2012) Fish cytokines and immune response. In: *New Advances and Contributions to Fish Biology* (ed Türker H), pp. 3–58. InTech.
- Riccioni G, Landi M, Ferrara G *et al.* (2010) Spatio-temporal population structuring and genetic diversity retention in depleted Atlantic bluefin tuna of the Mediterranean Sea. *Proceedings of the National Academy of Sciences of the United States of America*, **107**, 2102–2107.

- Rice P, Longden I, Bleasby A (2000) EMBOSS: the European Molecular Biology Open Software Suite. *Trends in Genetics*, **16**, 276–277.
- Roberts RJ, Agius C (2008) Pan-steatitis in farmed northern bluefin tuna, *Thunnus thynnus* (L.), in the eastern Adriatic. *Journal of Fish Diseases*, **31**, 83–88.
- Robledo D, Ronza P, Harrison PW *et al.* (2014) RNA-seq analysis reveals significant transcriptome changes in turbot (*Scophthalmus maximus*) suffering severe enteromyxosis. *BMC Genomics*, **15**, 1149.
- Rolland AD, Lareyre J-J, Goupil A-S *et al.* (2009) Expression profiling of rainbow trout testis development identifies evolutionary conserved genes involved in spermatogenesis. *BMC Genomics*, **10**, 546.
- Rooker JR, Secor DH, De Metrio G *et al.* (2008) Natal Homing and Connectivity in Atlantic Bluefin Tuna Populations. *Science*, **322**, 742–744.
- Rosenfeld H, Mylonas CC, Bridges CR *et al.* (2012) GnRHa-mediated stimulation of the reproductive endocrine axis in captive Atlantic bluefin tuna, *Thunnus thynnus*. *General and Comparative Endocrinology*, **175**, 55–64.
- Rozanov D V., Savinov AY, Golubkov VS *et al.* (2004) Cellular membrane type-1 matrix metalloproteinase (MT1-MMP) cleaves C3b, an essential component of the complement system. *The Journal of Biological Chemistry*, **279**, 46551–46557.
- Salzet M, Capron a., Stefano GB (2000) Molecular crosstalk in host-parasite relationships: Schistosome- and leech-host interactions. *Parasitology Today*, **16**, 536–540.
- Savan R, Aman A, Nakao M, Watanuki H, Sakai M (2005) Discovery of a novel immunoglobulin heavy chain gene chimera from common carp (*Cyprinus carpio* L.). *Immunogenetics*, **57**, 458–463.
- Sawada Y, Okada T, Miyashita S, Murata O, Kumai H (2005) Completion of the Pacific bluefin tuna *Thunnus orientalis* (Temminck et Schlegel) life cycle. *Aquaculture Research*, **36**, 413–421.
- Scharsack JP, Koch K, Hammerschmidt K (2007) Who is in control of the stickleback immune system: interactions between *Schistocephalus solidus* and its specific vertebrate host. *Proceedings of the Royal Society B: Biological Sciences*, **274**, 3151–3158.
- Schena M, Shalon D, Davis R, Brown P (1995) Quantitative monitoring of gene expression patterns with a complementary DNA microarray. *Science*, **270**, 467–470.
- Schmieder R, Edwards R (2011) Quality control and preprocessing of metagenomic datasets. *Bioinformatics*, **27**, 863–864.
- Secombes CJ, Chappell L (1996) Fish immune responses to experimental and natural infection with helminth parasites. *Annual Review of Fish Diseases*, **6**, 167–177.

- Secombes CJ, Cross AR, Sharp GJE, Garcia R (1992) NADPH oxidase-like activity in rainbow trout *Oncorhynchus mykiss* (Walbaum) macrophages. *Developmental & Comparative Immunology*, **16**, 405–413.
- Segers K, Dahlbäck B, Nicolaes GAF (2007) Coagulation factor V and thrombophilia: Background and mechanisms. *Thrombosis and Haemostasis*, **98**, 530–542.
- Selkoe K a., Toonen RJ (2006) Microsatellites for ecologists: A practical guide to using and evaluating microsatellite markers. *Ecology Letters*, **9**, 615–629.
- Selman K, Wallace RA, Sarka A, Qi X (1993) Stages of oocyte development in the zebrafish, *Brachydanio rerio*. *Journal of Morphology*, **218**, 203–224.
- Sher A (1976) Complement-dependent adherence of mast cells to schistosomula. *Nature*, **263**, 334–336.
- Shiels H, Di Maio A, Thompson S, Block B (2011) Warm fish with cold hearts: thermal plasticity of excitation–contraction coupling in bluefin tuna. *Proceedings of The Royal Society B Biological Sciences*, **278**, 18–27.
- Sitjà-Bobadilla A (2008) Living off a fish: A trade-off between parasites and the immune system. *Fish & Shellfish Immunology*, **25**, 358–372.
- Spellberg B, Edwards JE (2001) Type 1/Type 2 immunity in infectious diseases. *Clinical Infectious Diseases*, **32**, 76–102.
- Star B, Nederbragt AJ, Jentoft S *et al.* (2011) The genome sequence of Atlantic cod reveals a unique immune system. *Nature*, **477**, 207–210.
- Stavnezer J, Amemiya CT (2004) Evolution of isotype switching. *Seminars in Immunology*, **16**, 257–275.
- Su CW, Cao Y, Kaplan J *et al.* (2011) Duodenal helminth infection alters barrier function of the colonic epithelium via adaptive immune activation. *Infection and Immunity*, **79**, 2285–2294.
- Su AI, Wiltshire T, Batalov S *et al.* (2004) A gene atlas of the mouse and human protein-encoding transcriptomes. *Proceedings of the National Academy of Sciences of the United States of America*, **101**, 6062–6067.
- Tadiso TM, Krasnov A, Skugor S *et al.* (2011) Gene expression analyses of immune responses in Atlantic salmon during early stages of infection by salmon louse (*Lepeophtheirus salmonis*) revealed bi-phasic responses coinciding with the copepod–chalarinus transition. *BMC Genomics*, **12**, 141.
- Taggart JB, Bron JE, Martin SAM *et al.* (2008) A description of the origins, design and performance of the TRAITs-SGP Atlantic salmon *Salmo salar* L. cDNA microarray. *Journal of Fish Biology*, **72**, 2071–2094.

- Taylor NG, McAllister MK, Lawson GL, Carruthers T, Block BA (2011) Atlantic bluefin tuna: a novel multistock spatial model for assessing population biomass. *PLoS ONE*, **6**, e27693.
- Theocharidis A, van Dongen S, Enright AJ, Freeman TC (2009) Network visualization and analysis of gene expression data using BioLayout *Express*<sup>3D</sup>. *Nature Protocols*, **4**, 1535–1550.
- Titus TA, Yan Y-L, Wilson C *et al.* (2009) The Fanconi anemia/BRCA gene network in zebrafish: Embryonic expression and comparative genomics. *Mutation Research*, **668**, 117–132.
- Tóth G, Gáspári Z, Jurka J (2000) Microsatellites in different eukaryotic genomes: survey and analysis. *Genome Research*, **10**, 967–981.
- Untergasser A, Cutcutache I, Koressaar T *et al.* (2012) Primer3-new capabilities and interfaces. *Nucleic Acids Research*, **40**, e115.
- Uribe C, Folch H, Enriquez R, Moran G (2011) Innate and adaptive immunity in teleost fish: a review. *Veterinarni Medicina*, **56**, 486–503.
- Vandesompele J, De Preter K, Pattyn F *et al.* (2002) Accurate normalization of real-time quantitative RT-PCR data by geometric averaging of multiple internal control genes. *Genome Biology*, **3**, RESEARCH0034.
- Vasemägi A, Nilsson J, Primmer CR (2005) Expressed sequence tag-linked microsatellites as a source of gene-associated polymorphisms for detecting signatures of divergent selection in Atlantic salmon (*Salmo salar* L.). *Molecular Biology and Evolution*, **22**, 1067–1076.
- Vezzulli L, Moreno M, Marin V *et al.* (2008) Organic waste impact of capture-based Atlantic bluefin tuna aquaculture at an exposed site in the Mediterranean Sea. *Estuarine, Coastal and Shelf Science*, **78**, 369–384.
- Viñas J, Gordo A, Fernández-Cebrián R *et al.* (2011) Facts and uncertainties about the genetic population structure of Atlantic bluefin tuna (*Thunnus thynnus*) in the Mediterranean. Implications for fishery management. *Reviews in Fish Biology and Fisheries*, **21**, 527–541.
- Vita R, Marin A (2007) Environmental impact of capture-based bluefin tuna aquaculture on benthic communities in the western Mediterranean. *Aquaculture Research*, **38**, 331–339.
- Vita R, Marín A, Jiménez-Brinquis B *et al.* (2004) Aquaculture of Bluefin tuna in the Mediterranean: Evaluation of organic particulate wastes. *Aquaculture Research*, **35**, 1384–1387.
- Volff J-N (2005) Genome evolution and biodiversity in teleost fish. *Heredity*, **94**, 280–294.

- Walli A, Teo SLH, Boustany A *et al.* (2009) Seasonal movements, aggregations and diving behavior of Atlantic bluefin tuna (*Thunnus thynnus*) revealed with archival tags. *PLoS ONE*, **4**, e6151.
- Wang Z, Gerstein M, Snyder M (2009) RNA-Seq: a revolutionary tool for transcriptomics. *Nature Reviews Genetics*, **10**, 57–63.
- Wang T, Gorgoglione B, Maehr T *et al.* (2011a) Fish Suppressors of Cytokine Signaling (SOCS): Gene Discovery, Modulation of Expression and Function. *Journal of Signal Transduction*, **2011**, 20 pages.
- Wang T, Huang W, Costa MM, Martin S a M, Secombes CJ (2011b) Two copies of the genes encoding the subunits of putative interleukin (IL)-4/IL-13 receptors, IL-4R $\alpha$ , IL-13R $\alpha$ 1 and IL-13R $\alpha$ 2, have been identified in rainbow trout (*Oncorhynchus mykiss*) and have complex patterns of expression and modulation. *Immunogenetics*, **63**, 235–253.
- Wehrens R, Franceschi P (2012a) Meta-Statistics for Variable Selection: The R Package BioMark. *Journal of Statistical Software*, **51**, 1–18.
- Wehrens R, Franceschi P (2012b) Thresholding for biomarker selection in multivariate data using Higher Criticism. *Molecular BioSystems*, **8**, 2339–2346.
- Whitehead A, Crawford DL (2005) Variation in tissue-specific gene expression among natural populations. *Genome Biology*, **6**, R13.
- Whyte SK, Chappell LH, Secombes CJ (1989) Cytotoxic reactions of rainbow trout, *Salmo gairdneri* Richardson, macrophages for larvae of the eye fluke *Diplostomum spathaceum* (Digenea). *Journal of Fish Biology*, **35**, 333–345.
- Wickham H (2009) ggplot2 - Elegant Graphics for Data Analysis. Springer, New York.
- Wold S, Sjöström M, Eriksson L (2001) PLS-regression: A basic tool of chemometrics. *Chemometrics and Intelligent Laboratory Systems*, **58**, 109–130.
- Wolf JC, Wolfe MJ (2005) A brief overview of nonneoplastic hepatic toxicity in fish. *Toxicologic Pathology*, **33**, 75–85.
- Yamaguti S (1970) *Digenetic trematodes of Hawaiian fishes*. Keigaku Publishing Company, Tokyo.
- Yang BY, Arab M, Chen TT (1997) Cloning and characterization of rainbow trout (*Oncorhynchus mykiss*) somatolactin cDNA and its expression in pituitary and nonpituitary tissues. *General and Comparative Endocrinology*, **106**, 271–280.
- Yang M, Zhou H (2008) Grass carp transforming growth factor- $\beta$ 1 (TGF- $\beta$ 1): Molecular cloning, tissue distribution and immunobiological activity in teleost peripheral blood lymphocytes. *Molecular Immunology*, **45**, 1792–1798.

- Yu F, Li Y, Liu L, Li Y (2008) Comparative genomics of human-like *Schistosoma japonicum* genes indicates a putative mechanism for host-parasite relationship. *Genomics*, **91**, 152–157.
- Zhang J, Bai S, Zhang X, Nagase H, Sarras MP (2003) The expression of novel membrane-type matrix metalloproteinase isoforms is required for normal development of zebrafish embryos. *Matrix Biology*, **22**, 279–293.
- Zhang L, Liu W, Shao C *et al.* (2014) Cloning, expression and methylation analysis of piwil2 in half-smooth tongue sole (*Cynoglossus semilaevis*). *Marine Genomics*, pii: S1874–7787(14)00043–9.
- Zhao S, Fung-Leung W-P, Bittner A, Ngo K, Liu X (2014) Comparison of RNA-Seq and microarray in transcriptome profiling of activated T cells. *PloS ONE*, **9**, e78644.
- Zhou Y, Wang F, Liu S *et al.* (2012) Human chorionic gonadotropin suppresses expression of Piwis in common carp (*Cyprinus carpio*) ovaries. *General and Comparative Endocrinology*, **176**, 126–131.
- Zhu LY, Nie L, Zhu G, Xiang LX, Shao JZ (2013) Advances in research of fish immune-relevant genes: A comparative overview of innate and adaptive immunity in teleosts. *Developmental and Comparative Immunology*, **39**, 39–62.
- Zhulidov PA, Bogdanova EA, Shcheglov AS *et al.* (2004) Simple cDNA normalization using kamchatka crab duplex-specific nuclease. *Nucleic Acids Research*, **32**, e37.
- Zitka O, Kukacka J, Krizkova S *et al.* (2010) Matrix metalloproteinases. *Current Medicinal Chemistry*, **17**, 3751–3768.
- Zou J, Carrington A, Collet B *et al.* (2005) Identification and bioactivities of IFN- $\gamma$  in rainbow trout *Oncorhynchus mykiss*: the first Th1-type cytokine characterized functionally in fish. *The Journal of Immunology*, **175**, 2484–2494.

## 7 Summary

The largest of the tuna species, Atlantic bluefin tuna, *Thunnus thynnus* (Linnaeus, 1758), inhabits the North Atlantic Ocean and the Mediterranean Sea. It is considered to be endangered by overfishing and capture-based farming/fattening practices, stimulating research into development of self-sustained aquaculture technology. In this study an effort was made to construct a transcriptomic resource for Atlantic bluefin tuna, aiding the research of different biological and physiological aspects of this species. Normalized mixed-tissue cDNA library was constructed from adult *T. thynnus* and pyrosequenced. A total of 976,904 raw sequence reads were assembled into 33,105 unique transcripts having a mean length of 893 bp and an N50 of 870. Of these, 33.4% showed similarity to known proteins or gene transcripts and 86.6% of them were matched to the congeneric Pacific bluefin tuna (*T. orientalis*) genome. The sequences harbour significant potential for development of markers such as EST-SSRs. A novel 15K Agilent oligo-microarray for *T. thynnus* was designed and comparative tissue gene expression profiles were inferred for gill, heart, liver, ovaries and testes. Gills were particularly associated with immune system, signal transduction and cell communication processes, while ovaries displayed signatures of glycan biosynthesis, nucleotide metabolism, transcription, translation, replication and repair. These ground level gene expression data can serve in the design of new transcriptomic studies for this species. In another experiment, the interaction between *T. thynnus* and the digenean parasite *Didymosulcus katsuwonicola*, the core species of tuna parasite assemblages, was investigated at ultrastructural, using transmission electron microscopy, and transcriptomic level, using newly developed microarray. Numerous transiting vesicles were recorded in didymozoid's tegument in direct contact with host's loose collagen connective tissue capsule comprising fibrocytes, fibroblasts, eosinophilic-granulated mast cells, eosinophils and plasma cells, also encompassing a nerve composed of three neuronal axons. Transcriptionally, moderate gene regulation was observed in both directions including the complement system and pro-inflammatory cytokines, as well as endocrine, digestive and nervous functional pathways. The data are consistent with available literature and provide new insights on tuna immune system which can be further explored in more focused studies.

## 8 Sažetak

Atlantska plavoperajna tuna, *Thunnus thynnus* (Linnaeus, 1758), je pelagična migratorna vrsta iz porodice Scombridae koja nastanjuje Atlantski ocean i Sredozemno more. Neke od jedinstvenih evolucijskih prilagodbi na život u otvorenom moru su karakteristične za ovu vrstu: aerodinamični oblik tijela, povišena metabolička stopa i aerobna aktivnost, brzi rast, veliki fekunditet i sposobnost održavanja povišene tjelesne temperature u odnosu na okoliš u području mozga, mišića i probavnih organa, poznato kao regionalna endotermija. Vrsta je od iznimnog socio-ekonomskog značaja, s više od polovice svjetske proizvodnje koncentrirane u području Sredozemnog mora, uključujući i Jadran. Uzgoj tune je ovisan o godišnjem ulovu jedinki iz divljih populacija koje se prebacuju u uzgojne kaveze i intenzivno hrane s ciljem povećanja sadržaja masti i tržišne vrijednosti po izlovu. Ovakva aktivnost nije dugoročno održiva i smatra se da razvoj potpuno zatvorenog uzgojnog ciklusa u zatočeništvu može sačuvati vrstu za buduće generacije. Transkriptomika, istraživanje sastava RNA populacije, odraza genske aktivnosti koja uvjetuje nastanak određenog fenotipa, omogućava razvoj molekularnih biljega specifičnih za rast, razvoj i zdravstveno stanje organizama, jedan od ključnih alata za razvoj optimalnih i održivih akvakulturnih strategija. Cilj ove studije je bio razviti novi alat za istraživanje genske ekspresije kod vrste *T. thynnus* - DNA mikročip s 15 000 oligonukleotidnih probi, te po prvi put istražiti odnos ovog domaćina na razini transkriptoma, s nametnikom *Didymosulcus katsuwonicola* Pozdnyakov 1990 (Digenea, Didymozoidae), ključne vrste nametničkih zajednica plavoperajne tune.

Kako bi se proširila baza kodirajućih ili eksprimiranih sekvenci za *T. thynnus*, sintetizirana je normalizirana cDNA knjižnica na kalupu ukupne RNA iz različitih tkiva odraslih jedinki i pirosekvencirana. Ukupno je dobiveno 976 904 nukleotidnih sljedova, sastavljeno u 33 105 jedinstvenih sekvenci sa srednjom dužinom od 893 baze i N50 vrijednošću od 870. Trećina (33,4 %) transkripata je uspješno identificirana putem značajne sličnosti s RefSeq proteinskom bazom podataka, dok je 86,6 % spareno s genomom pacifičke plavoperajne tune *T. orientalis*. Na anotiranim sekvencama je putem MISA programa identificirano 730 mikrosatelitnih motiva (EST-SSRs) koji mogu poslužiti za razvoj novih populacijskih studija *T. thynnus*. Anotirani transkripti su nadalje odabrani kao kalup za dizajn specifičnih komplementarnih probi dužine 60 parova baza, korištenjem online dostupnog alata eArray (Agilent

Technologies), i osmišljen je DNA mikročip s 15 208 *T. thynnus* specifičnih probi i 536 pozitivnih i negativnih kontrola definiranih od strane proizvođača. Kako bi se provjerila njegova funkcionalnost, napravljena je usporedba transkriptoma metabolički različitih tkiva, škrge, srca, jetre te muških i ženskih gonada. Najveći je kontrast uočen između škrge, u kojima je zabilježena značajna ekspresija komponenti imunskog sustava, signalnih puteva i stanične komunikacije, u odnosu na ovarije, u kojima je bila istaknuta sinteza glikana, metabolizam nukleotida, transkripcija, translacija, replikacija i DNA popravak. Profili ekspresije odabranih transkriptata su provjereni lančanom reakcijom polimerazom u realnom vremenu (RT-qPCR). Podaci dobiveni putem DNA mikročipa i RT-qPCR su pokazali značajnu korelaciju. Tkivno-specifični profili genske ekspresije predstavljaju značajan alat u osmišljavanju novih ciljanih transkriptomskih studija.

Odnos između atlantske plavoperajne tune i metilja *D. katsuwonocola* je istražen u drugom eksperimentu, na razini transkriptoma korištenjem DNA mikročipa, i staničnoj razini putem elektronske transmisijske mikroskopije. *D. katsuwonocola* stvara vezivno-tkivne ciste na škržnim filamentima domaćina s induciranim lokalnim upalnim odgovorom, ali bez većih patoloških promjena. Uočeno je da broj cista ovog nametnika po domaćinu opada tijekom uzgoja, sukladno dinamici čitave nametničke zajednice, što predstavlja zanimljiv fenomen s obzirom na suprotan trend iz akvakulturne prakse drugih vrsta.

Za studiju je odabrano 7 zaraženih i nezaraženih uzoraka podrijetlom od različitih životinja. Ciste prosječne duljine 2 mm su otvorene skalpelom i nametnici su uklonjeni prije analize. Sukladno s kroničnim tipom ove infekcije, zabilježene su umjerene diferencijalne promjene u ekspresiji gena u inficiranom u odnosu na neinficirano tkivo, uključujući aktivirani sustav komplementa, proinflamatorne citokine, matriks metaloproteinaze te smanjenu ekspresiju neuro-endokrinih signalnih puteva te citoskeletnih elemenata i kolagena. Na staničnoj razini su uočeni brojni migrirajući vezikuli u tegumentu didimozoida u bliskom kontaktu s vezivno-tkivnom rahlom kolagenom stjenkom ciste domaćina. Cista je obuhvaćala niz razgranatih kapilara, živac s tri neuralna aksona te brojne fibroblaste, fibroците, mastocite, granulirane eozinofile, plazma stanice i mukozne stanice. Podatci rasvjetljavaju odnos između *T. thynnus* i *D. katsuwonocola* na molekularnoj razini te pružaju osnovu za razvoj studija s ciljem povezivanja ekspresije određenih transkriptata i staničnih tipova. Uz uzorke domaćina, na dva DNA mikročipa je napravljena heterologna

hibridizacija izolirane i amplificirane mRNA *D. katsuwonicola*. Podatci ukazuju na značajan unakrižno-hibridizacijski potencijal određenih probi, što sugerira postojanje nespecifičnih izvora, kontaminacije ili mogućnosti konvergentne evolucije i horizontalnog prijenosa gena između nametnika i domaćina, kao zanimljiv predmet za daljnja istraživanja.

## 9 Supporting Information

**Supplement 9.1** Table showing a sample from transcripts present in first six largest tissue-specific clusters obtained by Markov clustering algorithm in Biolayout Express 3D. Expression values are conditionally formatted to highlight patterns, with red denoting increased and blue decreased expression.

Probe_ID	DESCRIPTION	MCL Cluster	Tissue	Gill	Heart	Liver	Ovary	Testis
scf0247_1	aquaporin 3b	Cluster004	Gill	3.259349	-5.79942	-5.98322	-7.57313	-5.74896
scf0247_2	aquaporin 3b	Cluster004	Gill	2.983468	-5.50811	-5.01378	-7.82823	-4.86095
scf5010_1	ATPase, Ca++ transporting, cardiac muscle, slow twitch 2a	Cluster002	Heart	-3.30679	4.218201	-3.7007	-3.53275	-3.72021
scf5010_2	ATPase, Ca++ transporting, cardiac muscle, slow twitch 2a	Cluster002	Heart	-3.6418	4.407511	-3.82065	-3.65552	-4.72256
deg094517_1	fatty acid binding protein 2, intestinal	Cluster002	Heart	-0.48537	4.893098	-2.78097	-5.65885	1.148749
deg094517_2	fatty acid binding protein 2, intestinal	Cluster002	Heart	-0.2076	5.063862	-2.98283	-7.35284	1.243108
scf5580_1	coagulation factor V	Cluster003	Liver	-3.52139	-2.5996	4.962723	-1.7626	-3.27198
scf5580_2	coagulation factor V	Cluster003	Liver	-3.43468	-2.44368	5.299647	-2.11824	-2.87811
deg132539_1	complement C4-like	Cluster003	Liver	-1.5402	-0.7653	4.186786	-6.6477	-1.8066
deg136111_1	complement C4-like	Cluster003	Liver	-1.08468	0.151068	5.349956	-3.02329	-2.08389
scf0491_1	cytochrome P450 2G1-like	Cluster003	Liver	0.202052	-7.25543	4.614479	-4.00606	-5.7397
scf0491_2	cytochrome P450 2G1-like	Cluster003	Liver	0.090786	-9.08044	4.626906	-4.17393	-5.72359
scf1454_1	cytochrome P450, family 1, subfamily C, polypeptide 2	Cluster003	Liver	-6.99969	2.766839	5.540385	-3.43131	0.10649
scf1454_2	cytochrome P450, family 1, subfamily C, polypeptide 2	Cluster003	Liver	-7.84169	2.865815	5.804614	-4.50442	0.223588
deg087332_1	cytochrome P450, family 2, subfamily AD, polypeptide 2	Cluster003	Liver	-4.45709	0.990049	4.757481	-3.45246	2.382616
deg087332_2	cytochrome P450, family 2, subfamily AD, polypeptide 2	Cluster003	Liver	-3.26614	0.934163	4.863984	-2.9621	2.231383
scf5151_1	cytochrome P450, family 2, subfamily K, polypeptide17	Cluster003	Liver	-3.96145	-2.09981	4.177924	0.373326	-4.00443
scf5151_2	cytochrome P450, family 2, subfamily K, polypeptide17	Cluster003	Liver	-2.05597	-1.27638	4.415216	0.360502	-3.62232
scf2250_1	cytochrome P450, family 2, subfamily N, polypeptide 13	Cluster003	Liver	0.395962	-4.54165	5.823495	-6.73016	-2.96604
scf2250_2	cytochrome P450, family 2, subfamily N, polypeptide 13	Cluster003	Liver	0.653168	-3.05588	5.751476	-8.0096	-1.64139
scf1728_1	cytochrome P450, family 2, subfamily X, polypeptide 9	Cluster003	Liver	-7.15634	-6.25475	5.481219	-7.22275	-1.1367
scf1728_2	cytochrome P450, family 2, subfamily X, polypeptide 9	Cluster003	Liver	-5.88491	-4.96105	5.108408	-4.82765	-1.06291

scf0564_1	cytochrome P450, family 24, subfamily A, polypeptide 1	Cluster003	Liver	-5.11135	-8.28414	4.089981	-8.09996	-5.85785
scf0564_2	cytochrome P450, family 24, subfamily A, polypeptide 1	Cluster003	Liver	-5.21005	-8.02331	4.05393	-7.88569	-6.03418
scf0600_1	cytochrome P450, family 3, subfamily A, polypeptide 65	Cluster003	Liver	0.247121	-3.30313	5.009157	-6.99961	-3.12353
scf0600_2	cytochrome P450, family 3, subfamily A, polypeptide 65	Cluster003	Liver	0.291971	-3.68223	5.313509	-8.6316	-3.15795
deg072631_1	cytochrome P450, family 3, subfamily c, polypeptide 1	Cluster003	Liver	0.770029	0.257655	4.647134	-1.60919	-2.29339
deg071131_1	cytochrome P450, family 4, subfamily T, polypeptide 8	Cluster003	Liver	-1.10785	-2.8436	5.061296	-1.6464	1.365499
deg071131_2	cytochrome P450, family 4, subfamily T, polypeptide 8	Cluster003	Liver	-0.90066	-2.69449	4.974909	-1.35202	1.377406
scf5633_1	cytochrome P450, family 4, subfamily V, polypeptide 2	Cluster003	Liver	-4.05242	-1.08672	5.698996	-2.8283	-3.34674
scf5633_2	cytochrome P450, family 4, subfamily V, polypeptide 2	Cluster003	Liver	-4.33283	-3.10471	5.993162	-1.78563	-3.84885
scf0435_1	cytochrome P450, family 7, subfamily A, polypeptide 1a	Cluster003	Liver	0.841465	-6.39737	5.488637	-7.90533	-5.20466
scf0435_2	cytochrome P450, family 7, subfamily A, polypeptide 1a	Cluster003	Liver	0.724075	-6.40592	4.876761	-6.42524	-4.74039
deg135222_1	aquaporin 1a, tandem duplicate 1	Cluster001	Ovary	-4.13975	-2.57171	-2.94097	0.611103	-4.91452
deg135223_1	aquaporin 1a, tandem duplicate 2	Cluster001	Ovary	-7.56544	-5.32488	-7.05806	0.090796	-7.6111
scf6477_1	cathepsin S, b.1	Cluster001	Ovary	-5.80561	-4.81362	-6.03813	-0.01709	-5.88301
scf6477_2	cathepsin S, b.1	Cluster001	Ovary	-7.2698	-4.86362	-6.60056	0.581903	-7.70246
scf6497_1	exosome component 2	Cluster001	Ovary	-2.38233	-2.77171	-2.21158	0.36548	-1.54661
scf6497_2	exosome component 2	Cluster001	Ovary	-2.15994	-1.71695	-1.75491	0.369375	-0.94222
deg134977_2	pescadillo	Cluster001	Ovary	-2.46516	-2.05467	-2.59828	0.823552	-1.89149
scf5276_1	pescadillo	Cluster001	Ovary	-2.25663	-1.59421	-1.41093	0.699624	-2.0136
scf5276_2	pescadillo	Cluster001	Ovary	-1.70726	-1.3913	-1.13984	0.49965	-1.46991
scf0415_1	zona pellucida glycoprotein 3a.1	Cluster001	Ovary	-3.60236	-2.74464	-3.07432	0.568651	-3.79486
scf0250_1	zona pellucida sperm-binding protein 4-like	Cluster001	Ovary	-7.13403	-5.04761	-6.6122	0.435495	-6.66699
scf4104_1	Fanconi anemia, complementation group I	Cluster005	Ovary/Testis	-1.55598	-4.51085	-4.72566	0.011115	0.576036
scf4104_2	Fanconi anemia, complementation group I	Cluster005	Ovary/Testis	-1.76525	-3.16136	-3.31869	0.116925	0.447419
scf6480_1	mediator complex subunit 6	Cluster005	Ovary/Testis	-0.37628	-1.05629	-1.71848	0.091365	0.577759
scf6480_2	mediator complex subunit 6	Cluster005	Ovary/Testis	-0.15019	-0.81912	-1.12509	0.184281	0.616288
deg101622_1	piwi-like 2	Cluster005	Ovary/Testis	-5.00058	-2.99428	-3.48851	0.702191	0.836825
deg101622_2	piwi-like 2	Cluster005	Ovary/Testis	-5.16557	-2.58909	-3.50027	0.724842	0.821166
TTncbi48_1	<i>Thunnus thynnus</i> sl mRNA for somatolactin, complete cds	Cluster006	Testis	-4.77958	-2.28548	-0.97133	-2.14568	3.571196

TTncbi48_2	<i>Thunnus thynnus</i> sl mRNA for somatolactin, complete cds	Cluster006	Testis	-3.75034	-1.84224	-0.95443	-1.18245	3.384852
TTncbi50_1	Tuna mRNA for growth hormone	Cluster006	Testis	-3.55051	-3.6588	-3.16574	-2.41224	3.474931
TTncbi50_2	Tuna mRNA for growth hormone	Cluster006	Testis	-3.24579	-2.97125	-2.62168	-2.22003	3.26653
deg092184_1	t-complex-associated testis-expressed protein 1-like	Cluster006	Testis	-5.80269	-3.31178	-1.78217	-3.76756	3.50558
scf0501_1	vasa homologue	Cluster006	Testis	-7.11718	-3.74656	-6.31242	-0.05708	2.57166
scf0501_2	vasa homologue	Cluster006	Testis	-6.95518	-3.76251	-5.96982	-0.14806	2.585666

**Supplement 9.2.** Tables giving results of functional KEGG pathway analyses of tissue-specific expressional profiles using GAGE analyses. First table displays pathways for single tissues and the second for tests run for combinations of two tissues against all other samples. Data are given only for statistically significant pathways ( $q < 0.1$ ) and the sign of stat. mean value indicates the direction of regulation.

KEGG Pathway	Gill		Heart		Liver		Ovary		Testis	
	stat.mean	q.value								
Adherens junction	1.801	0.001								
Adipocytokine signaling pathway							-1.490	0.009		
Alanine, aspartate and glutamate metabolism	-1.623	0.027			1.153	0.090				
Aminoacyl-tRNA biosynthesis							2.120	0.000		
Antigen processing and presentation	1.382	0.015								
Apoptosis	1.559	0.006								
Arginine and proline metabolism							-1.367	0.015		
Axon guidance	1.912	0.001					-1.186	0.033		
B cell receptor signaling pathway	3.183	0.000					-1.687	0.003		
Basal transcription factors					-1.772	0.007	2.380	0.000		
Base excision repair					-1.739	0.008	1.664	0.006	1.442	0.076
Bile secretion					1.329	0.046				
Calcium signaling pathway			2.145	0.003			-1.402	0.012		
Carbon fixation in photosynthetic organisms							-1.102	0.048		
Cardiac muscle contraction			4.169	0.000			-2.364	0.000		
Cell adhesion molecules (CAMs)	2.487	0.000					-1.997	0.001		
Cell cycle					-1.684	0.008	2.945	0.000		
Cell cycle - yeast	-1.374	0.075	-1.809	0.070	-2.352	0.000	3.926	0.000		
Chemokine signaling pathway	3.186	0.000					-2.231	0.000	-1.553	0.053
Cholinergic synapse	1.074	0.053					-0.910	0.085		
Circadian entrainment							-1.289	0.022		
Citrate cycle (TCA cycle)			2.644	0.000						
Complement and coagulation cascades					6.746	0.000	-3.751	0.000		

KEGG Pathway	Gill		Heart		Liver		Ovary		Testis	
	stat.mean	q.value								
Cysteine and methionine metabolism					1.224	0.068				
Cytokine-cytokine receptor interaction	2.819	0.000			1.270	0.069	-4.150	0.000		
DNA replication					-3.001	0.000	2.790	0.000	2.605	0.000
Dopaminergic synapse	0.909	0.099					-1.180	0.033		
Drug metabolism - other enzymes					1.574	0.016				
ECM-receptor interaction	2.045	0.000	1.482	0.069			-2.009	0.001		
Endocytosis	1.705	0.002					-1.565	0.006		
ErbB signaling pathway	1.022	0.064								
Estrogen signaling pathway	1.373	0.015					-1.241	0.027		
Fanconi anemia pathway	-1.526	0.055			-2.036	0.003	3.081	0.000	1.819	0.020
Fat digestion and absorption					1.825	0.004				
Fatty acid degradation			2.186	0.003						
Fc epsilon RI signaling pathway	2.653	0.000					-1.701	0.003		
Fc gamma R-mediated phagocytosis	3.652	0.000					-2.211	0.000		
Focal adhesion	2.333	0.000	2.681	0.000			-2.344	0.000		
GABAergic synapse							-1.515	0.009		
Galactose metabolism					1.376	0.044				
Gap junction	1.730	0.002								
Gastric acid secretion	1.266	0.026					-1.145	0.040		
Glutamatergic synapse	1.248	0.028	1.511	0.060			-2.170	0.000		
Glycerolipid metabolism	-1.559	0.038			2.677	0.000	-0.907	0.094		
Glycerophospholipid metabolism					1.306	0.046				
Glycine, serine and threonine metabolism	-1.507	0.038			1.415	0.035				
Glycolysis / Gluconeogenesis			1.564	0.052			-1.036	0.058		
Glyoxylate and dicarboxylate metabolism	-1.370	0.073	1.563	0.058	1.157	0.090				
GnRH signaling pathway	1.597	0.005					-1.144	0.038		
Hematopoietic cell lineage	2.065	0.001					-1.473	0.012		
HIF-1 signaling pathway							-1.341	0.016		

KEGG Pathway	Gill		Heart		Liver		Ovary		Testis	
	stat.mean	q.value								
Hippo signaling pathway	1.159	0.036								
Histidine metabolism					2.041	0.002				
Homologous recombination					-1.761	0.008	1.739	0.005	1.460	0.077
Inositol phosphate metabolism							-1.243	0.027		
Insulin secretion							-1.267	0.025		
Jak-STAT signaling pathway	1.186	0.034					-2.016	0.000		
Leukocyte transendothelial migration	2.334	0.000	1.560	0.052			-1.455	0.011	-1.444	0.078
Long-term depression	1.575	0.006								
Long-term potentiation	1.080	0.053								
Lysosome	1.304	0.020	-1.630	0.070					-1.537	0.053
MAPK signaling pathway	2.669	0.000	2.312	0.001			-2.420	0.000	-1.389	0.085
Meiosis - yeast					-1.567	0.013	2.785	0.000		
Melanogenesis	1.301	0.021								
Mismatch repair					-1.721	0.010	1.647	0.007	1.453	0.077
mRNA surveillance pathway					-1.542	0.013	1.230	0.049		
Natural killer cell mediated cytotoxicity	3.418	0.000					-2.672	0.000		
Neuroactive ligand-receptor interaction	1.529	0.006					-1.809	0.001		
Neurotrophin signaling pathway	1.842	0.001					-0.876	0.094		
NF-kappa B signaling pathway	2.887	0.000					-2.296	0.000		
N-Glycan biosynthesis							1.272	0.043		
NOD-like receptor signaling pathway	1.455	0.011					-1.176	0.035		
Nucleotide excision repair					-1.950	0.003	2.110	0.000	1.693	0.021
Oocyte meiosis							2.213	0.000		
Osteoclast differentiation	2.995	0.000					-2.684	0.000		
Ovarian steroidogenesis					1.320	0.046				
Oxidative phosphorylation			4.009	0.000			-1.428	0.012		
Pancreatic secretion							-1.481	0.010		
Pentose and glucuronate interconversions					2.325	0.000				

KEGG Pathway	Gill		Heart		Liver		Ovary		Testis	
	stat.mean	q.value								
Peroxisome	-1.588	0.027			1.689	0.006				
Phagosome	1.851	0.001					-0.971	0.069	-1.528	0.053
Phosphatidylinositol signaling system	1.567	0.006					-1.126	0.041		
PI3K-Akt signaling pathway	2.140	0.000					-1.767	0.002		
PPAR signaling pathway					2.410	0.000	-1.943	0.001		
Progesterone-mediated oocyte maturation							2.156	0.000		
Prolactin signaling pathway	1.210	0.030					-1.681	0.003		
Propanoate metabolism			1.961	0.010			-1.107	0.046		
Proteasome	1.136	0.041								
Protein digestion and absorption							-2.715	0.000		
Proximal tubule bicarbonate reclamation							-1.244	0.031		
Purine metabolism									1.554	0.026
Pyrimidine metabolism			-1.693	0.070			1.665	0.005		
Pyruvate metabolism			1.828	0.017			-0.972	0.071		
Regulation of actin cytoskeleton	2.442	0.000					-0.977	0.069	-1.902	0.014
Retinol metabolism					2.798	0.000	-1.632	0.007		
Retrograde endocannabinoid signaling							-0.943	0.079		
Ribosome			-1.969	0.032	-1.922	0.003			2.282	0.000
Ribosome biogenesis in eukaryotes	-1.814	0.020	-1.685	0.070			3.154	0.000		
RIG-I-like receptor signaling pathway	1.330	0.020					-0.925	0.083		
RNA degradation					-1.222	0.078	2.278	0.000		
RNA polymerase					-1.433	0.037	2.051	0.001		
RNA transport	-1.728	0.020	-2.019	0.032	-1.956	0.003	3.625	0.000	1.674	0.020
Salivary secretion	1.677	0.004					-1.168	0.037		
Serotonergic synapse	0.918	0.099					-0.974	0.069		
Spliceosome					-2.405	0.000	2.295	0.000		
Starch and sucrose metabolism					1.966	0.002	-0.893	0.094		
T cell receptor signaling pathway	2.978	0.000					-1.454	0.011		

KEGG Pathway	Gill		Heart		Liver		Ovary		Testis	
	stat.mean	q.value								
TGF-beta signaling pathway	1.313	0.020					-1.415	0.012		
Thyroid hormone synthesis	0.963	0.085								
Tight junction	1.035	0.061								
TNF signaling pathway	2.439	0.000					-2.156	0.000		
Toll-like receptor signaling pathway	1.583	0.006					-1.393	0.013		
Tryptophan metabolism					2.857	0.000	-1.158	0.040		
Tyrosine metabolism					1.821	0.004	-0.998	0.069		
Ubiquitin mediated proteolysis					-1.533	0.013	1.672	0.004		
Valine, leucine and isoleucine degradation	-2.233	0.002	2.941	0.000						
Various types of N-glycan biosynthesis							1.618	0.007		
Vascular smooth muscle contraction	1.304	0.020					-1.946	0.001		
Vasopressin-regulated water reabsorption	0.912	0.099					-0.957	0.073		
VEGF signaling pathway	1.597	0.005					-1.445	0.011		
Wnt signaling pathway	1.217	0.029					-0.984	0.069		

KEGG Pathway	Gill_Heart		Gill_Liver		Gill_Ovary		Gill_Testis		Heart_Liver		Heart_Ovary		Heart_Testis		Liver_Ovary		Liver_Testis		Ovary_Testis	
	stat. mean	q.value	stat. mean	q.value	stat. mean	q.value	stat. mean	q.value	stat. mean	q.value	stat. mean	q.value	stat. mean	q.value	stat. mean	q.value	stat. mean	q.value	stat. mean	q.value
ABC transporters	0.708	0.079	0.842	0.034															-1.058	0.006
Adherens junction	1.416	0.001	1.072	0.007	0.854	0.057											-0.978	0.046	-1.195	0.002
Adipocytokine signaling pathway	0.781	0.050	0.943	0.017					0.938	0.031									-1.292	0.001
Alanine, aspartate and glutamate metabolism					-1.492	0.000			1.169	0.009						1.162	0.011			
Aldosterone-regulated sodium reabsorption																			-0.624	0.074
Amino sugar and nucleotide sugar metabolism			0.823	0.035																
Aminoacyl-tRNA biosynthesis	-1.256	0.010	-1.210	0.004					-0.907	0.069	1.066	0.035			1.007	0.048			1.637	0.000
Antigen processing and presentation			1.359	0.001							-1.042	0.043							-0.858	0.020
Apoptosis	1.243	0.002	0.909	0.022										-0.713	0.071				-1.033	0.006
Arachidonic acid metabolism																			-0.836	0.023
Arginine and proline metabolism					-1.555	0.000			1.069	0.014			0.969	0.089			1.164	0.011		
Axon guidance	1.802	0.000	0.809	0.039			0.887	0.056							-1.303	0.001	-0.912	0.059	-1.225	0.001
B cell receptor signaling pathway	2.282	0.000	2.044	0.000	1.020	0.035	1.268	0.005			-1.197	0.016			-1.276	0.002	-1.027	0.046	-2.052	0.000
Basal transcription factors	-0.913	0.074	-1.616	0.000	1.215	0.011			-1.751	0.000	1.214	0.016							2.079	0.000
Base excision repair	-0.977	0.058	-1.645	0.000					-1.738	0.000									2.118	0.000
beta-Alanine metabolism					-1.037	0.015			1.004	0.025										
Bile secretion			1.093	0.006					0.974	0.026									-1.116	0.003
Calcium signaling pathway	1.717	0.000							1.104	0.011					-1.072	0.006			-1.523	0.000
Carbon fixation in photosynthetic organisms					-0.885	0.043			1.000	0.026									-0.820	0.028
Cardiac muscle contraction	1.955	0.000			-2.020	0.000			1.980	0.000			2.518	0.000	-1.996	0.000			-1.482	0.000
Cell adhesion molecules (CAMs)	2.103	0.000	1.604	0.000			1.142	0.012			-1.100	0.037			-1.454	0.000			-1.915	0.000
Cell cycle	-1.211	0.011	-1.887	0.000	1.269	0.006			-1.639	0.000	1.667	0.001			0.860	0.098	-0.852	0.074	2.304	0.000
Cell cycle - yeast	-2.015	0.000	-2.540	0.000	1.740	0.000			-2.713	0.000	1.771	0.001			1.073	0.048			3.527	0.000

KEGG Pathway	Gill_Heart		Gill_Liver		Gill_Ovary		Gill_Testis		Heart_Liver		Heart_Ovary		Heart_Testis		Liver_Ovary		Liver_Testis		Ovary_Testis	
	stat. mean	q.value	stat. mean	q.value	stat. mean	q.value	stat. mean	q.value	stat. mean	q.value	stat. mean	q.value	stat. mean	q.value	stat. mean	q.value	stat. mean	q.value	stat. mean	q.value
Chemokine signaling pathway	2.878	0.000	2.005	0.000			1.113	0.012			-0.991	0.048			-1.689	0.000	-1.226	0.013	-2.580	0.000
Cholinergic synapse	1.362	0.001													-0.943	0.017			-0.978	0.009
Circadian entrainment	1.136	0.005											0.973	0.089	-1.328	0.001			-0.635	0.071
Citrate cycle (TCA cycle)					-1.030	0.019	-1.493	0.002	1.743	0.000	1.332	0.009							-0.804	0.034
Complement and coagulation cascades			3.773	0.000	-3.384	0.000	-1.901	0.001	4.671	0.000	-2.827	0.000			2.042	0.002	3.524	0.000	-3.633	0.000
Cysteine and methionine metabolism					-0.989	0.019			0.993	0.025							0.875	0.074		
Cytokine-cytokine receptor interaction	2.676	0.000	2.788	0.000	-0.907	0.050	1.331	0.005	1.570	0.001	-2.302	0.000			-1.963	0.000			-3.421	0.000
DNA replication	-1.710	0.001	-2.816	0.000	1.132	0.019	1.006	0.056	-3.047	0.000	1.090	0.035							3.678	0.000
Dopaminergic synapse	1.253	0.002													-1.267	0.001			-0.734	0.040
Drug metabolism - other enzymes			0.940	0.020					0.935	0.037									-0.760	0.039
ECM-receptor interaction	2.307	0.000	0.922	0.024			1.034	0.026							-1.842	0.000	-0.832	0.083	-1.730	0.000
Endocrine and other factor-regulated calcium reabsorption	0.695	0.081													-0.692	0.082				
Endocytosis	1.754	0.000	1.123	0.004											-1.106	0.005			-1.635	0.000
ErbB signaling pathway	0.817	0.039	0.688	0.070															-0.771	0.033
Estrogen signaling pathway	1.157	0.005	1.101	0.005											-0.680	0.086			-1.270	0.001
Fanconi anemia pathway	-2.046	0.000	-2.428	0.000	1.060	0.035			-2.410	0.000	1.245	0.018							3.341	0.000
Fat digestion and absorption					-0.928	0.035	-1.005	0.050	1.324	0.004					0.986	0.056	0.909	0.074	-0.594	0.097
Fatty acid degradation	0.859	0.039							1.169	0.010									-0.744	0.043
Fc epsilon RI signaling pathway	2.074	0.000	1.519	0.000			1.278	0.005			-1.036	0.043			-1.449	0.000	-0.820	0.093	-1.690	0.000
Fc gamma R-mediated phagocytosis	2.245	0.000	2.493	0.000	0.983	0.044	1.852	0.000			-1.943	0.000			-1.505	0.000			-2.145	0.000
Focal adhesion	3.198	0.000	0.946	0.017			0.781	0.099	0.856	0.047					-2.243	0.000	-1.454	0.001	-2.408	0.000
GABAergic synapse	0.869	0.033			-0.860	0.046							1.223	0.023	-1.341	0.001				
Galactose metabolism			0.655	0.091					0.897	0.042									-0.573	0.099
Gap junction	1.453	0.000	0.638	0.094	0.923	0.044									-0.798	0.046	-1.131	0.020	-0.845	0.022
Gastric acid secretion	1.436	0.001													-1.090	0.006			-1.061	0.006
Glutamatergic synapse	1.755	0.000					1.160	0.012					1.187	0.030	-1.984	0.000			-1.170	0.002

KEGG Pathway	Gill_Heart		Gill_Liver		Gill_Ovary		Gill_Testis		Heart_Liver		Heart_Ovary		Heart_Testis		Liver_Ovary		Liver_Testis		Ovary_Testis	
	stat. mean	q.value	stat. mean	q.value	stat. mean	q.value	stat. mean	q.value	stat. mean	q.value	stat. mean	q.value	stat. mean	q.value	stat. mean	q.value	stat. mean	q.value	stat. mean	q.value
Glycerolipid metabolism	-0.967	0.062	0.763	0.062	-1.682	0.000	-1.347	0.007	2.059	0.000					1.207	0.038	1.542	0.002	-0.902	0.019
Glycerophospholipid metabolism							-1.050	0.032	1.107	0.011					0.883	0.080			-0.753	0.037
Glycine, serine and threonine metabolism					-1.372	0.001	-0.864	0.093	1.266	0.005							1.128	0.012		
Glycolysis / Gluconeogenesis					-1.253	0.002			1.523	0.000									-0.907	0.014
Glyoxylate and dicarboxylate metabolism					-1.517	0.000	-1.058	0.036	1.719	0.000									-0.707	0.052
GnRH signaling pathway	1.866	0.000													-1.288	0.001	-1.001	0.046	-1.274	0.001
Hematopoietic cell lineage	2.013	0.000	1.263	0.003											-1.150	0.005	-0.917	0.074	-1.776	0.000
HIF-1 signaling pathway	1.039	0.010							0.958	0.027					-0.653	0.096			-1.253	0.001
Hippo signaling pathway	1.521	0.000	0.612	0.100											-0.714	0.071	-0.916	0.057	-1.273	0.001
Histidine metabolism	-0.999	0.058	0.917	0.029	-1.012	0.022			0.956	0.039	-1.065	0.043					1.491	0.002		
Homologous recombination	-1.027	0.058	-1.549	0.000	0.838	0.067			-1.920	0.000									2.181	0.000
Inositol phosphate metabolism	0.713	0.077	1.277	0.001					0.863	0.046									-1.390	0.000
Insulin secretion	0.914	0.025													-0.836	0.036			-0.900	0.015
Insulin signaling pathway	0.822	0.039	0.787	0.041					0.767	0.074									-1.152	0.002
Jak-STAT signaling pathway	1.022	0.012	1.511	0.000					0.911	0.037	-1.265	0.012			-0.672	0.094			-1.678	0.000
Leukocyte transendothelial migration	2.558	0.000	1.126	0.005											-1.458	0.000	-1.450	0.001	-1.976	0.000
Long-term depression	1.152	0.005	0.793	0.044											-0.744	0.063			-0.819	0.026
Long-term potentiation	1.009	0.013																	-0.580	0.095
Lysosome			1.453	0.000	1.373	0.003							-2.029	0.000	1.048	0.042			-0.564	0.099
MAPK signaling pathway	3.228	0.000	1.336	0.001			0.873	0.056	0.815	0.059					-2.134	0.000	-1.431	0.001	-2.597	0.000
Meiosis - yeast	-1.423	0.004	-1.781	0.000	1.187	0.013			-1.796	0.000	1.313	0.009							2.427	0.000
Melanogenesis	1.090	0.008	0.778	0.046															-0.931	0.013
Mismatch repair	-0.986	0.062	-1.698	0.000					-1.665	0.000									2.114	0.000
mRNA surveillance pathway			-1.135	0.006	0.755	0.091			-1.291	0.003									1.316	0.001
Natural killer cell mediated cytotoxicity	2.675	0.000	2.464	0.000			1.465	0.002			-1.675	0.000			-1.688	0.000			-2.687	0.000

KEGG Pathway	Gill_Heart		Gill_Liver		Gill_Ovary		Gill_Testis		Heart_Liver		Heart_Ovary		Heart_Testis		Liver_Ovary		Liver_Testis		Ovary_Testis	
	stat. mean	q.value	stat. mean	q.value	stat. mean	q.value	stat. mean	q.value	stat. mean	q.value	stat. mean	q.value	stat. mean	q.value	stat. mean	q.value	stat. mean	q.value	stat. mean	q.value
Neuroactive ligand-receptor interaction	1.457	0.000	1.235	0.002							-0.927	0.062			-1.041	0.008			-1.583	0.000
Neurotrophin signaling pathway	1.640	0.000	1.003	0.012											-0.850	0.031	-0.968	0.046	-1.312	0.001
NF-kappa B signaling pathway	1.917	0.000	2.155	0.000			1.517	0.001			-1.784	0.000			-1.379	0.001			-2.016	0.000
N-Glycan biosynthesis					0.979	0.035			-1.256	0.004									1.087	0.008
NOD-like receptor signaling pathway	0.882	0.032	1.189	0.003							-0.997	0.048							-1.039	0.006
Notch signaling pathway			0.678	0.079																
Nucleotide excision repair	-1.324	0.007	-2.085	0.000					-1.925	0.000	0.975	0.057							2.593	0.000
Oocyte meiosis	-0.914	0.062	-1.137	0.006	0.899	0.049			-0.827	0.095	1.306	0.009			0.982	0.048			1.400	0.000
Osteoclast differentiation	2.835	0.000	1.944	0.000			1.264	0.005			-1.222	0.015			-1.928	0.000	-0.876	0.074	-2.608	0.000
Ovarian steroidogenesis					-1.071	0.011			1.145	0.010							0.879	0.074		
Oxidative phosphorylation	1.701	0.000	-1.163	0.006	-1.536	0.000			1.662	0.000	1.271	0.012	2.238	0.000	-1.574	0.000			-1.024	0.007
p53 signaling pathway					0.806	0.067														
Pancreatic secretion	0.851	0.035	0.668	0.079											-0.906	0.023			-0.916	0.013
Pentose and glucuronate interconversions	-0.937	0.080	0.846	0.047	-1.253	0.003	-0.916	0.093	1.499	0.001					1.071	0.048	1.408	0.004	-0.691	0.069
Peroxisome	-1.012	0.046			-1.253	0.002	-1.097	0.029	1.328	0.002					0.981	0.048	1.137	0.011		
Phagosome	1.265	0.002	1.758	0.000															-1.703	0.000
Phosphatidylinositol signaling system	1.028	0.012	1.300	0.001							-0.895	0.078							-1.213	0.001
PI3K-Akt signaling pathway	2.174	0.000	1.280	0.001											-1.384	0.000	-0.870	0.069	-1.895	0.000
Porphyrin and chlorophyll metabolism					-0.739	0.098			1.107	0.011									-0.652	0.065
PPAR signaling pathway			1.011	0.012	-1.957	0.000	-1.020	0.041	2.456	0.000							1.255	0.006	-1.712	0.000
Progesterone-mediated oocyte maturation			-1.237	0.003	0.865	0.056					1.502	0.002					-0.829	0.079	1.273	0.001
Prolactin signaling pathway	1.279	0.002	1.371	0.001					0.986	0.026									-1.766	0.000
Propanoate metabolism					-1.583	0.000			1.602	0.000			1.177	0.032					-0.701	0.053
Proteasome							1.109	0.012	-0.853	0.086					-0.870	0.029				
Protein digestion and			0.633	0.100	-1.725	0.000	0.978	0.042	0.915	0.039	-1.556	0.001	1.276	0.023	-1.344	0.001	1.359	0.004	-1.000	0.009

KEGG Pathway	Gill_Heart		Gill_Liver		Gill_Ovary		Gill_Testis		Heart_Liver		Heart_Ovary		Heart_Testis		Liver_Ovary		Liver_Testis		Ovary_Testis		
	stat. mean	q.value	stat. mean	q.value	stat. mean	q.value	stat. mean	q.value	stat. mean	q.value	stat. mean	q.value	stat. mean	q.value	stat. mean	q.value	stat. mean	q.value	stat. mean	q.value	
absorption																					
Protein processing in endoplasmic reticulum			0.607	0.100	0.822	0.061															
Proximal tubule bicarbonate reclamation					-0.972	0.025			1.196	0.009										-1.018	0.008
Purine metabolism	-1.209	0.010							-1.045	0.021										1.422	0.000
Pyrimidine metabolism	-1.376	0.004	-0.792	0.084	0.746	0.094			-1.389	0.001										1.715	0.000
Pyruvate metabolism					-1.276	0.002			1.260	0.005			1.122	0.037						-0.589	0.093
Regulation of actin cytoskeleton	2.413	0.000	1.324	0.001	0.999	0.034									-1.007	0.010	-1.638	0.000	-1.962	0.000	
Retinol metabolism			1.570	0.000	-1.451	0.001	-1.045	0.053	2.260	0.000	-0.904	0.099					1.201	0.012	-1.819	0.000	
Retrograde endocannabinoid signaling	0.830	0.039													-1.214	0.002					
Ribosome	-0.955	0.058	-1.149	0.006	0.828	0.061	1.718	0.000	-2.498	0.000										2.222	0.000
Ribosome biogenesis in eukaryotes	-2.258	0.000	-2.024	0.000	0.914	0.051			-1.788	0.000	1.290	0.011			1.363	0.011				2.943	0.000
RIG-I-like receptor signaling pathway	0.942	0.022	1.004	0.012																-0.996	0.008
RNA degradation	-1.300	0.007	-1.362	0.001	1.024	0.034			-1.619	0.000										2.074	0.000
RNA polymerase	-1.227	0.015	-1.456	0.001	0.919	0.056			-1.748	0.000										2.148	0.000
RNA transport	-2.388	0.000	-2.512	0.000	1.293	0.006			-2.551	0.000	1.436	0.004			1.138	0.038				3.613	0.000
Salivary secretion	1.358	0.001	0.754	0.055			1.033	0.025							-1.186	0.003				-0.907	0.016
Serotonergic synapse	1.238	0.002													-0.923	0.020				-0.924	0.013
Sphingolipid metabolism			0.780	0.045																	
Spliceosome			-1.757	0.000	1.448	0.002			-2.320	0.000	1.037	0.035					-0.873	0.070	2.332	0.000	
Starch and sucrose metabolism			0.727	0.067	-1.222	0.003	-1.099	0.032	1.789	0.000							0.854	0.090	-1.094	0.005	
Synaptic vesicle cycle					0.963	0.035															
T cell receptor signaling pathway	2.195	0.000	1.780	0.000	1.039	0.034	1.176	0.010			-0.970	0.053			-1.242	0.002	-1.104	0.027	-1.846	0.000	
TGF-beta signaling pathway	1.409	0.001	0.761	0.048											-1.098	0.005				-1.211	0.001
Thyroid hormone synthesis	0.824	0.039	0.642	0.091																-0.772	0.033
Tight junction	1.475	0.000													-0.875	0.027	-0.950	0.046	-0.990	0.008	
TNF signaling pathway	2.059	0.000	1.917	0.000			0.913	0.054			-1.224	0.015			-1.216	0.002				-2.220	0.000
Toll-like receptor	1.181	0.004	1.248	0.002							-0.945	0.060			-0.781	0.050				-1.296	0.001

KEGG Pathway	Gill_Heart		Gill_Liver		Gill_Ovary		Gill_Testis		Heart_Liver		Heart_Ovary		Heart_Testis		Liver_Ovary		Liver_Testis		Ovary_Testis		
	stat. mean	q.value	stat. mean	q.value	stat. mean	q.value	stat. mean	q.value	stat. mean	q.value	stat. mean	q.value	stat. mean	q.value	stat. mean	q.value	stat. mean	q.value	stat. mean	q.value	
signaling pathway																					
Tryptophan metabolism			1.373	0.001	-1.364	0.001	-1.200	0.026	2.085	0.000					1.158	0.042	1.322	0.006	-1.415	0.000	
Tyrosine metabolism					-1.526	0.000	-0.901	0.089	1.657	0.000							1.186	0.011	-0.736	0.043	
Ubiquitin mediated proteolysis			-0.953	0.025	1.232	0.006			-1.176	0.008	1.113	0.020					-1.155	0.015	1.030	0.012	
Valine, leucine and isoleucine degradation			-1.246	0.004	-1.608	0.000	-1.794	0.000	1.970	0.000	1.590	0.002	1.396	0.013							
Various types of N-glycan biosynthesis					1.262	0.006			-1.203	0.008									0.989	0.021	
Vascular smooth muscle contraction	1.515	0.000	0.813	0.039			0.845	0.069							-1.403	0.000			-1.370	0.000	
Vasopressin-regulated water reabsorption	0.678	0.086													-0.777	0.050					
VEGF signaling pathway	1.728	0.000	0.882	0.027											-1.192	0.003			-1.442	0.000	
Wnt signaling pathway	1.043	0.010	0.864	0.028															-1.030	0.006	

**10 CURRICULUM VITAE****Željka Trumbić**

Date and place of birth: 06.10.1981. Split, Croatia  
 Contact address: Livanjska 5/III, 21 000 Split, Croatia  
 Mob: 00 385 91 315 4284  
 Mail: ztrumbic@unist.hr

**CURRENT POSITION**

2009– present Novice in science (PhD student)/ Teaching Assistant  
 University of Split, Department of Marine Studies, Croatia  
 Teaching: undergraduate level practical courses in Molecular biology, Genetics and Applied Histology at Home University.

**EDUCATION**

2010– present Postgraduate PhD degree programme: Interdisciplinary Study of Molecular Biosciences, University of Josip Juraj Strossmayer, Osijek  
 2008 MASTER II; University of Bordeaux 1, France  
 Master of Science and Technologies - Functioning of Aquatic Ecosystems  
 2006 DIPLOMA: MSc in Marine Biology and Ecology, University of Split, Centre for Marine Studies, Croatia

**WORKSHOPS AND CONFERENCES**

2012. ENGAGE/GEUVADIS RNA-seq Workshop – practical course, European Bioinformatics Institute, Cambridge, UK  
 2010. Phylogenetic reconstruction: techniques and uses, Institute for Oceanography and Fisheries, Split, Croatia  
 2009. Oligo arrays/Expression R1087A - Agilent training course, Institute Gustave Roussy, Paris, France  
 CEFAS Histopathology Workshop, Weymouth, United Kingdom  
 EUROTOX Basic Toxicology Course, Tirana, Albania  
 Introduction to Bioinformatics; Practical course:, Faculty of Science, University of Zagreb, Croatia

**SCHOLARSHIPS AND VISITS TO FOREIGN INSTITUTIONS**

2013. ERASMUS student placement Life Long Learning Program  
 Research visit to Institute of Aquaculture, University of Stirling, Scotland, United Kingdom

2011. Fellowship for Doctoral Students, Croatian Science Foundation  
Research visit to Institute of Aquaculture, University of Stirling, Scotland, United Kingdom
- 2007/2008 Scholarship of the French Government in collaboration with the Croatian Ministry of Science, Education and Sports  
Research visit to Marine station in Arcachon, University of Bordeaux 1, France

PERSONAL SKILLS AND COMPETENCES
---------------------------------

- |                 |  |
|-----------------|--|
| Languages       | Croatian (mother tongue); English (fluent);<br>French (reading, writing and verbal skills: good)       |
| Computer skills | Microsoft Office, STATISTICA, GIMP, Genespring, basics of C++ programming, Perl and Python, R software |
| Other           | Holder of type B driver's license<br>One star diver, R1 CMAS   |

PUBLICATIONS
--------------

- Lepen Pleić I, Bušelić I, **Trumbić Ž**, Bočina I, Šprung M, Ivona M. 2015. Expression analysis of the Atlantic bluefin tuna (*Thunnus thynnus*) pro-inflammatory cytokines, IL-1 $\beta$ , TNF $\alpha$ 1 and TNF $\alpha$ 2 in response to parasites *Pseudocycnus appendiculatus* (Copepoda) and *Didymosulcus katsuwonicola* (Digenea). Fish Shellfish Immunol. 45: 946–954.
- Popović Z, Mladineo I, Ezgeta-Balić D, **Trumbić Ž**, Vrgoč N, Peharda M. 2013. Reproductive cycle and gonad development of *Venus verrucosa* L.(Bivalvia: Veneridae) in Kaštela Bay, Adriatic Sea. Mar. Biol. Res. 9:229–239.
- Šegvić-Bubić T, Boban J, Grubišić L, **Trumbić Ž**, Radman M, Perčić M, Čož-Rakovac R. 2013. Effects of propolis enriched diet on growth performance and plasma biochemical parameters of juvenile European sea bass (*Dicentrarchus labrax* L.) under acute low-temperature stress. Aquac. Nutr. 19:877–885.
- Šegvić-Bubić T, Lepen I, **Trumbić Ž**, Ljubković J, Sutlović D, Matić-Skoko S, Grubišić L, Glamuzina B, Mladineo I. 2011. Population genetic structure of reared and wild gilthead sea bream (*Sparus aurata*) in the Adriatic Sea inferred with microsatellite loci. Aquaculture 318:309–315.
- Dang C, de Montaudouin X, Caill-Milly N, **Trumbić Ž**. 2010. Spatio-temporal patterns of perkinsosis in the Manila clam *Ruditapes philippinarum* from Arcachon Bay (SW France). Dis. Aquat. Organ. 91:151–159.
- Mladineo I, **Trumbić Ž**, Jozić S, Šegvić T. 2009. First report of *Cryptosporidium* sp. (Coccidia, Apicomplexa) oocysts in the black mussel (*Mytilus galloprovincialis*) reared in the Mali Ston Bay, Adriatic Sea. J. Shellfish Res. 28:541–546.